

PUNCHING SHEAR BEHAVIOUR OF REINFORCED CONCRETE SLABS



BY

A. K. M. JAHANGIR ALAM

A thesis submitted to the Department of Civil Engineering,
Bangladesh University of Engineering and Technology, Dhaka,
in partial fulfillment of the requirements for the degree

of

MASTER OF SCIENCE IN CIVIL ENGINEERING

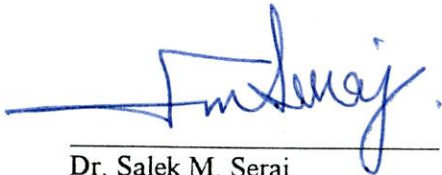


#91690#

SEPTEMBER, 1997

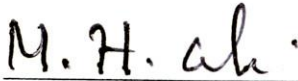
PUNCHING SHEAR BEHAVIOUR OF REINFORCED CONCRETE SLABS

Approved as to style and contents by :



Dr. Salek M. Seraj
Associate Professor
Department of Civil Engineering
BUET, Dhaka.

Chairman
(Supervisor)



Dr. Md. Hossain Ali
Professor
Head of the Department
Department of Civil Engineering
BUET, Dhaka.

Member



Dr. Alamgir Habib
Professor
Department of Civil Engineering
BUET, Dhaka.

Member



Mr. A. S. M. Abdul Hamid
Director *
Civil and Structural Engineering
Development, Design Consultants Ltd.
21, New Eskaton Road
Dhaka-1000.

Member
(External)

Director **
Khaled and Partners Ltd.
8/9, Lalmatia
1st floor, Block-C
Dhaka-1207.

* Upto the end of June '97

** From July '97

To

my parents

DECLARATION

Declared that except where specific references are made to other investigators, the work embodied in this thesis is the result of the investigation carried out by the author under the supervision of Dr. Salek M. Seraj, Associate Professor, Department of Civil Engineering, Bangladesh University of Engineering & Technology, Dhaka, Bangladesh. Neither this thesis nor any part of it has been submitted or is being concurrently submitted elsewhere for any other purpose (except for publication).

September, 1997



A. K. M. Jahangir Alam

ACKNOWLEDGMENT

The author wishes to express his deepest gratitude to his supervisor Dr. Salek M. Seraj, Associate Professor, Department of Civil Engineering, Bangladesh University of Engineering & Technology (BUET), for his constant guidance, continued encouragement, generous help and unfailing enthusiasm at all the stages of this research work. His active interest in this topic and valuable advice were the source of the author's inspiration.

Sincere appreciation and gratitude are also expressed to Dr. Md. Hossain Ali, Professor and Head, Department of Civil Engineering, BUET, for his encouragement and cooperation. Thanks are also due to Dr. M. Azadur Rahman, Professor, Department of Civil Engineering, for his co-operation during his tenure as Head, Department of Civil Engineering, BUET.

The author owes his thanks to the members of the Board of Post Graduate Studies of the Department of Civil Engineering, BUET, and also to the members of the Committee of Advanced Studies and Research for kindly approving the research proposal and financing the experimental work reported in this thesis.

The author is greatly indebted to Dr. A. B. M. Badruzzaman, Associate Professor, Department of Civil Engineering, BUET, for his generous help at the Computer Laboratory at different stages of the work. The author is also grateful to Mr. M. M. Abdul Alim, Executive Engineer (Civil), Engineering Office, BUET, for his kind support during the present study.

The technical staff of the Concrete Structures and Strength of Materials Laboratories were very helpful during the experimental work. Almost all the technical personnel were involved in the experimental work some way or other. I would like to extend my special thanks to Messrs. Md. Abdul Karim, Md. Barkat Ullah, Banard Rojario, Julhas Uddin, Md. Abdul Berek and Md. Golam Rabbani.

Finally, the author wishes to thank his family and friends who helped him with necessary advice and information during the course of the study.

ABSTRACT

Punching shear is an important consideration in the design of reinforced concrete flat plates, flat slabs, and column footings. Present design rules for punching shear failure of reinforced concrete slabs, given in various Codes of practice, are largely based on studies of the behaviour and strength of simply-supported, conventional specimens extending to the nominal line of contraflexure. As punching shear provisions incorporated in various Codes of practice are a direct result of the empirical procedures, they do not usually provide an accurate estimate of the ultimate punching load capacity of a slab with its edges restrained against rotation. This is because no direct account is taken of the significant enhancement of punching capacity due to the in-plane restraint in many types of reinforced concrete slab systems.

The present study describes punching tests conducted on reinforced concrete slabs with their edges restrained as well as unrestrained. Here, edge restraint has been provided, by means of edge beams of various dimensions, to mimic the behaviour of continuous slabs. A total of 16 model slabs have been tested in an effort to ascertain the influence of the degree of boundary restraint, percentage of steel reinforcement, and slab thickness of the slab models on their structural behaviour and punching load-carrying capacity. The cracking pattern and load-deflection behaviour of the slabs tested have also been monitored closely. The test program was carried out to provide basic information on the real punching behaviour of restrained slabs subjected to concentrated loading and may also be usefully applied in the assessment of existing structures with laterally restrained slab construction.

The significant positive effect of edge restraint on the punching failure load, resulting in enhancing the ultimate punching strength, has been noticed. The code-specified strength of the specimens was calculated in accordance with the American, British, Canadian and European codes. It became apparent that no code-specified method predicts an enhancement in the punching shear strength of a restrained reinforced concrete slab with an increase in the degree of such restraints. Present Codes do not recognize the role of percentage of longitudinal steel on the punching strength effectively either. It has been understood that inclusion of the findings of the study in the design Codes will result in a rational design of structural systems where punching phenomenon plays a vital role.

CONTENTS

	<u>Page No.</u>
DECLARATION	iv
ACKNOWLEDGMENT	v
ABSTRACT	vi
CONTENTS	vii
LIST OF FIGURES	xi
LIST OF TABLES	xv
NOTATIONS	xvi
CHAPTER ONE GENERAL CONSIDERATIONS	1
1.1 INTRODUCTION	1
1.2 PRESENT STATE OF ART OF THE RESEARCH TOPIC	2
1.3 OBJECTIVE OF THE STUDY	5
1.4 METHODOLOGY	5
CHAPTER TWO CODE PROVISIONS AND SPECIMEN DETAILS	8
2.1 INTRODUCTION	8
2.2 CODE PROVISIONS	8
2.2.1 American (ACI 318-95) Code provision	8
2.2.2 British (BS 8110-85) Code provision	9
2.2.3 Canadian (CAN3-A23.3-M84) Code provision	10
2.2.4 European (CEB-FIP) Code provision	10
2.2.5 Bangladesh National Building Code (BNBC-93) provision	11
2.2.6 Summary of Code provisions	11
2.3 SPECIMEN DETAILS	13
2.3.1 General	13

	<u>Page No.</u>
2.3.2 Major variables of specimens	20
2.4 DESIGN STRENGTH OF MODEL SLABS	21
CHAPTER THREE	MATERIALS USED AND CASTING
	PROCEDURE
	25
3.1 GENERAL	25
3.2 PORTLAND CEMENT	25
3.3 AGGREGATES	25
3.3.1 General	25
3.3.2 Fine Aggregates	26
3.3.3 Coarse Aggregates	26
3.4 WATER	27
3.5 REINFORCEMENT	27
3.5.1 General	27
3.5.2 Fabrication of steel	28
3.6 CONCRETE TRIAL MIX PROPORTIONING	28
3.7 FORM WORK	31
3.8 MIXING OF CONCRETE	31
3.9 PLACING OF CONCRETE	31
3.10 CASTING OF CYLINDER	32
3.11 CURING	32
CHAPTER FOUR	TESTING PROGRAMME
	35
4.1 INTRODUCTION	35
4.2 TESTING ARRANGEMENT	35
4.3 TESTING PROCEDURE	36
4.3.1 Calibration of test rig	36
4.3.2 Instrumentation	36

	<u>Page No.</u>
4.4 TEST RESULTS	37
4.4.1 General	37
4.4.2 Details of test results	40
CHAPTER FIVE	DISCUSSION OF RESULTS
	61
5.1 GENERAL	61
5.2 ULTIMATE LOAD CARRYING CAPACITY	61
5.3 EFFECT OF EDGE RESTRAINT	63
5.4 EFFECT OF STEEL REINFORCEMENT	65
5.5 EFFECT OF SLAB THICKNESS	66
5.6 DEFLECTION	67
5.7 CRACKING	67
5.8 DETERMINATION OF SIZE SENSITIVITY VIA SLAB16	72
5.9 COMPARISON OF TEST RESULTS WITH DIFFERENT CODE PREDICTIONS	72
CHAPTER SIX	CONCLUSION AND RECOMMENDATIONS
	79
6.1 CONCLUSIONS	79
6.2 RECOMMENDATIONS FOR FUTURE RESEARCH	80
REFERENCES	81
<i>APPENDIX A</i> <i>Details section and reinforcement of all slabs.</i>	84
<i>APPENDIX B</i> <i>Calculation of design strength of slabs.</i>	93

DESIGN B-1	Design of slab samples of slab thickness = 80 mm (SLAB1, SLAB2, SLAB3, SLAB7, SLAB10 and SLAB13)	94
DESIGN B-2	Design of slab samples of slab thickness = 60 mm (SLAB4, SLAB5, SLAB6, SLAB8, SLAB9, SLAB11, SLAB12, SLAB14, SLAB15 and SLAB16)	96
B-3	Calculation of torsional rigidity of slabs	98
<i>APPENDIX C</i>	<i>Weight of the sample and slab movement</i>	100
<i>APPENDIX D</i>	<i>Deflections of slab and edge beam</i>	106
<i>APPENDIX E</i>	<i>Test Results in table</i>	118

LIST OF FIGURES

	<u>Page No.</u>
<i>Figure 1.1</i>	A square column tends to shear out a pyramid from a footing or column. 6
<i>Figure 2.1</i>	Dimension and reinforcement details of model slabs. 15
<i>Figure 2.2A</i>	Reinforcement details of (a) SLAB1, (b) SLAB2, (c) SLAB3 and (d) SLAB4. 16
<i>Figure 2.2B</i>	Reinforcement details of (a) SLAB5, (b) SLAB6, (c) SLAB7 and (d) SLAB8. 17
<i>Figure 2.2C</i>	Reinforcement details of (a) SLAB9, (b) SLAB10, (c) SLAB11 and (d) SLAB12. 18
<i>Figure 2.2D</i>	Reinforcement details of (a) SLAB13, (b) SLAB14 and (c) SLAB15. 19
<i>Figure 3.1</i>	Details of typical formwork. 33
<i>Figure 3.2</i>	(a) Bottom portion of formwork system, (b) Reinforcement casing in the completed formwork. 34
<i>Figure 4.1</i>	Test rig and testing set-up. 38
<i>Figure 4.2</i>	Typical cracking pattern on the top surface of a model slab. 39
<i>Figure 4.3</i>	Cracking pattern of bottom surface of (a) SLAB1 and (b) SLAB2. 42
<i>Figure 4.4</i>	Cracking pattern of bottom surface of (a) SLAB3 and (b) SLAB4. 45
<i>Figure 4.5</i>	Cracking pattern of bottom surface of (a) SLAB5 and (b) SLAB6. 48
<i>Figure 4.6</i>	Cracking pattern of bottom surface of (a) SLAB8 and (b) SLAB9. 51
<i>Figure 4.7</i>	Cracking pattern of bottom surface of (a) SLAB10 and (b) SLAB11. 53
<i>Figure 4.8</i>	Cracking pattern of bottom surface of (a) SLAB12 and (b) SLAB13. 56

	<u>Page No.</u>
<i>Figure 4.9</i> Cracking pattern of bottom surface of (a) SLAB14 and (b) SLAB15.	58
Figure 4.10 Cracking pattern of bottom surface of SLAB16.	60
<i>Figure 5.1</i> Effect of edge restraint for 1.0 percent reinforcement	68
<i>Figure 5.2</i> Effect of edge restraint for slab thickness of 60 mm.	69
<i>Figure 5.3</i> Effect of edge restraint for same width of edge beam.	70
<i>Figure 5.4</i> Central deflection of all slabs under different loading.	71
<i>Figure 5.5</i> Comparison of ultimate load for different Code predicted load at slab thickness = 80 mm and reinforcement ratio = 1.0 percent.	74
<i>Figure 5.6</i> Comparison of ultimate load for different Code predicted load at slab thickness = 60 mm and reinforcement ratio = 1.0 percent.	75
<i>Figure 5.7</i> Comparison of ultimate load for different Code predicted load at slab thickness = 60 mm and reinforcement ratio = 0.5 percent.	76
<i>Figure 5.8a</i> Normalized punching shear strength for 1.0 percent reinforcement	77
<i>Figure 5.8b</i> Normalized punching shear strength for slab thickness of 60 mm.	77
<i>Figure 5.8c</i> Normalized punching shear strength for same width of edge beam.	77
<i>Figure A-1</i> (a) Plan (b) Section and reinforcement details of SLAB1	85
<i>Figure A-2</i> (a) Plan (b) Section and reinforcement details of SLAB2	85
<i>Figure A-3</i> (a) Plan (b) Section and reinforcement details of SLAB3	86
<i>Figure A-4</i> (a) Plan (b) Section and reinforcement details of SLAB4	86
<i>Figure A-5</i> (a) Plan (b) Section and reinforcement details of SLAB5	87
<i>Figure A-6</i> (a) Plan (b) Section and reinforcement details of SLAB6	87
<i>Figure A-7</i> (a) Plan (b) Section and reinforcement details of SLAB7	88
<i>Figure A-8</i> (a) Plan (b) Section and reinforcement details of SLAB8	88
<i>Figure A-9</i> (a) Plan (b) Section and reinforcement details of SLAB9	89
<i>Figure A-10</i> (a) Plan (b) Section and reinforcement details of SLAB10	89
<i>Figure A-11</i> (a) Plan (b) Section and reinforcement details of SLAB11	90
<i>Figure A-12</i> (a) Plan (b) Section and reinforcement details of SLAB12	90
<i>Figure A-13</i> (a) Plan (b) Section and reinforcement details of SLAB13	91
<i>Figure A-14</i> (a) Plan (b) Section and reinforcement details of SLAB14	91

	<u>Page No.</u>
<i>Figure A-15</i> (a) Plan (b) Section and reinforcement details of SLAB15	92
<i>Figure A-16</i> (a) Plan (b) Section and reinforcement details of SLAB16.	92
<i>Figure B-1</i> Dimension of L-section for torsional rigidity	98
<i>Figure C-1</i> Lifting of the slab at the casting yard.	103
<i>Figure C-2</i> Slab placed on trolley.	103
<i>Figure C-3</i> Trolley along with slab being pushed and pulled towards the laboratory.	104
<i>Figure C-4</i> Lifting of slab with two cranes for placement in the test rig.	104
<i>Figure C-5</i> Slabs without edge beam (SLAB13-SLAB15) placed on test rig.	105
<i>Figure D-1</i> Central deflection of slab for different loading of (a) SLAB1, (b) SLAB2, (c) SLAB3 and (d) SLAB4.	107
<i>Figure D-2</i> Central deflection of slab for different loading of (a) SLAB5, (b) SLAB6, (c) SLAB7 and (d) SLAB8.	108
<i>Figure D-3</i> Central deflection of slab for different loading of (a) SLAB9, (b) SLAB10, (c) SLAB11 and (d) SLAB12.	109
<i>Figure D-4</i> Central deflection of slab for different loading of (a) SLAB13, (b) SLAB14, (c) SLAB15 and (d) SLAB16.	110
<i>Figure D-5</i> Upward deflection of edge beam at the mid-section under different loading of (a) SLAB1, (b) SLAB2, (c) SLAB3 and (d) SLAB4.	111
<i>Figure D-6</i> Upward deflection of edge beam at the mid-section under different loading of (a) SLAB5 and (b) SLAB6.	112
<i>Figure D-7</i> Central deflection of slab under different loading of same width of edge beam (245 mm) for (a) h=80 mm and (b) h=60 mm.	113
<i>Figure D-8</i> Central deflection of slab under applied loading for various width of edge beam at same reinforcement ratio (ρ) =1.0 percent for (a) h=80 mm and (b) h=60 mm.	114
<i>Figure D-9a</i> Central deflection of slab under different loading of same slab thickness (60 mm) for (1) b=245 mm and (2) b=175 mm.	115
<i>Figure D-9b</i> Central deflection of slab under different loading of same slab thickness (60 mm) for (1) b=105 mm and (2) b=0 mm.	116

- Figure D-10* Central deflection of slab under applied loading for various width of edge beam (b) at slab thickness (h) = 60 mm and reinforcement ratio (ρ) = 0.5 percent. 117
- Figure D-11* Upward deflection of edge beam at the mid-section of SLAB1 to SLAB6. 117

LIST OF TABLES

	<u>Page No.</u>
<i>Table 2.1</i> Summary of Various Code Provisions Related to Punching Shear Strength of Concrete.	12
<i>Table 2.2</i> Details of Reinforced Concrete Slab Specimens	14
<i>Table 2.3</i> Slab Grouping Based on Size of Edge Restraint	23
<i>Table 2.4</i> Slab Grouping Based on Reinforcement Ratios	23
<i>Table 2.5</i> Punching Shear Capacity of all the Slabs Tested	24
<i>Table 3.1</i> Trial mix Proportion and Strength of Concrete	30
<i>Table 5.1</i> Comparison of Load Carrying Capacity with Code Predictions	62
<i>Table 5.2</i> Non-dimensional and Normalized Punching Shear Strength of Reinforced Concrete Slabs	64
<i>Table C-1</i> Weight of the Sample	101
<i>Table C-2</i> The Actual Load and Monitored Load.	102
<i>Table E-1</i> Ultimate Strength of Slabs and Cylinder Strength of Concrete.	119
<i>Table E-2a</i> Central Deflection of Slab for Different Loading of SLAB1 to SLAB6.	120
<i>Table E-2b</i> Central Deflection of Slab for Different Loading of SLAB7 to SLAB12.	121
<i>Table E-2c</i> Central Deflection of Slab for Different Loading of SLAB13 to SLAB16	122

NOTATIONS

- b = Width of edge beam in millimeter (mm)
- b_0 = Perimeter of critical section of slab or footing in millimeter or inch
- C = Torsional rigidity of slabs in mm^4
- c = Length or width of column or loaded area in millimeter or inch
- d = Effective depth (Distance from extreme compression fiber to centroid of longitudinal tension reinforcement) in millimeter or inch
- f'_c = Uniaxial cylinder (compressive) strength of concrete in MPa or psi
- f_{cu} = Uniaxial cube (compressive) strength of concrete in MPa or psi
- h = Total thickness of slab
- P_u = Ultimate load in kilo-Newton (kN)
- V_c, V_p = Punching shear strength provided by concrete in Newtons or pounds.
- β_e = Ratio of long side to short side of concentrated load or reaction area
- ρ = Reinforcement ratio in percentage



CHAPTER ONE

GENERAL CONSIDERATIONS

1.1 INTRODUCTION

Punching shear is an important consideration in the design of reinforced concrete punching shear flat plates, flat slabs, and column footings. Present design rules for punching shear strength of reinforced concrete slabs, given in various Codes of practice, are largely based on the studies of the behaviour and strength of simply-supported conventional specimens extending to the nominal line of contraflexure.

Column tend to punch through the flat plates, flat slabs and footings because of the shear stresses which act in them around the perimeter of the columns. At the same time the concentrated compression stresses from the column spread out into them (flat plate, flat slab and footing) so that the concrete adjacent to the column remains in vertical or slightly inclined compression, in addition to shear. In consequence, if failure occurs, the failure takes the form of the truncated cone or pyramid with sides slopping outwards at an angle approximately 45° around the reaction area. The punching shear provisions incorporated in various Codes of practice are deficient as they are usually based on tests conducted on simply-supported slabs, sometimes extended to the point of contraflexure and thus fail to mimic the punching behaviour of continuous slab construction, where all panel edges can not rotate freely, in contrast to its simply supported slab counterpart. Consequently, test results of simple slab specimens do not usually provide an accurate prediction of the ultimate load capacity of a slab having lateral restraint. Apart from the fact that as the present Codes rely heavily on test conducted on simply supported small-sized specimens, some of the present-day Code provisions usually specifies the punching shear strength as a function of concrete strength alone. Thus, these Codes fail to take adequate account of the possible role of specimen size and edge restraint. Again, some Codes do not acknowledge the possible effect of percentage of longitudinal reinforcement on the punching shear behaviour of reinforced concrete slabs. Under the circumstances, a study comprising of a planned

series of testing on restrained as well as unrestrained slabs is deemed essential in order to have an insight on the real punching behaviour of reinforced concrete slabs.

Shear failure, both beam and punching type, may be considered more dangerous than flexure failure. This may be so because of greater uncertainty in predicting certain other modes of collapse, or because of the catastrophic nature of some other types of failure, should they occur. Shear failure is difficult to predict accurately. Shear failure is likely to occur suddenly, with no advance warning of distress.

1.2 PRESENT STATE OF ART OF THE RESEARCH TOPIC

A large number of investigators, on the basis of their experimental studies on the punching shear behaviour of slabs, have expressed their opinion against the present punching shear provisions. They have shown that the Code does not usually provide an accurate prediction of the punching shear strength of reinforced concrete slab for various end conditions, reinforcement ratio, span-to-depth ratio, etc.

Kuang and Morley (1992) tested 12 restrained reinforced concrete slabs with varying span-to-depth ratio, percentage of reinforcement, degree of edge restraint and reported that the punching shear strengths are much higher than those predicted by ACI 318 (1989) and BS 8110 (1985). They opined that no code specified method predicts an enhancement in punching shear strength of restrained concrete slabs with an increase in the degree edge restraint. In reality, they have suggested that there is a definite enhancement in punching shear strength as the degree of edge restraint increases. The Codes do not give accurate predictions of the punching shear capacity of restraint slab, and in view of the magnitude of the strength enhancement, the authors have opined that it would evidently be beneficial if the effect of compressive membrane action could be allowed for in the design Codes.

Results of an experimental investigation on the punching shear strength of reinforced concrete slabs with varying span-to-depth ratio have been summarized by Lovrovich and McLean (1990). They have reported that the ACI Building Code does not recognize span-to-depth ratio effects or the effects of restraining action at the support

when treating punching shear in reinforced concrete slabs. They observed that punching shear strength were much greater than the values permitted by the ACI Building Code. This was especially true for those specimens with smaller span-to-depth ratios. The higher strengths were a result of smaller span-to-depth ratios, in-plane compressive forces caused by restraining action at the support and excellent anchorage provided for the shear reinforcement.

Yamada, et al. (1992) performed a research programme for the determination of the effect of shear reinforcement type and ratio on punching shear strength of monolithic slab to column connections. Their experimental study showed that ACI 318-89 provisions for the computation of shear strength considering the reinforcement contribution are justifiably conservative at low reinforcement ratios (upto approximately 0.6 percent). They also showed that the hat-shaped reinforcement (this type of reinforcement did not conform to the requirements of ACI 318-89) was not effective because of lack of proper anchorage and large spacing. Double hooked reinforcement showed high effectiveness, which resulted in a considerable increment of the punching shear resistance of the connections.

Gardner (1990) presents the result of an investigation relating punching shear to concrete strength and steel ratio. He concluded that the shear capacity is proportional to the cube root of concrete strength and steel ratio and that the ACI 318 (1983) and CSA A23.3-M84 (1984) provision should be reviewed. He also opined that the shear perimeter should be increased by using large columns and column capitals, if the punching shear capacity is in doubt.

Punching shear tests of geometrically similar reinforced concrete slabs of different sizes have been carried out by Bazant and Coa (1987). They have summarized that the punching shear failure of slab without stirrup is not plastic but brittle. They have found that larger the slab thickness, steeper the post-peak decline of the load deflection diagram, thus the punching shear behaviour of thin slab is closer to plasticity and that of thick slab is closer to linear elastic fracture mechanics.

McLean et al. (1990) concluded from their experimental work that punching shear strengths are much higher than those predicted by ACI 318 (1983). They cited some reasons for such higher strengths. The authors stated that the ACI Building Code allows only half of concrete contribution to the punching shear strength in a slab with shear reinforcement than it allows in a slab without shear reinforcement. From the test results, they have shown that the strength provided by the concrete is the same in the specimens with and without shear reinforcement. The researchers stated that the Code recognizes only the shear reinforcement activated by the assumed 45° degree failure surfaces. In the test specimens, the cracks were generally much flatter than 45° degree, thus activating substantially more shear reinforcement than is recognized by the Code. The study revealed that the relatively small span-to-thickness ratios of the specimens resulted in different internal cracking patterns than those of thinner slabs. This cracking was indicative of development of internal compression struts similar to those observed in deep beams. They also argued with the Code specified upper limits on the punching shear strength in a slab, regardless of the amount of shear reinforcement provided.

Regan and Jorabi (1988) have shown that analysis using current Code provision and making separate calculations of full width shear strength and punching shear are inappropriate. They proposed that design checks should be based on nominal shear stresses obtained as the sum of stresses arising from two components of load bearing action. The first is a symmetrical spreading of concentrated load and the second is the spanning of the slab carrying the spread load between supports.

Rankin and Long (1987a,1987b) from their experiment recognized the importance of the flexure and shear modes of punching failure to produce more consistent and economic design procedure. They have drawn out that the punching strength of full panel specimen is significantly greater than that of equivalent conventional slab, for the effect of compressive membrane action in the full panel specimen gives significantly better correlation with test result than present Code method and other procedures.

From the above discussion, it can be concluded that the present punching shear strength provision on different Codes should either be changed or modified or further

experimental investigations may be conducted in an effort to understand the punching behaviour of slab systems satisfactorily.

1.3 OBJECTIVE OF THE STUDY

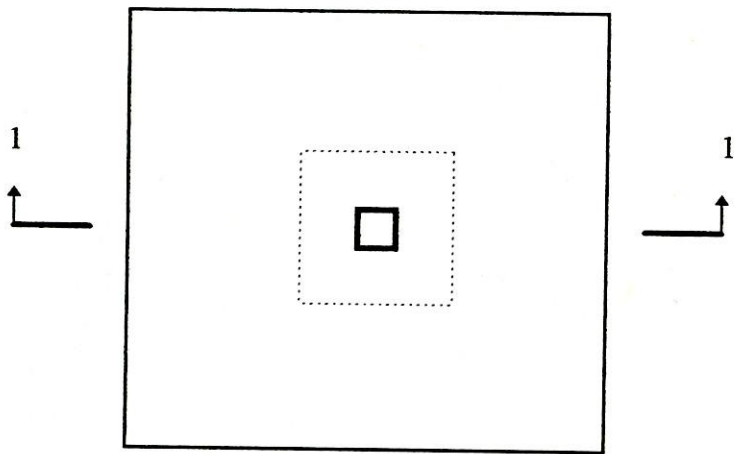
The objectives of this research work are as follows :

- i) To study the punching shear capacity of slabs
- ii) To study the effects of edge restraint on the punching shear strength of concrete.
- iii) To find out the effect of reinforcement ratio on the punching shear strength of concrete.
- iv) To study the effect of slab thickness on the punching shear strength.
- v) To study the crack patterns.
- vi) To compare the test results with various Code provisions.

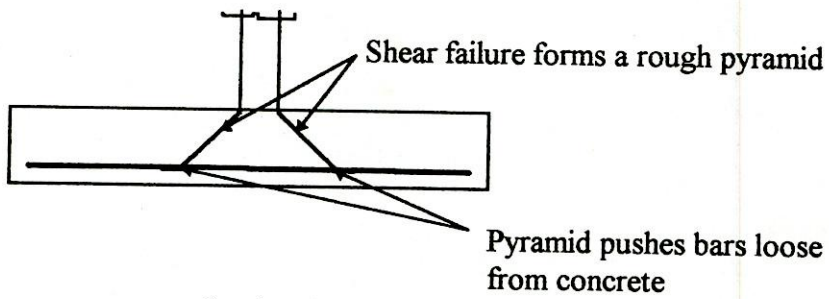
1.4 METHODOLOGY

When a two-way slab is heavily loaded with a concentrated load or where a column rests on a two-way footing, diagonal tension cracks form that encircle the load or column. These cracks are not visible, except as flexural cracks. Such cracks extend into compression area of the slab and encounter resistant resistance near the load similar to the shear-compression condition. The slab or footing continue to take load and finally fails around and against the load or column, punching out a pyramid of concrete as indicated in *Figure 1.1*. Diagonal cracks do not form further out from the load or column because of rapid increase in the failure perimeter. The initial diagonal cracks thus proceed to failure in punching shear type of failure directly around the load.

In compromising between initial cracking and the final punching shear condition at failure for different ratios between column (or load) dimension and footing (or slab) thickness, different Codes recommended a single punching shear strength calculation at



Plan



Section 1-1

Figure 1.1 A square column tends to shear out a pyramid from a footing or slab.

a pseudocritical distance from the column face or edge of the load and American Code (ACI 318-95), Canadian Code (CAN3-23-3-M84), European Code (CEB-FIP), Bangladesh National Building Code recommend this strength calculation at a distance of $d/2$ from the column face or edge of the load.

In the present case, an extensive experimental study have been conducted on slabs subjected to concentrated loading to failure. These slabs had variable edge restraint and variations in slab thickness, span length and reinforcement ratio. The details of all the slab specimens tested along with punching shear provisions of various Codes are given in Chapter Two. Materials used in this experimental programme as well as casting procedure are given in Chapter Three.

The test samples were designed to simulate continuous slab construction. Each slab was subjected to concentrated loading at the geometrical center using a universal testing machine. The details of test programme, testing set-up, test results are described in Chapter Four. Again, the test results obtained from this study have been analyzed and critically discussed in Chapter Five. The findings of the present study have been summarized in Chapter Six as conclusions. In this chapter recommendations for the future course of study have also been incorporated.

Some information pertaining to the details of the specimens tested, calculations of design strength as predicted by various Codes, experimental results, movement of slabs, etc. have been incorporated in Appendices A - E, for ready reference.

CHAPTER TWO

CODE PROVISIONS AND SPECIMEN DETAILS

2.1 INTRODUCTION

A total of 16 slabs have been tested in an effort to ascertain the influence of the degree of boundary restraint (provided by edge beams of various dimensions), percentage of steel reinforcement and span-to-depth ratio of slab specimens on their structural behaviour and punching load carrying capacity. The Code specified strengths of the specimens were calculated in accordance with the American (ACI 318, 1995), British (BS 8110, 1985), Canadian (CAN3-23.3-M84, 1984), European (CEB-FIP, 1978) and Bangladesh (BNBC, 1993) Codes.

2.2 CODE PROVISIONS

For the design of flat plates, flat slabs, bridge decks and column footings punching shear strength of concrete in the vicinity of columns, concentrated loads or reactions is one of the design criterion which governs the design. Thus, the critical shear section for this type of shear should be located so as the perimeter of critical section is a minimum, but need not approach closer than a certain distance from edge or corners of columns, concentrated load or reaction areas. Different Code provisions provide the location of this critical section differently. But for all the Codes, when this is done, the shear strength is taken almost independent of the column size, slab depth, span-to-depth ratio and edge restraint.

2.2.1 American (ACI 318,1995) Code provision

According to ACI 318 (1995) Code provision, the critical section for shear in slabs subjected to bending in two directions follow the perimeter (b_0) located at a distance $d/2$ from the periphery of the concentrated load. According to this Code, for non-

prestressed slabs and footing, nominal punching shear strength provided by concrete (V_c in pounds or Newtons) shall be smallest of the following three equations,

$$V_c = (2 + 4 / \beta_c) \sqrt{f'_c} b_0 d \quad (\text{FPS unit}) \quad (2.1a)$$

$$V_c = (1 + 2 / \beta_c) \sqrt{f'_c} b_0 d / 6 \quad (\text{SI unit}) \quad (2.1b)$$

$$V_c = (2 + a_s d / b_0) \sqrt{f'_c} b_0 d \quad (\text{FPS unit}) \quad (2.2a)$$

$$V_c = (1 + 0.5 a_s d / b_0) \sqrt{f'_c} b_0 d / 6 \quad (\text{SI unit}) \quad (2.2b)$$

$$V_c = 4 \sqrt{f'_c} b_0 d \quad (\text{FPS unit}) \quad (2.3a)$$

$$V_c = 0.33 \sqrt{f'_c} b_0 d \quad (\text{SI unit}) \quad (2.3b)$$

Here,

β_c = Ratio of long side to short side of concentrated load or reaction area.

f'_c = Uniaxial cylinder (compressive) strength of concrete in MPa or psi.

b_0 = Perimeter of critical section of slab or footing in millimeter or inch.

d = Effective depth (Distance from extreme compression fiber to the centroid of longitudinal tension reinforcement) in millimeter or inch.

a_s = 40 for interior column, 30 for edge column, 20 for corner column

2.2.2 British (BS 8110, 1985) Code provision

According to BS 8110 (1985) Code the b_0 is calculated at a distance of $1.5d$ from the edge of column and the punching shear strength of concrete is given by the following equation,

$$V_p = 0.79 \sqrt[3]{100\rho} \sqrt[3]{f_{cu} / 25} \sqrt[4]{400 / d} [4(c + 3d)] d \quad (2.4)$$

Where,

$\rho \leq 3.0$ percent, $400/d \geq 1.0$ and $f_{cu} \leq 40$ MPa

Here,

V_p = Punching shear strength in Newtons (N).

ρ = Reinforcement ratio in percentage.

f_{cu} = Uniaxial cube (compressive) strength of concrete in MPa.

c = Length or width of column or loaded area in millimeter (mm).

d = Effective depth (Distance from extreme compression fiber to centroid of longitudinal tension reinforcement) in millimeter (mm).

2.2.3 Canadian (CAN3-A23.3-M84, 1984) Code provision

According to CAN3-A23.3-M84 (1984) Code, the critical section for punching shear in slabs the perimeter (b_0) located at a distance $d/2$ from the periphery of the concentrated load. The punching shear strength provided by the concrete is given by the following equation,

$$V_p = 0.4 \sqrt{f'_c} b_0 d \quad (2.5)$$

Here,

V_p = Punching shear strength provided by concrete in Newtons (N).

f'_c = Uniaxial cylinder (compressive) strength of concrete in MPa

b_0 = Perimeter of critical section of slab or footing in millimeter (mm).

d = Effective depth (Distance from extreme compression fiber to centroid of longitudinal tension reinforcement) in millimeter (mm).

2.2.4 European (CEB-FIP, 1978) Code provision

According to CEB-FIP (1978) Code, the critical section for punching shear follows the perimeter (b_0) located at a distance $d/2$ from the periphery of the concentrated load. The punching shear strength is given by the following equation,

$$V_p = v_c b_0 d \quad (2.6)$$

Where,

$$v_c = 1.6 \tau_{rd} k (1 + \rho/2)$$

$$\tau_{rd} = 0.075 (f'_c)^{2/3}$$

$$k = (1.6 - d/1000) \geq 1.0$$

$$\rho \leq 0.8 \text{ percent}$$

Here,

V_p = Punching shear strength in Newtons (N).

f'_c = Uniaxial cylinder (compressive) strength of concrete in MPa.

ρ = Reinforcement ratio in percentage.

b_0 = Perimeter of critical section of slab or footing in millimeter (mm).

d = Effective depth (Distance from extreme compression fiber to centroid of longitudinal tension reinforcement) in millimeter (mm).

2.2.5 Bangladesh (BNBC, 1993) Code provision

According to this Code, for non-prestressed slabs and footing, the critical section for shear in slabs subjected to bending in two directions follow the perimeter (b_0) located at a distance $d/2$ from the periphery of the concentrated load. According to this Code, for non-prestressed slabs and footing, nominal punching shear strength provided by concrete (V_c in Newtons) shall be smallest of the following three equations,

$$V_c = 0.17(1 + 2 / \beta_c) \sqrt{f'_c} b_0 d \quad (2.7)$$

$$V_c = 0.17(1 + a_s d / b_0) \sqrt{f'_c} b_0 d \quad (2.8)$$

$$V_c = 0.33 \sqrt{f'_c} b_0 d \quad (2.9)$$

Here,

β_c = Ratio of long side to short side of concentrated load or reaction area.

f'_c = Uniaxial cylinder (compressive) strength of concrete in MPa.

b_0 = Perimeter of critical section of slab or footing in millimeter.

d = Effective depth (Distance from extreme compression fiber to centroid of longitudinal tension reinforcement) in millimeter.

a_s = 20 for interior column, 15 for edge column, 10 for corner column.

It is to be noted that the provisions of punching shear strength of BNBC (1993) Code is very much akin to ACI 318 (1995) and, thus, during the course of comparing experimental results with various Code provisions reference will be made only to ACI 318 (1995) Code.

2.2.6 Summary of Code provisions

The punching shear provisions of various Codes are summarized in *Table 2.1*. The meaning of variables used in this table have already been explained earlier.

Table 2.1 Summary of Various Code Provisions Related to Punching Shear Strength of Concrete.

Serial no.	Codes	Used equations
1.	ACI 318 (1995)	$V_c = (2 + 4 / \beta_c) \sqrt{f'_c} b_0 d \quad (\text{FPS unit}) \quad (2.1a)$ $V_c = (1 + 2 / \beta_c) \sqrt{f'_c} b_0 d / 6 \quad (\text{SI unit}) \quad (2.1b)$ $V_c = (2 + a_s d / b_0) \sqrt{f'_c} b_0 d \quad (\text{FPS unit}) \quad (2.2a)$ $V_c = (1 + 0.5 a_s d / b_0) \sqrt{f'_c} b_0 d / 6 \quad (\text{SI unit}) \quad (2.2b)$ $V_c = 4 \sqrt{f'_c} b_0 d \quad (\text{FPS unit}) \quad (2.3a)$ $V_c = 0.33 \sqrt{f'_c} b_0 d \quad (\text{SI unit}) \quad (2.3b)$ <p>V_c (in pounds or Newtons) shall be smallest of the above values. Where, $b_0 = 4(c+d)$</p>
2.	BS 8110 (1985)	$V_p = 0.79 \sqrt[3]{100\rho} \sqrt[3]{f_{cu}} / 25 \sqrt[4]{400/d} [4(c+3d)]d \quad (2.4)$ <p>Where, $\rho \leq 3.0$ percent, $400/d \geq 1.0$ and $f_{cu} \leq 40$ MPa</p>
3.	CAN3-A23.3-M84 (1984)	$V_p = 0.4 \sqrt{f'_c} b_0 d \quad (2.5)$ <p>Where, $b_0 = 4(c+d)$</p>
4.	CEB-FIP (1978)	$V_p = v_c b_0 d \quad (2.6)$ <p>Where, $v_c = 1.6 \tau_{rd} k (1 + \rho/2)$ $\tau_{rd} = 0.075 (f'_c)^{2/3}$ $k = (1.6 - d/1000) \geq 1.0$ $\rho \leq 0.8 \text{ percent}$ $b_0 = 4(c+d)$ </p>
5.	BNBC (1993)	$V_c = 0.17(1 + 2 / \beta_c) \sqrt{f'_c} b_0 d \quad (2.7)$ $V_c = 0.17(1 + a_s d / b_0) \sqrt{f'_c} b_0 d \quad (2.8)$ $V_c = 0.33 \sqrt{f'_c} b_0 d \quad (2.9)$ <p>V_c (in Newton) will be smallest of equations (2.7), (2.8) and (2.9). Where, $b_0 = 4(c+d)$</p>

2.3 SPECIMEN DETAILS

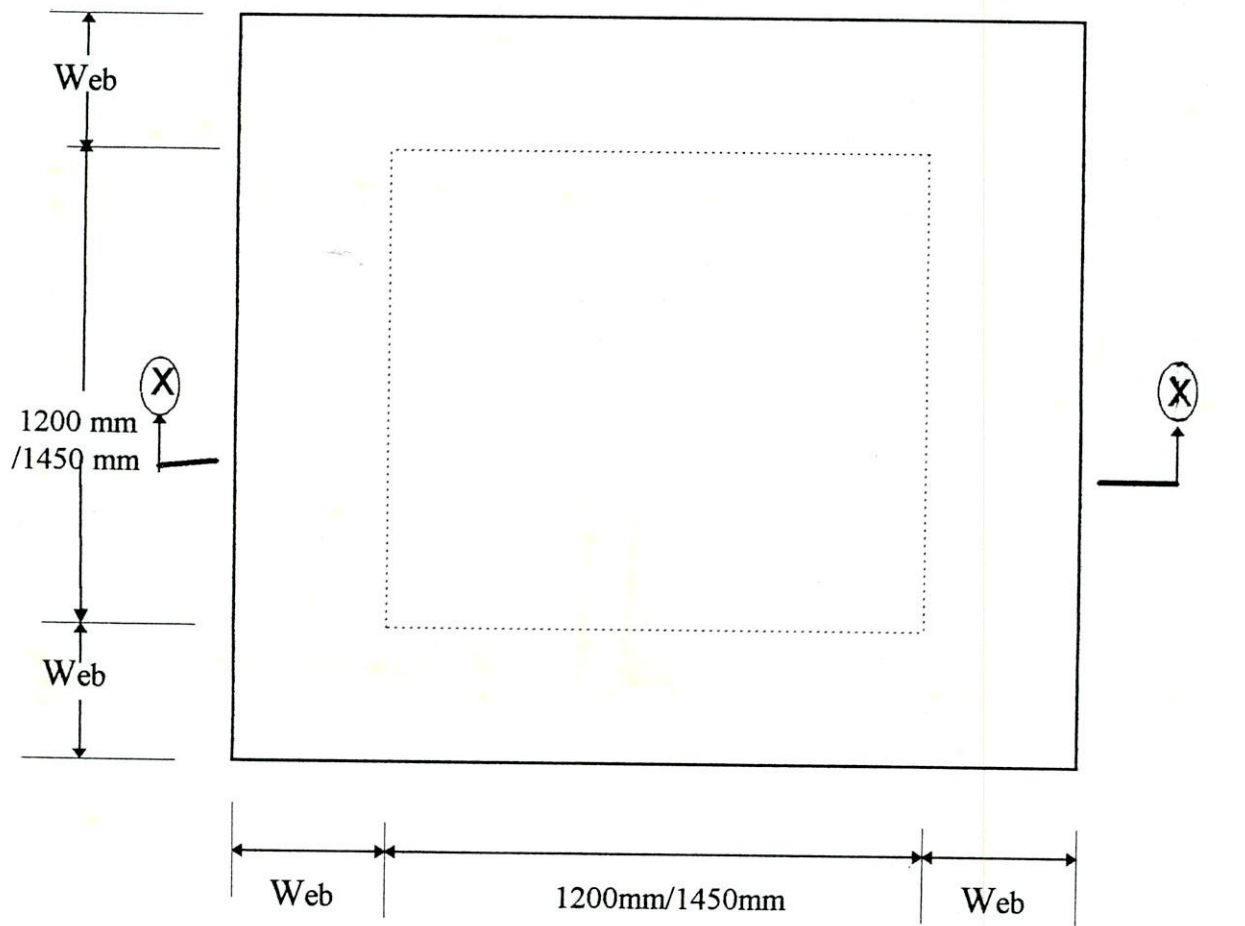
2.3.1 General

Several approximately one-fifth scale square reinforced concrete slab specimens have been constructed and tested in this study. Thirteen of these slabs had edge restraints in the form of edge beam, whereas other three samples were plain normal slabs having no edge beams. Width of edge beam, slab thickness and reinforcement ratio were the variable elements for different samples having one or more than one variability. The main reasons for casting several slabs by varying parameters was to compare the slab samples with one another and also to compare the results with different Code of predictions. Details of the slab samples can be gathered from *Figure 2.1* and *Table 2.2*. Whereas reinforcement details of all the model specimens can be seen in *Figure 2.2*, the relevant detailed sketches of plan, section and reinforcement of all the slab samples are given in *Appendix A*.

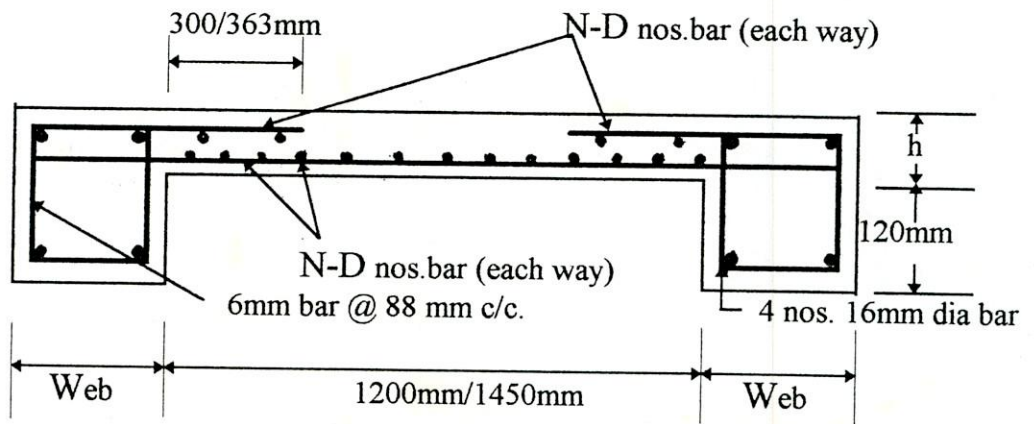
Table 2.2 Details of Reinforced Concrete Slab Specimens

SLAB	Width of edge beam (Web)	Slab thickness (h)	Reinforcement ratio (ρ)	Main bars in each direction N-D	Extra top bars in each direction N-D	Edge beam reinforcement
	mm	mm	%	no.-mm ϕ	no.-mm ϕ	no.-mm ϕ
SLAB1	245	80	0.5	15-6	15-6	4-16
SLAB2	245	80	1.0	30-6	30-6	4-16
SLAB3	245	80	1.5	16-10	16-10	4-16
SLAB4	245	60	0.5	11-6	11-6	4-16
SLAB5	245	60	1.0	22-6	22-6	4-16
SLAB6	245	60	1.5	33-6	33-6	4-16
SLAB7	175	80	1.0	30-6	30-6	4-16
SLAB8	175	60	0.5	11-6	11-6	4-16
SLAB9	175	60	1.0	22-6	22-6	4-16
SLAB10	105	80	1.0	30-6	30-6	4-16
SLAB11	105	60	0.5	11-6	11-6	4-16
SLAB12	105	60	1.0	22-6	22-6	4-16
SLAB13	0	80	1.0	30-6	30-6	*3-16
SLAB14	0	60	0.5	11-6	11-6	*3-16
SLAB15	0	60	1.0	22-6	22-6	*3-16
SLAB 16	340	60	1.0	26-6	26-6	4-16

* These reinforcements were provided at the extended bottom section of slab.
 All stirrups for edge beam were 6 mm ϕ @ 88 mm c/c.
 For SLAB1 to SLAB15, span=1200 mm and for SLAB16, span=1450 mm



PLAN



SECTION X -- X

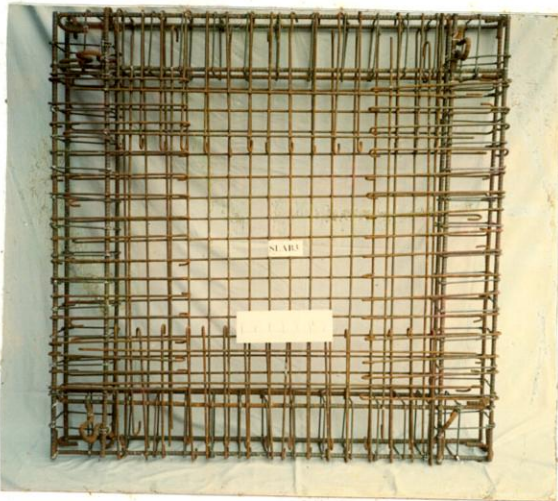
Figure 2.1 Dimension and reinforcement details of model slabs.



(a)



(b)



(c)



(d)

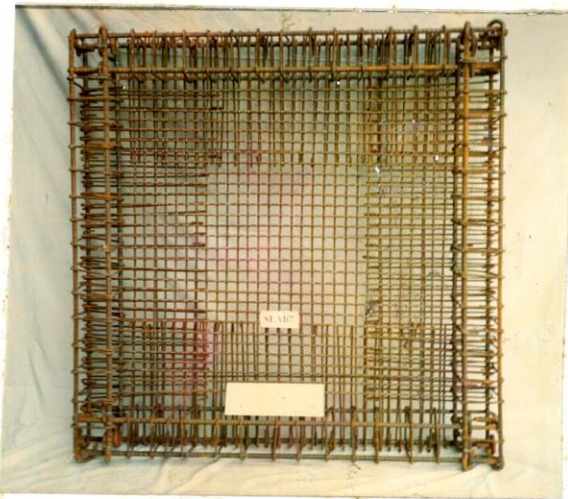
Figure 2.2A Reinforcement details of (a) SLAB1, (b) SLAB2, (c) SLAB3 and (d) SLAB4



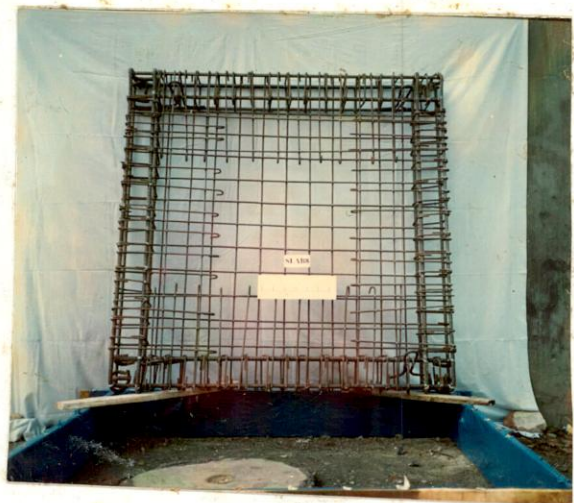
(a)



(b)

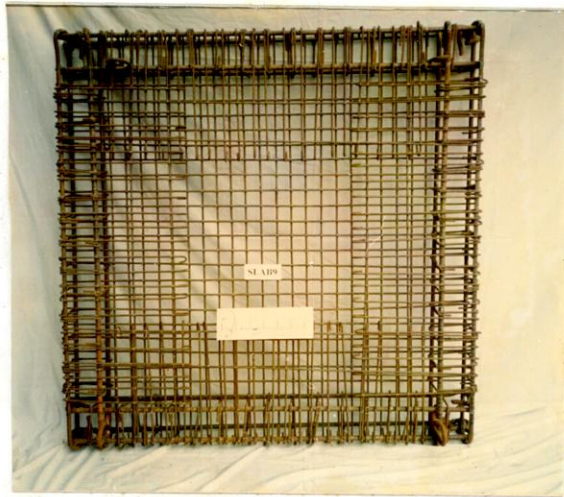


(c)

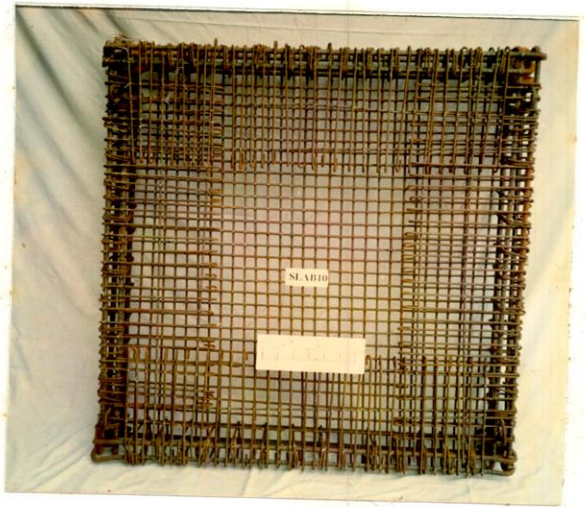


(d)

Figure 2.2B Reinforcement details of (a) SLAB5, (b) SLAB6, (c) SLAB7 and (d) SLAB8



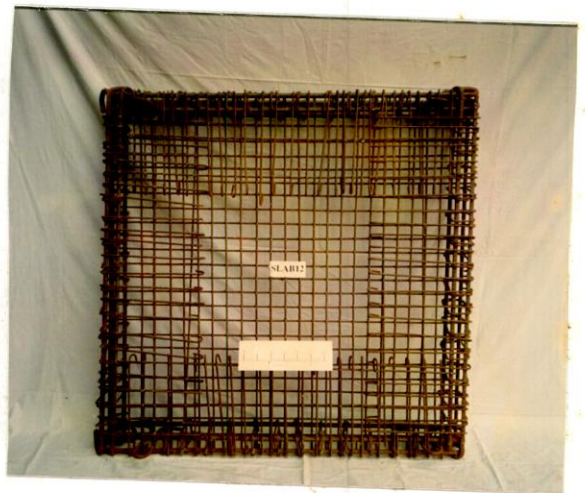
(a)



(b)

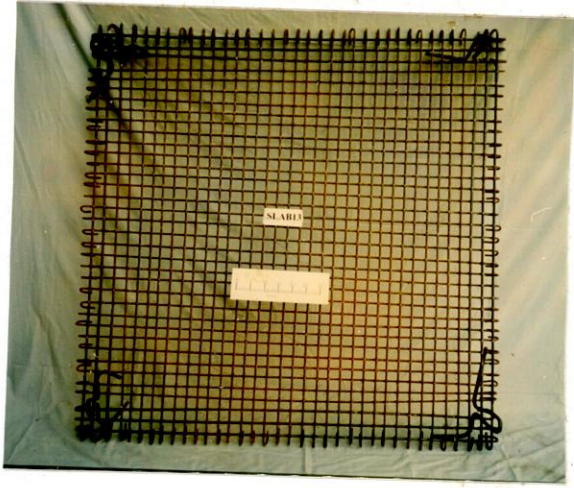


(c)



(d)

Figure 2.2C Reinforcement details of (a) SLAB9, (b) SLAB10, (c) SLAB11 and (d) SLAB12



(a)



(b)



(c)

Figure 2.2D Reinforcement details of (a) SLAB13, (b) SLAB14 and (c) SLAB15

2.3.2 Major variables of specimens

A total of 15 square reinforced concrete slab specimens with a clear span of 1200 mm and a 16th one with a clear span of 1450 mm were constructed and tested. The major variable of all specimens were as follows :

A. Degree of edge restraint

The experimental model slabs with edge restraints consist of a typically isolated slab-beam panel system, and the slab panel was supported and restrained on all four sides by edge beams. The edge beams were integrally connected with the slab, and the strength ratio of the beam to slab was such that the beams remain elastic until failure of the slab.

The different degrees of edge restraint imposed at the slab (SLAB1-SLAB15) surrounds were provided by having three different values of rigidity of the edge beams and the beam widths were 245 mm, 175 mm and 105 mm. For the slabs having no edge restraint in the form of beams (SLAB13, SLAB14 and SLAB15), slab thickness were 80 mm and 60 mm and reinforcement ratio (ρ) were 0.5 and 1.0 percent. During testing, although these slabs were provided with supports on all the four sides, absence of integrally connected edge beams allowed them to rotate at the sides.

The edge beams have imposed torsional rigidity to the slab-beam system. For the present study, the torsional rigidity (C) of various edge beams have been calculated. The torsional rigidity for SLAB1 to SLAB3= 2.36×10^8 mm⁴, for SLAB4 to SLAB6= 1.32×10^8 mm⁴, for SLAB7= 1.72×10^8 mm⁴, for SLAB8 and SLAB9= 1.31×10^8 mm⁴, for SLAB10= 0.64×10^8 mm⁴, for SLAB11 and SLAB12= 0.50×10^8 mm⁴, for SLAB13= 0.21×10^8 mm⁴, for SLAB14 and SLAB15= 0.10×10^8 mm⁴. The relevant calculations for torsional rigidity are given in *Appendix B*.

In *Table 2.3*, all the slab samples tested have been grouped on the basis of their edge beam size.

B. Span-to-depth ratio

Different span-to-depth ratios were achieved by varying slab thickness of the test specimens. In slabs SLAB1-SLAB15, the thickness was kept at 80 mm and 60 mm, giving ratios of 15 and 20, respectively. For SLAB16, the slab thickness was chosen to be 60 mm, ensuring span-to-depth ratio being 24.17.

The slab samples SLAB1, SLAB2, SLAB3, SLAB7, SLAB10 and SLAB13 had 80 mm thick with a span-to-depth ratio of 15. On the other hand, SLAB4, SLAB5, SLAB6, SLAB8, SLAB9, SLAB11, SLAB12, SLAB14 and SLAB15 had 60 mm thick slab with a span-to-depth ratio is 20. Again, SLAB16, which had a clear span of 1450 mm in contrast to the other slabs of 1200 mm span, had a 60 mm thick slab with a span-to-depth ratio equal to 24.17.

C. Reinforcement ratio (ρ)

Three level of steel reinforcement ratios for slab panels, 0.5 percent, 1.0 percent and 1.5 percent in both directions were selected. The details are shown in *Table 2.4*.

2.4 DESIGN STRENGTH OF MODEL SLABS

Concrete slabs are relatively thin, flat structural element whose main function is to transmit loads normal to their plane. In order to model a slab and its support faithfully, and to interpret the results of tests conducted on a model slabs, it is essential to understand how a slab behaves in reality so that actual field condition can be mimicked while preparing the scaled down model specimens and testing them later in the laboratory. Here, the edge beams at the four sides of slab models acts as the restraining element of slabs - a very limited effort to simulate continuity of slab edges. Again, for the slab models having no edge restraint, the edge beams were omitted, in those cases, however, external supports were placed at all the edges during testing.

However, since the present-day Codes do not acknowledge the possible role of edge restraint/continuity on the design strength, the punching shear strength of slab samples were evaluated using recommended formula of different Code provisions as stated earlier in the Section 2.2, taking the uniaxial (cylinder) compressive strength of concrete equals to 36 MPa ($f'_c=36$ MPa), which was found from trial mixes. On the other hand, clear cover of concrete was assumed to 10 mm, which was maintained during the casting of the slabs. Design strength of all the slab samples are shown in *Table 2.5*, and the relevant design calculations of all the slabs, for various Codes consideration, are available in the *Appendix B*.

Table 2.3 Slab Grouping Based on Size of Edge Restraint

Slab Group	Width of edge beam	SLABS
GROUP 1	245 mm	SLAB1, SLAB2, SLAB3, SLAB4, SLAB5, SLAB6
GROUP 2	175 mm	SLAB7, SLAB8 and SLAB9
GROUP 3	105 mm	SLAB10, SLAB11 and SLAB12
GROUP 4	0 mm	SLAB13, SLAB14 and SLAB15
GROUP 5	340 mm	SLAB16

Table 2.4 Slab Grouping Based on Reinforcement Ratios.

Reinforcement ratio in percent	Slab samples
0.50	SLAB1, SLAB4, SLAB8, SLAB11 and SLAB14
1.00	SLAB2, SLAB5, SLAB7, SLAB9, SLAB10, SLAB12, SLAB13, SLAB15 and SLAB16
1.50	SLAB3 and SLAB6

Table 2.5 Punching Shear Capacity of all the Slabs Tested

Slab	Design load in kN (Considering $f'_c = 36$ MPa)							
	ACI 318-89	BS 8110-85			CAN3- A23.3- 84	CEB-FIP		
		$\rho=0.5\%$	$\rho=1.0\%$	$\rho=1.5\%$		$\rho=0.5\%$	$\rho=1.0\%$	$\rho=1.5\%$
SLAB1	105.34	104.77	---	---	127.68	133.12	---	---
SLAB2	105.34	---	132.00	---	127.68	---	149.09	---
SLAB3	105.34	---	---	151.10	127.68	---	---	149.09
SLAB4	67.32	66.60	---	---	81.60	86.19	---	---
SLAB5	67.32	---	83.91	---	81.60	---	96.53	---
SLAB6	67.32	---	---	96.05	81.60	---	---	96.53
SLAB7	105.34	---	132.00	---	127.68	---	149.09	---
SLAB8	67.32	66.60	---	---	81.60	86.19	---	---
SLAB9	67.32	---	83.91	---	81.60	---	96.53	---
SLAB10	105.34	---	132.00	---	127.68	---	149.09	---
SLAB11	67.32	66.60	---	---	81.60	86.19	---	---
SLAB12	67.32	---	83.91	---	81.60	---	96.53	---
SLAB13	105.34	---	132.00	---	127.68	---	149.09	---
SLAB14	67.32	66.60	---	---	81.60	86.19	---	---
SLAB15	67.32	---	83.91	---	81.60	---	96.53	---
SLAB16	67.32	---	83.91	---	81.60	---	96.53	---

CHAPTER THREE

MATERIALS USED AND CASTING PROCEDURE

3.1 GENERAL

The concrete used in the specimens consisted of ordinary Portland cement, natural sand and coarse stone aggregate with maximum size 10 mm. The water cement ratio for concrete was 0.45. Both 6 mm and 10 mm diameter plain steel bars having an average yield strength of 421 MPa were used in the slab panels and stirrup of edge beams. Flexural reinforcement in the edge beam were provided by 16 mm diameter deformed bar with an average yield strength 414 MPa. An average cylinder compressive strength of concrete of 36 MPa at the age of 28 days was obtained from trial mixes.

3.2 PORTLAND CEMENT

The requirement of the cement is given below :

- a) All cement used for the casting of model slabs and cylinder were ordinary Portland cement conforming to the requirements of the ASTM.
- b) All types of casting were performed with same brand of cement. The accepted brand of cement was selected from the trial mix proportion.
- c) All cement for casting purposes were delivered from the same shipment and stored of the laboratory. The storage cement was carefully protected against moisture and exposure to air.

3.3 AGGREGATES

3.3.1 General

Aggregates comprises about 85% volume of concrete. Aggregate used for concrete were chemically inert, strong, hard, durable, limited porosity and free from adverse

coating clay lumps, coal, coal residues and organic or other impurities that may cause corrosion of the reinforcement or may impair the strength or durability of the concrete.

3.3.2 Fine Aggregates

Fine aggregates are natural sand or sand derived by crushing gravel or stone and free from coagulated lump, alkaline or acidic reaction and other deleterious matters. Sand is normally dredged from river beds and stream in the dry season when the river bed is dry or when there is not much flow in the river. Under such situation along with the sand, decayed vegetable matter, humus organic matter and other impurities are likely to settle down. But if sand is dredged when there is a good flow of water from very deep bed, the organic matters are likely to get washed away at the time of dredging. Fine aggregates coming from tidal river or from pits near sea shore generally contains some percentage of silt. The contamination of aggregates by silt usually affects the setting properties and ultimate strength of concrete. Opinions are divided on the question whether the silts contained in aggregates would cause corrosion of reinforcement. But studies have indicated that the usual percentages of silt generally contained in the fine aggregates usually do not cause corrosion in any appreciable manner. However, it is a good practice to wash sand containing silt more than 3 percent.

Sylhet sand was used in this study as fine aggregate. Sylhet sand is available from the eastern part of the Bangladesh and is obtained from the bed of flowing river. The fineness modulus (F.M) of this aggregates was tested and found to be equal to 2.66.

3.3.3 Coarse Aggregates

Coarse aggregates used here were crushed stone, comprising of angular or rounded in shape and had granular or crystalline or smooth non powdery surface, free from friable, flaky and laminated pieces, mica and shale and all other materials which might be injurious to the concrete. The maximum size of coarse aggregate used in this study was 10 mm in an effort to minimize size effect in the model slabs.

3.4 WATER

Water is an important ingredient of concrete as it actively participates in the chemical reaction with cement. It has been estimated that on an average 23% of water by weight of cement is required for chemical reaction with Portland cement compound, which is known as bound water. A certain quantity of water is imbedded within the gel-pores. This water is known as gel water. It can be said that bound water and gel water are complimentary to each other. If the quantity of water is inadequate to fill up the gel-pores, the formations of gel itself will stop and if the formation of gel stops there is no question of gel pores being present. It has been further estimated that about 15 percent by weight of cement is required to fill up the gel pores. Therefore a total 38 percent of water by weight of cement is required for the complete chemical reactions and to occupy the space within gel-pores. Since quality of water usually affects the strength properties of hardened concrete, only pure water should be used for casting purpose. Suitability of water for curing of concrete is also a considerable factor. Water that contains impurities may cause staining and is objectionable for curing of concrete. The most common cause of staining is usually high concentration of iron or organic matter in the water. Water that contains more than 0.08 ppm of iron may be avoided for curing if the appearance of concrete is important. Similarly the use of sea water may also be avoided in such case. It is worth mentioning here that, in the present study, water used in casting of concrete and curing purposes were obtained from deep tube-well and this water was suitable for drinking purpose. No materials injurious to concrete can be expected to be available in the water used.

3.5 REINFORCEMENT

3.5.1 General

For reinforced concrete, in comparison to concrete, steel is a high strength material. The useful strength of ordinary reinforcing steels is used in tension as well as compression. On the other hand steel is a high costing material compared to concrete. It follows that the two materials are best used in combination if concrete is made to

resist the compressive stresses and the steel the tensile stresses. However, reinforcement steel is also used for resisting compressive forces primarily where it is desired to reduce the cross-sectional dimensions of compressive members. For most effective reinforcing action, it is essential that steel and concrete deform together, i.e. that there be a sufficiently strong bond between the two materials to ensure that no relative movements of the steel bar and the surrounding concrete occur. This bond is provided by the relatively large chemical adhesion which develops at the steel concrete interface by the natural roughness of the mill scale of hot rolled reinforcing bars.

For the present study, both 6 mm and 10 mm diameter plain steel bars having an average yield strength of 421 MPa were used in the slab panels and stirrup of edge beam. For all slabs other than SLAB3, main bar as well as extra top reinforcements were used by 6 mm diameter plain bar. Only for SLAB3, 10 mm diameter bars were used as slab reinforcement. Flexural reinforcement in the edge beam of all the slabs were provided by 16 mm diameter deformed bar with an average yield strength 414 MPa.

3.5.2 Fabrication of steel

All reinforcing steel was cut and bent cold, strictly in accordance with the drawing and firmly tied with 16 gauge G.I wires. Precast mortar blocks was used as spacers in forms to maintain required clearance between the reinforcement and the surface.

3.6 CONCRETE TRIAL MIX PROPORTIONING

Strength properties of concrete of a given proportion usually scatter from batch to batch. It is, thus, necessary to select a proportion which is expected to furnish an average strength greater than the design strength.

For the present study, a water-cement ratio 0.45 was selected and several small trial batches with varying amounts of cement contents as well as aggregates were produced to obtain the required strength. All the ingredients of trial mix proportions were

measured by the weight basis. Strength obtained from various trial mixes along with the mix proportions used are given in *Table 3.1*. Strength obtained from the trial mix no. 5, was used during the casting of actual slab samples in the laboratory. Actual strength of concrete of individual slab samples was determined on the day of testing individual slabs. Here, mix ratio for actual slabs were determined from 7-day cylinder strength for convenience. The 28-day strength for mix no. 5 was found to be 36 MPa.

Table 3.1 Trial mix Proportion and Strength of Concrete

Trial mix no.	Mix proportion by weight	Crushing Strength of Cylinder at the age of 7 days (MPa)	Average Strength of Concrete(Cylinder) at the age of 7 days (MPa)
1	1.00 : 2.50 : 3.25	19.40	19.03
		18.02	
		19.68	
2	1.00 : 2.75 : 3.15	18.30	17.24
		17.00	
		16.42	
3	1.00 : 2.00 : 2.00	26.34	23.70
		20.00	
		24.76	
4	1.00 : 2.00 : 2.50	19.14	19.62
		19.89	
		19.83	
5	1.00 : 1.50 : 2.50	30.45	29.80
		29.32	
		29.63	
Here, 7 days strength was considered for comparison purposes only. For all the trial mixes, w/c=0.45			

3.7 FORM WORK

The design and construction of the formwork was performed as per size and shape of the slab concerned along with its edge beams. The bottom surface of the form was composed of brick flat soling on the compacted soil. Above the brick flat soling, cement mortar with neat cement finishing was applied to make the surface flat and polythine was also given to make the surface fully leakproof. Formwork for the outer sides of the edge beams were constructed tightly by 38 mm thick wooden plank and were sufficiently anchored to prevent lateral movement of any part of the formwork system during concrete placement. The formwork at the bottom surface was not reused and all surfaces of the forms were properly cleaned before placing the concrete. The details of formwork and formwork system for this work is shown in *Figures 3.1 and 3.2*.

3.8 MIXING OF CONCRETE

The concrete ingredients of right proportions were mixed thoroughly in the mixing machine in its revolving condition. A commercial mixing machine of 0.35 cubic meter capacity was used for this purpose.

3.9 PLACING OF CONCRETE

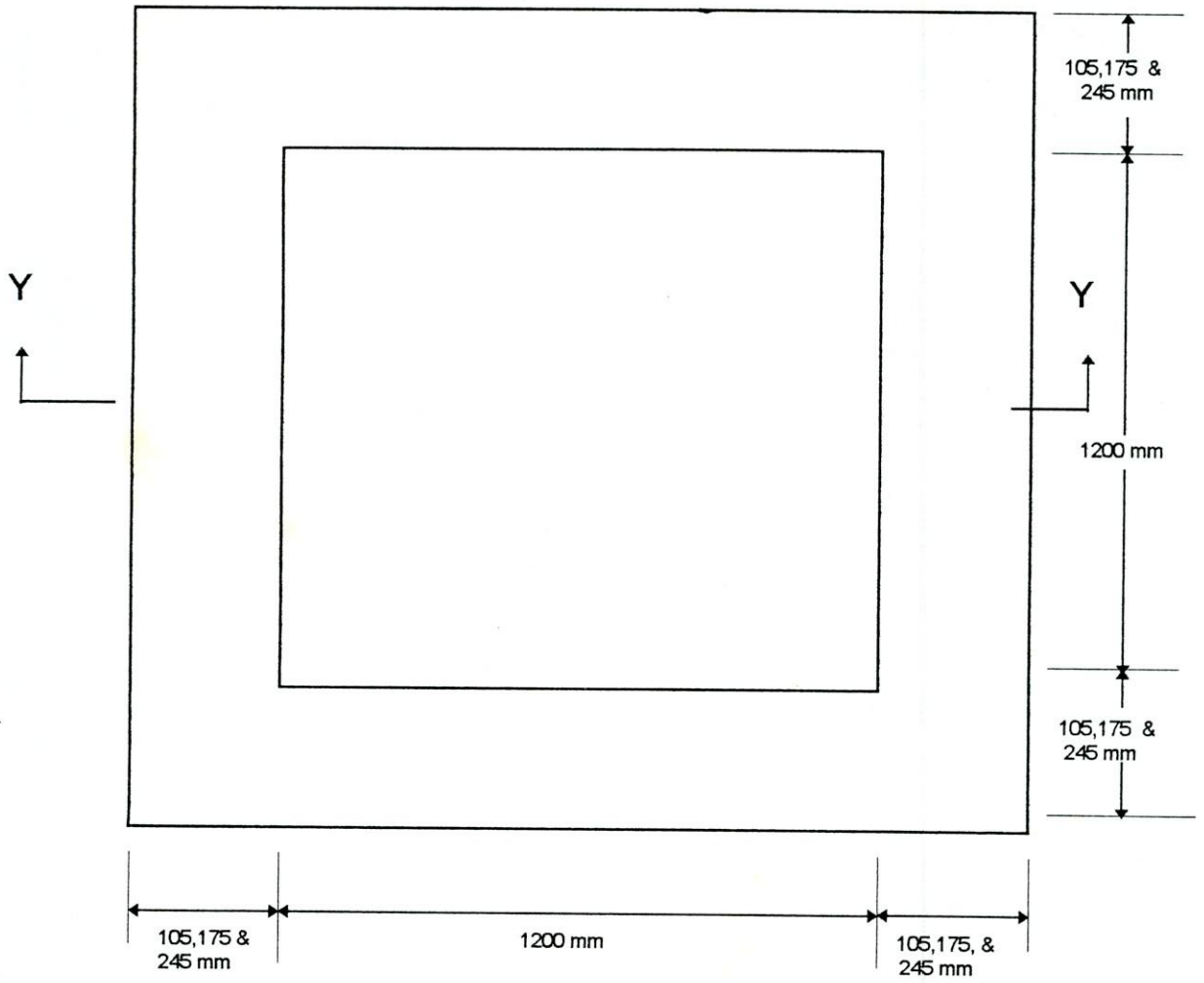
The method and equipment used for transporting concrete was such that concrete having the required composition and consistency was delivered to the work, without objectionable segregation or loss of slump. The concrete was deposited continuously in layers of appropriate thickness so that no concrete was deposited on concrete which has hardened sufficiently. After depositing, the concrete was thoroughly consolidated around reinforcement by rodding, spading and, of course, by using a electric vibrator.

3.10 CASTING OF CYLINDER

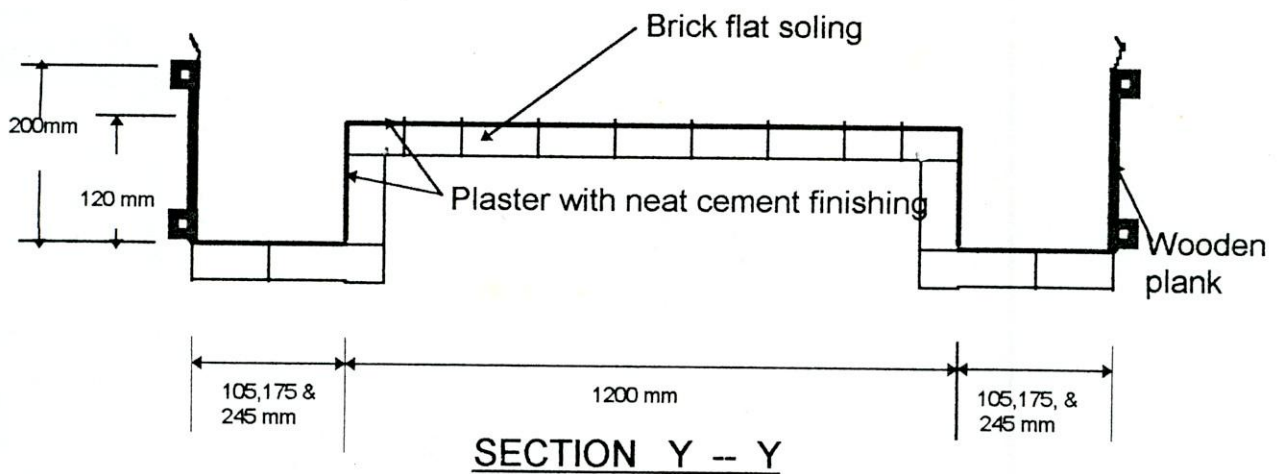
Two cylinders were taken for each type of slab during the casting of slab so that the ingredients as well as water/cement ratio of concrete of the cylinders and respective slab remain similar.

3.11 CURING

Concrete was cured with water and kept wet 28 consecutive days immediately following placement by covering it by water saturated material. Curing of the test cylinders were performed using the same process as adopted for slab curing. Water used for curing was met by the requirements of the specifications for water used for mixing concrete.



PLAN



SECTION Y -- Y

Figure 3.1 Details of typical formwork.



(a)



(b)

Figure 3.2 (a) Bottom portion of formwork system, (b) Reinforcement casing in the completed formwork.

CHAPTER FOUR

TESTING PROGRAMME

4.1 INTRODUCTION

The tests were designed to simulate conditions in actual structures. Each slab was subjected to concentrated loading at the geometric center using a universal testing machine. Layers of steel plate and steel blocks were used to help distribute the load from the universal testing machine to the test sample. During testing, corner sides of each sample was properly anchored. Loading was applied to specimen at an approximately constant rate up to the peak load, at the same time deflections were measured. Failure occurred abruptly in all specimens and loading was stopped after failure.

4.2 TESTING ARRANGEMENT

For SLAB1 to SLAB12 and SLAB16, each of the specimens was put on four separate reaction blocks as pedestals. The pedestals were 250mm x 250mm x 150mm in size. All the pedestals were constructed by using reinforced cement concrete with high percentage of reinforcement in them. The pedestals were supported by a pair of steel joist, which were clamped to the laboratory floor. To simulate continuous beam construction and prevent lifting of the other part of the specimen at the corners during testing, a channel was used at each of the corners, and securely anchoring them to the steel joist by threaded rods as shown in *Figure 4.1*.

For SLAB12 to SLAB15, each sample slab was put on a previously tested slab sample with edge beam which was turned up side down. The turned slab was supported by the pair of steel joist as clamped to the laboratory floor. To prevent lifting of any part of the specimen during testing, a channel was also used at each of the corners, and securely anchoring them to the steel joist by threaded rods as shown in *Appendix C*. This arrangement ensured vertical support of the plane slabs on its edges. Such vertical restraints were equivalent to similar slabs having their edges restrained.

It is worth mentioning here that the average weight of each of the specimens was 6.9 kN (705.19 kg) and it was extremely difficult even to move these slabs from the casting yard to the testing rig. *Figures C-1, C-2, C-3, C-4* of *Appendix C* show a sequence which was followed in order to move one of such specimens from the yard to the rig. The actual placement of each of the heavy slabs in the rig accurately in not so well equipped laboratory, thus, was quite a formidable task indeed. The weight of all slab samples are also given in the *Appendix C*.

4.3 TESTING PROCEDURE

4.3.1 Calibration of test rig

The test rig was calibrated twice, once at the beginning of the testing of the first slab and later on completion of the testing of all model slabs. The calibration was performed by applying load to a proving ring from the test rig. The proving ring was earlier calibrated at different temperature levels. Since, both the calibration exercises resulted in very similar relationship between the applied load and the actual load, an average of the two tests have been considered in the present study. In *Table C-2* of *Appendix C*, the actual load and monitored load are given.

4.3.2 Instrumentation

A test rig (consisting mainly of steel girder, hydraulic jack) was designed for the purpose of loading slabs of various sizes under loading arrangements to failure. A 300 kN capacity hydraulic jack was used for the application of punching load. The load from the jack was applied to the model slabs at their geometric center through a 20 mm thick steel plate of 120mm x 120mm size, simulating a concentrated load. The applied load was measured using an accurately calibrated load cell. Loading was applied to the specimens in increments of 8.90 kN upto 75.00 kN and than in the increments of 4.45 kN upto failure with measurements of deflections after each load increment loading. The testing set up is also shown in *Figure 4.1*.

Deformations were measured by a number of Linear Variable Displacement Transducers (LVDTs). The central slab deflection and vertical deflection of edge beam were measured to obtain deflection profiles of the slabs. There was one LVDT at the mid-span to measure the central slab deflection, one LVDT was placed at the middle span of one of the edge beams to measure the central vertical deflection of the edge beam and four LVDTs at the corner of edge beams to assess the performance of the supports.

At each load increment, the load was maintained constant for about 2 minutes in order to monitor the load, deformation response of the edge beam and mark the crack (if any). Once the applied load exceeded by about twice the load predicted load by ACI 318-95, the LVDT at the centre point of the slab was removed to avoid loss of the LVDT.

4.4 TEST RESULTS

4.4.1 General

All model slabs were not tested on the same day. All the models underwent punching type of failure with its inherent brittle characteristics. Most of the slab samples failed at a load much higher than what have been predicted by the Codes of practices. The cracking pattern of the top surface of all the slabs were very much localized and approximately had a size of 120mm x 120mm as shown in *Figure 4.2*. The cracking patterns of the bottom surface were more or less of same type for the same group of samples as grouped in *Table 2.3*. For the same group of specimens, cracking at the bottom surface of slabs having low percentage of reinforcement were more severe than those having higher percentages of steel. Again, it has been noticed that the surface area of cracked zone for the slabs having wider edge beams were more than those slabs having smaller edge beams. It has also been seen for all the slab samples, the deflection at the support was negligible pointing out to the fact that support fixity was ensured, albeit approximately, during the testing of the model slabs. The central deflection of all the slabs and deflection of the edge beams are accumulated in *Appendix D*.

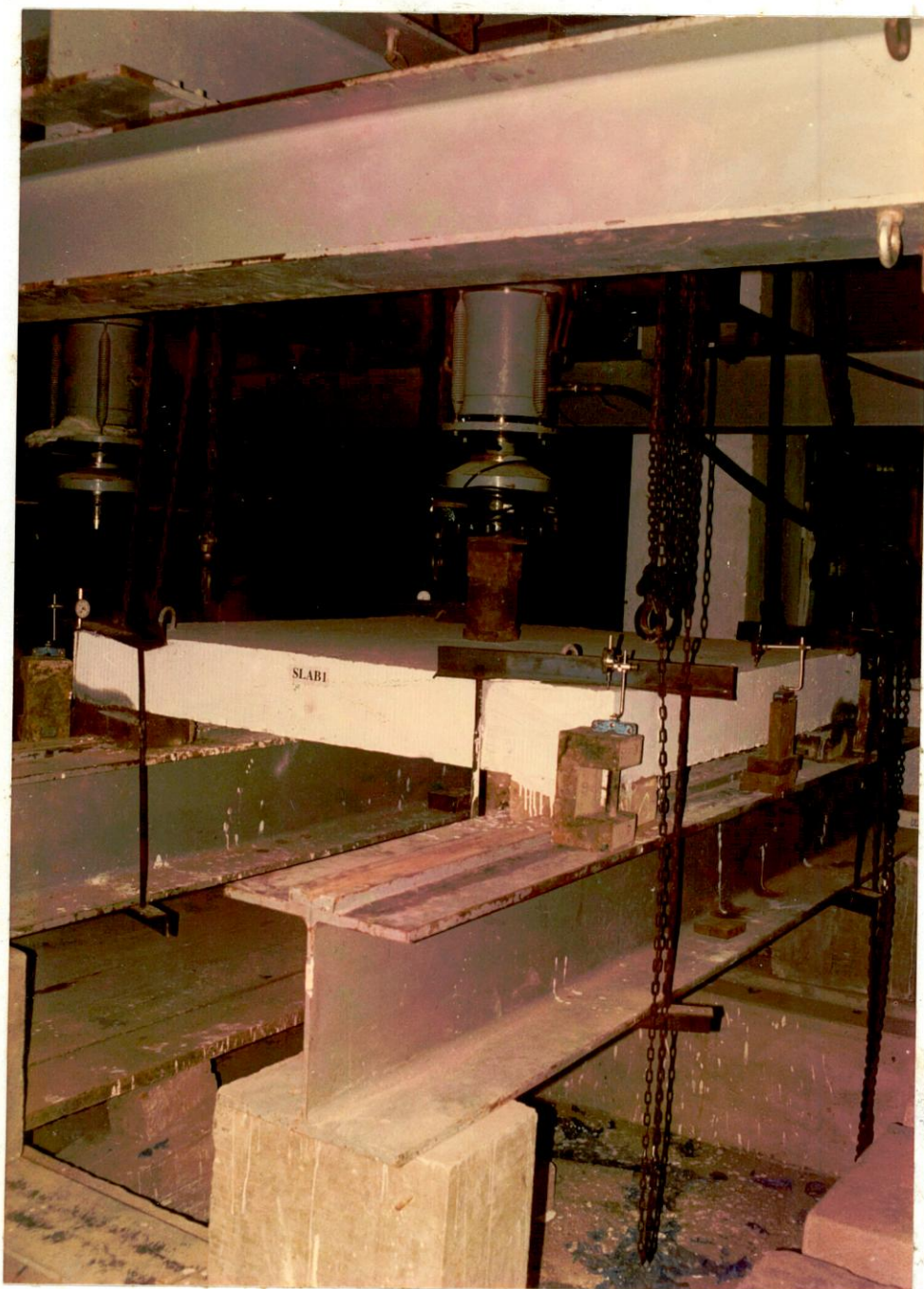


Figure 4.1 Test rig and testing set-up



Figure 4.2 Typical cracking pattern on the top surface of a model slab

4.4.2 Details of test results

I) SLAB1

SLAB1 was a 80 mm thick restrained slab with low percentage of reinforcement ($\rho=0.5$ percent). The predicted failure load for this slab in accordance with ACI 318-95, BS 8110-85, CAN3-A23.3-M84 and CEB-FIP-78 were 108.78 kN, 104.77 kN, 132.06 kN and 139.23 kN, respectively. During the test, the slab actually failed at a load of 225.16 kN. Thus the failure load has been found to be much higher than the loads predicted by all the above Codes.

In this slab, the first crack was visible at a load of 64.92 kN at the central portion of the bottom surface of slab. A few more cracks were formed in the adjacent regions at subsequent load steps. The cracking of the bottom surface propagated from the middle part of the slab towards the edge beam as the load increased. The number of cracks also increased with the increase of load. However, none of the cracks could reach the edge beam. Crack propagation from the central portion of the slab towards the supports of the edge beam were smaller. No cracks of the top surface of the slab and slab portion adjacent to edge beam were visible.

Due to safety reasons, the marking of crack propagation was not continued once the applied load reached a level around the Code predicted loads. The LVDT from the central portion was also removed. Thus the central deflection of the slab could not be measured after a load of 142.95 kN. At this level a central slab deflection of 4.93 mm was recorded.

After failure of the slab at a load of 225.16 kN, all the cracks at the bottom surface of the slab were marked. The cracking pattern at the bottom surface of the slab is shown in *Figure 4.3a*. From the cracking profile, it can be seen a regular deep boundary like cracking at the middle portion of slab, where spalling of concrete were also found. Some cracks crossed each other at the bottom surface of slab. The average uniaxial

compressive (cylinder) strength of concrete (f'_c) for this slab was found to be 38.51 MPa on the day of testing.

II) SLAB2

The slab thickness of this slab was 80 mm and this was also a restrained slab with moderate percentage of reinforcement ($\rho=1.0$ percent). The predicted failure load for this slab as per ACI 318-95, BS 8110-85, CAN3-A23.3-M84 and CEB-FIP-78 were 107.24 kN, 132.00 kN, 130.17 kN and 152.98 kN, respectively. The slab failed at a load of 242.09 kN which was, once again, much higher than the loads predicted by the Codes of practice.

Here, first crack was visible at a load of 75.00 kN at the bottom surface of the slab. The cracking pattern and propagation of cracking were similar to those of SLAB1. Number of cracks in the diagonal direction towards the edge beams for this slab was more in number than that of SLAB1. Once again, no cracks of the top surface of the slab and slab portion adjacent to edge beams were visible, before actual punching failure.

The cracks were no longer marked after the application of a load of 191.30 kN due to safety reason. Similarly the central deflection of the slab could not be measured after 191.30 kN load. The central deflection of slab measured at this level of load was 7.32 mm.

After failure of the slab at a load of 242.09 kN, all cracks at the bottom surface of the slab were marked. The cracking pattern of the bottom surface of the slab is shown in *Figure 4.3b*. It can be seen that no spalling of concrete after failure occurred in this slab. All cracks reached to the boundary line of cracking. The number of cracks of this slab were higher than SLAB1. The average uniaxial compressive (cylinder) strength of concrete (f'_c) for this slab was tested and found to be equal to 37.42 MPa on the same date of testing the slab.



(a)



(b)

Figure 4.3 Cracking pattern of bottom surface of (a) SLAB1 and (b) SLAB2

III) SLAB3

SLAB3 was a 80 mm thick restrained slab with high percentage of reinforcement ($\rho=1.5$ percent). The predicted failure load for this slab as per ACI 318-95, BS 8110-85, CAN3-A23.3-M84 and CEB-FIP-78 were 93.07 kN, 144.85 kN, 112.98 kN and 126.66 kN, respectively. During the test, the slab actually failed at a load of 142.95 kN.

In this slab, first crack was visible at a load of 57.44 kN at the bottom surface of slab. The cracking pattern and propagation of cracking were very much akin to SLAB1 and SLAB2. No cracks of the top surface of the slab and slab portion adjacent to edge beam were visible. Degree of cracking was, however, higher than those of SLAB1 and SLAB2.

Due to safety reasons, the cracks were no longer been marked after the load application exceeding to 133.27 kN. Again, the central deflection of the slab could not be measured after a load of 133.27 kN. At this level, central deflection of this slab was recorded to be 5.64 mm.

After failure of the slab at the load of 142.95 kN, all cracks at the bottom surface of the slab was marked and the cracking pattern of the bottom surface of this slab is shown in *Figure 4.4a*. From the cracking profile, it is seen that some cracks crossed one another. Here, spalling of concrete took place after failure. The average uniaxial compressive (cylinder) strength of concrete (f'_c) for this slab was found to be equal to 28.19 MPa on the same day of testing.

IV) SLAB4

SLAB4 was a 60 mm thick restrained slab with low percentage of reinforcement ($\rho=0.5$ percent). The predicted failure load for this slab as per ACI 318-95, BS 8110-85, CAN3-A23.3-M84 and CEB-FIP-78 were 69.28 kN, 66.60 kN, 84.10 kN and 89.73 kN, respectively. The slab failed at a load of 138.12 kN.

Here, first crack was visible at a load of 46.36 kN at the bottom surface of slab. A few more cracks were formed in the adjacent regions at subsequent load steps. The cracking of bottom surface were propagated from the middle span of the slab toward the edge beam with applied loading. The number of cracks were also increased with the increment of loading, however none of them could reach the edge beam. Crack propagation from the central position of slab along the direction to the support of edge beams were higher than those towards the middle section of edge beam. No cracks of the top surface of the slab and slab portion adjacent to edge beam were visible.

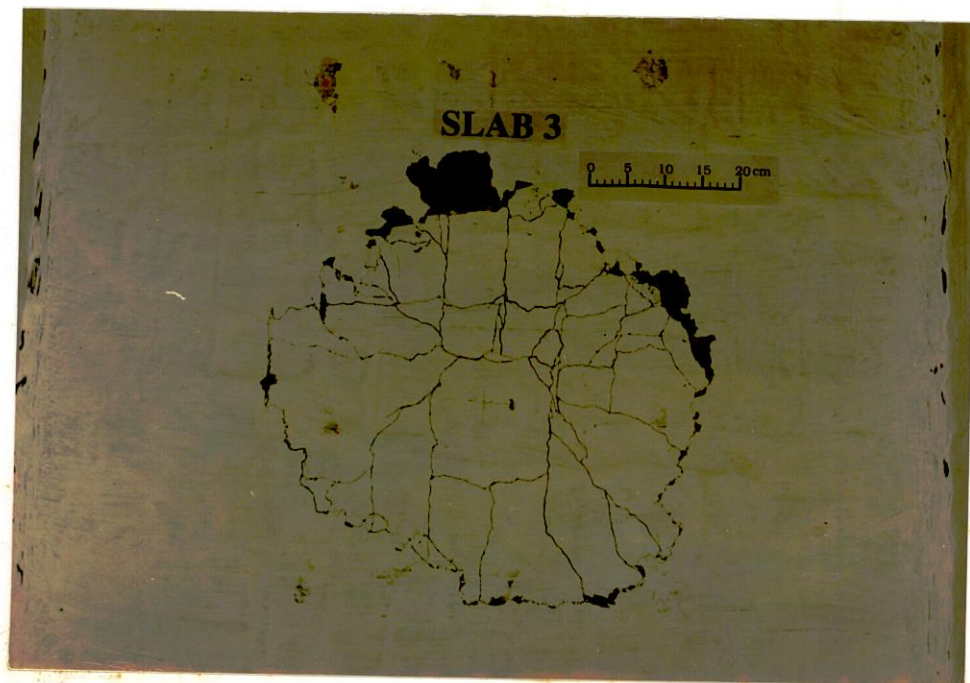
Due to safety reasons, the cracks were no longer been marked after the load of 104.98 kN. The central deflection of this slab as recorded at this load was 6.05 mm.

After failure of the slab at the load of 138.12 kN, all cracks at the bottom surface of the slab were marked. The cracking pattern of the bottom surface of the slab is shown in *Figure 4.4b*. From the cracking profile, it is evident that deep cracking around the middle portion of slab coupled with spalling of concrete took place in this case. Some cracks cross each other at the bottom surface of slab. The average uniaxial compressive (cylinder) strength of concrete (f'_c) for this slab was found to be 38.24 MPa on the day of testing.

V) SLAB5

The slab thickness of this restrained slab was 60 mm. It was reinforced with a medium percentage of reinforcement ($\rho=1.0$ percent). The predicted failure load for this slab in accordance with ACI 318-95, BS 8110-85, CAN3-A23.3-M84 and CEB-FIP-78 were 67.77 kN, 83.91 kN, 82.28 kN and 97.60 kN, respectively. During the test, the slab actually failed at a load of 147.59 kN.

In this slab, first crack was visible at a load of 46.36 kN at the bottom surface of the slab. The cracking pattern and propagation of cracking followed that of SLAB4.



(a)



(b)

Figure 4.4 Cracking pattern of bottom surface of (a) SLAB3 and (b) SLAB4

However, degree of cracking were much greater than SLAB4 and cracking in the diagonal direction towards edge beam for this slab was more pronounced than that of SLAB4. No cracks of the top surface of the slab and slab portion adjacent to edge beam were visible.

Due to safety reasons, the marking of crack propagation was not continued once the applied load reached a level around the Code prediction loads. The central deflection of the slab could not be measured after the application of this load level of 115.51 kN. At this level, a central deflection of 6.22 mm was recorded.

After failure of the slab at the load of 147.59 kN, all cracks at the bottom surface of the slab were marked. The cracking pattern of the bottom surface of the slab is shown in *Figure 4.5a*. The rate of propagation of crack at the bottom surface of slab increased, from the middle part of the slab towards the edge beam, as the load increased. No spalling of concrete took place after failure. The average uniaxial compressive (cylinder) strength of concrete (f'_c) for this slab was tested and found to be equal to 36.60 MPa on the day of testing.

VI) SLAB6

SLAB6 was a 60 mm thick restrained slab with high percentage of reinforcement ($\rho=1.5$ percent). The predicted failure load for this slab in accordance with ACI 318-95, BS 8110-85, CAN3-A23.3-M84 and CEB-FIP-78 were 72.56 kN, 96.05 kN, 88.09 kN and 106.89 kN, respectively. The slab failed at a load of 130.51 kN.

Here, first crack was visible at a load of 35.61 kN at the bottom surface of slab. The cracking pattern and propagation of cracking were similar to those of SLAB4 and SLAB5. No cracks of the top surface of the slab and slab portion adjacent to edge beam were visible.

Similar to the other slabs, the cracks were no longer marked after a load of 124.40 kN when LVDT from underneath the slab was also removed. Thus the central deflection

of the slab could not be measured after the load of 124.40 kN and central deflection of slab at this load was found to be equal to 6.93 mm.

After failure of the slab at an applied load of 130.51 kN, all cracks at the bottom surface of the slab was marked. The cracking pattern of the bottom surface of the slab is shown in *Figure 4.5b*. From the cracking profile, it is seen that some cracks crossed one another. Whereas most of the cracks were continued to a almost circular boundary around the loading area, a few cracks crossed the boundary and propagated towards the edge beam. The average uniaxial compressive (cylinder) strength of concrete (f'_c) for this slab was found to be 41.95 MPa on the same day of testing.

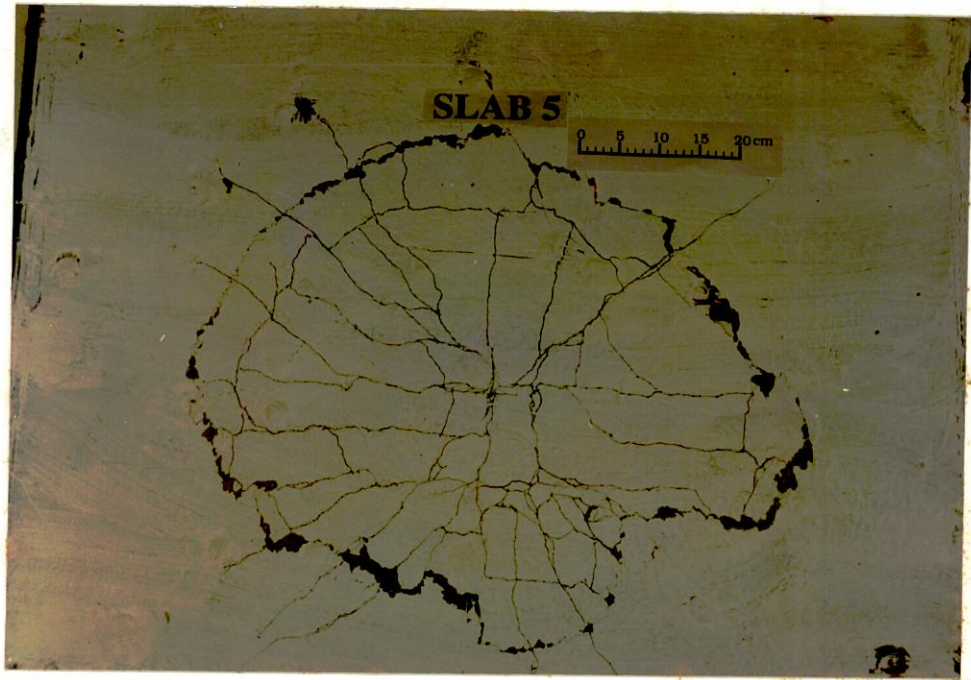
VII) SLAB7

This was a moderately restrained slab (width of edge beam=175 mm) with 1.0 percent reinforcement ($\rho=1.0$ percent). The slab thickness of this slab was 80 mm and the predicted failure load for this slab in accordance with ACI 318-95, BS 8110-85, CAN3-A23.3-M84 and CEB-FIP-78 were 99.86 kN, 132.00 kN, 121.22 kN and 139.12 kN, respectively. During the test, the slab actually failed at a load of 181.64 kN.

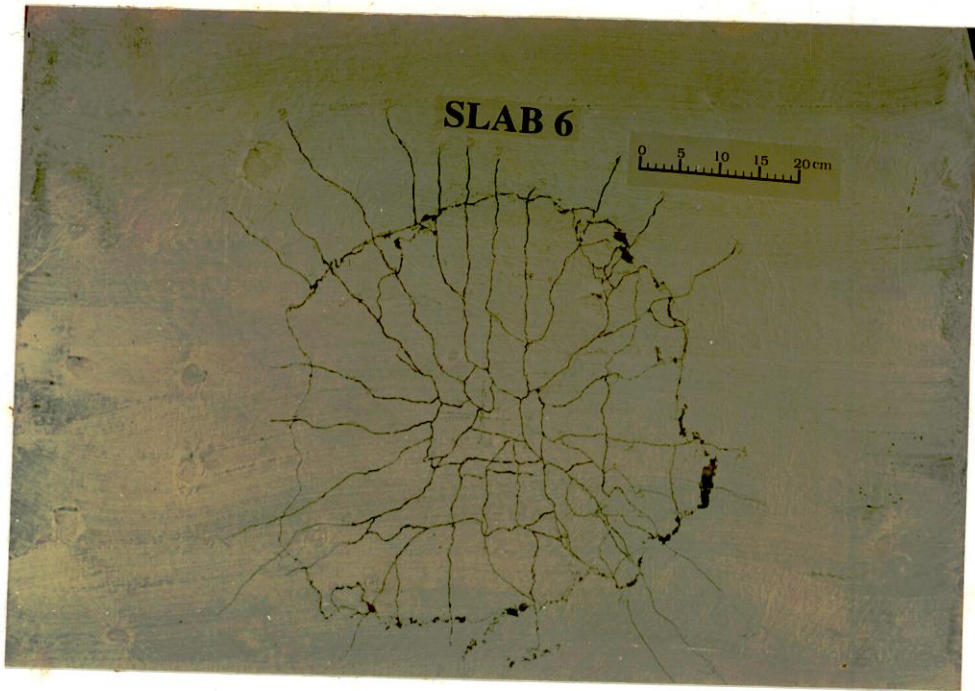
In this slab, first crack was visible at a load of 75.00 kN at the bottom surface of the slab. A few more cracks were formed in the adjacent regions at subsequent load steps. The nature of crack propagation of this slab was similar to that of SLAB2. No cracks of the top surface of the slab and slab portion adjacent to edge beam were visible. The central deflection of the slab as recorded at a load of 181.64 kN was 8.66 mm. The average uniaxial compressive (cylinder) strength of concrete (f'_c) for this slab was tested and found to be equal to 32.45 MPa on the same day of testing.

VIII) SLAB8

SLAB8 was also a 60 mm thick moderately restrained slab (width of edge beam=175mm) with lower percentage of reinforcement ($\rho=0.5$ percent). The predicted



(a)



(b)

Figure 4.5 Cracking pattern of bottom surface of (a) SLAB5 and (b) SLAB6

failure load for this slab as per ACI 318-95, BS 8110-85, CAN3-A23.3-M84 and CEB-FIP-78 were 72.00 kN, 66.60 kN, 87.40 kN and 94.45 kN, respectively. The slab failed at a load of 133.27 kN.

In this slab, first crack was visible at a load of 57.44 kN at the bottom surface of the slab. A large number of diagonal cracks were formed in this slab and propagation of cracks had similar to other 60 mm thick restrained slab samples. No cracks on the top surface of the slab and slab portions adjacent to edge beam were visible. The central deflection of this slab at the failure load was found to be 15.24 mm.

After failure of the slab at a load of 133.27 kN, all cracks at the bottom surface of the slab were marked. The cracking pattern of the bottom surface of the slab is shown in *Figure 4.6a*. From the cracking profile, it is evident that major cracks with large amount of spalling characterized the final failure pattern of the underside of the slab. The average uniaxial compressive (cylinder) strength of concrete (f'_c) for this slab was tested and found to be 41.30 MPa on the day of testing of the slab.

IX) SLAB9

The slab thickness of moderately restrained SLAB9 was 60 mm. The slab had a moderate percentage of reinforcement ($\rho=1.0$ percent). The predicted failure load for this slab in accordance with ACI 318-95, BS 8110-85, CAN3-A23.3-M84 and CEB-FIP-78 were 64.49 kN, 83.91 kN, 78.29 kN and 91.34 kN, respectively. The SLAB9 failed at a load of 115.51 kN.

Here, the very first crack was visible at a load of 46.36 kN at the bottom surface of the slab. Although the crack pattern and its propagation followed those of SLAB8, here the amount of cracking was much greater than SLAB8. No cracks of the top surface of the slab and slab portion adjacent to edge beam were, once again, visible. The central deflection of this slab at the load step before failure load (at the loading of 105 kN) was measured to be equal to 7.11 mm.

After failure of this slab at a load of 115.51 kN, all cracks at the bottom surface of the slab were marked. The cracking pattern of the bottom surface of the slab is shown in *Figure 4.6b*. From the final cracking profile, it can be seen that cracking around the mid portion of slab and small spalling of concrete marked the ultimate failure. The average uniaxial compressive (cylinder) strength of concrete (f'_c) for this slab was tested and found to be 33.14 MPa on the same day of testing.

X) SLAB10

SLAB10 was a lightly restrained slab (width of edge beam=105 mm) with moderate percentage of reinforcement ($\rho=1.0$ percent). The slab thickness of this slab was 80 mm and the predicted failure load for this slab in accordance with ACI 318-95, BS 8110-85, CAN3-A23.3-M84 and CEB-FIP-78 were 107.27 kN, 132.00 kN, 130.22 kN and 153.06 kN, respectively. During the test, the slab actually failed at a load of 188.89 kN.

In this slab, first crack was visible at a load of 57.44 kN at the bottom surface of slab. A few more cracks were formed in the adjacent region at subsequent load steps. The cracking of bottom surface were propagated similar to those of SLAB2 and SLAB7. No cracks of the top surface of the slab and slab portion adjacent to edge beam were visible, once again.

The marking of crack propagation was not continued once the applied load reached a level to 152.62 kN. The central deflection of this slab was not measured after the load of 152.62 kN either. At this level of load, a deflection of 7.0 mm was recorded.

After failure of the slab at a load of 188.89 kN, all cracks at the bottom surface of the slab was marked. The cracking pattern of the bottom surface of the slab is shown in *Figure 4.7a*. From the cracking profile, it can be seen that some cracks crossed one another and all cracks reached at a regular boundary around the middle portion of slab. However, some cracks crossed the boundary and progressed toward the edge beam.



(a)



(b)

Figure 4.6 Cracking pattern of bottom surface of (a) SLAB8 and (b) SLAB9

The average uniaxial compressive (cylinder) strength of concrete (f'_c) for this slab was tested and was found to be 37.45 MPa on the day of testing.

XI) SLAB11

SLAB11 was a 60 mm thick lightly restrained slab (width of edge beam = 105 mm) with lower percentage of reinforcement ($\rho=0.5$ percent). The predicted failure load for this slab as per ACI 318-95, BS 8110-85, CAN3-A23.3-M84 and CEB-FIP-78 were 71.23 kN, 66.60 kN, 86.48 kN and 93.12 kN, respectively. This slab failed at a load of 112.88 kN.

Here, first crack was visible at a load of 35.61 kN at the bottom surface of slab. A large amount of diagonal cracks were formed in this slab. The nature of propagation of cracks was similar to other 60 mm thick restrained slab samples. No cracks of the top surface of the slab and slab portion adjacent to edge beam were visible.

Due to safety reasons, the cracks were no longer marked after the application of a load of 84.73 kN. Again, the central deflection of this slab could not be measured after 84.73 kN load either. The central deflection of slab as measured at this level of load was 7.11 mm.

After failure of the slab at a load of 112.88 kN, all cracks at the bottom surface of the slab were marked. The cracking pattern of the bottom surface of the slab is shown in the *Figure 4.7b*. From the cracking profile, it is clear that cracking was concentrated around the middle portion of slab where spalling of concrete also took place. Some cracks crossed each other at the bottom surface of slab. The average uniaxial compressive (cylinder) strength of concrete (f'_c) for this slab was tested and was found to be equal to 40.43 MPa on the day of testing.



(a)



(b)

Figure 4.7 Cracking pattern of bottom surface of (a) SLAB10 and (b) SLAB11

XII) SLAB12

The slab thickness of SLAB12 slab was 60 mm and this was also a lightly restrained slab with moderate percentage of reinforcement ($\rho=1.0$ percent). The predicted failure load for this slab in accordance with ACI 318-95, BS 8110-85, CAN3-A23.3-M84 and CEB-FIP-78 were 68.18 kN, 83.91 kN, 82.77 kN and 98.38 kN, respectively. During the test, SLAB12 actually failed at a load of 115.73 kN.

In this slab, first crack was visible at a load of 46.36 kN at the bottom surface of the slab. The cracking pattern and propagation of cracking was similar to other restrained slabs of 60 mm thickness. No cracks of the top surface of the slab and slab portion adjacent to edge beam were visible.

Due to safety reasons, the cracks were no longer marked after the application of 75.00 kN load. Thus the central deflection of the slab could not be measured after 75.00 kN load. Central deflection of 3.94 mm was recorded at this level of load.

After failure of the slab at the load of 115.73 kN, all cracks at the bottom surface of the slab were marked. The cracking pattern of the bottom surface of the slab is shown in the *Figure 4.8a*. From the cracking profile, it can be seen that little amount of spalling of concrete and cracking around the middle portion of slab bottom characterized the failure. The average uniaxial compressive (cylinder) strength of concrete (f'_c) for this slab was found to be equal to 37.04 MPa on the same day of testing.

XIII) SLAB13

SLAB13 was a 80 mm thick unrestrained reinforced concrete slab sample with moderate percentage of reinforcement ($\rho=1.0$ percent). The predicted failure load for this slab in accordance with ACI 318-95, BS 8110-85, CAN3-A23.3-M84 and CEB-FIP-78 were 107.66 kN, 132.00 kN, 130.69 kN and 158.80 kN, respectively. This slab failed at a load of 171.96 kN.

In this slab, first crack was visible at a load of 57.44 kN at the center portion of the bottom surface of slab. A few more cracks were formed in the adjacent regions at subsequent load steps. The cracking of bottom surface were propagated from the middle span of the slab towards the edges of the slab with applied loading. The number of cracks were also increased with the increase of loading. However none of them could reach the corner of the slab. Inclined cracks from the corner of the top surface of the slab with an inclination about 45° degree from all the four supports were also visible.

Due to safety reasons, the cracks were no longer marked after applying a load of 133.27 kN. Thus, the central deflection of the slab could not be measured after 133.27 kN load. The central deflection of slab as recorded at this level of load was equal to 8.76 mm.

After failure of the slab at the load of 171.96 kN, all cracks at the bottom surface of the slab were marked. The cracking pattern of the bottom surface of the slab is shown in the *Figure 4.8b*. From the cracking profile, it is seen that cracking was concentrated around the middle portion of slab where small spalling of concrete were also found. The average uniaxial compressive (cylinder) strength of concrete (f_c') for this slab was found to be equal to 37.72 MPa on the same day of testing.

XIV) SLAB14

SLAB14 was a unrestrained type of slab of 60 mm thickness with lower percentage of reinforcement ($\rho=0.5$ percent). The predicted failure load for this slab as per ACI 318-95, BS 8110-85, CAN3-A23.3-M84 and CEB-FIP-78 were 66.00 kN, 66.60 kN, 88.12 kN and 84.11 kN, respectively. During the test, the slab actually failed at a load of 84.73 kN.

Here, first crack was visible at a load of 35.61 kN at the bottom surface of slab. The corners of the slab also underwent cracking.



(a)



(b)

Figure 4.8 Cracking pattern of bottom surface of (a) SLAB12 and (b) SLAB13

The cracks were no longer marked after the load application of 75.00 kN. The central deflection of this slab could not be measured after the load of 75.00 kN and central deflection of slab as recorded at this load was equal to 13.21 mm.

After failure of the slab at the load of 84.73 kN, all cracks at the bottom surface of the slab were marked. The cracking pattern of the bottom surface of the slab is shown in the *Figure 4.9a*. From the cracking profile, it is seen a regular that cracking was more pronounced around the middle portion of slab where spalling of concrete also took place. The average uniaxial compressive (cylinder) strength of concrete (f_c') for this slab was found to be 34.71 MPa on the day of testing.

XV) SLAB15

SLAB15 was also a unrestrained type of 60 mm thick slab with moderate percentage of reinforcement ($\rho=1.0$ percent). The predicted failure load for this slab as per ACI 318-95, BS 8110-85, CAN3-A23.3-M84 and CEB-FIP-78 were 64.38 kN, 83.91 kN, 78.16 kN and 91.14 kN, respectively. During the test, the slab actually failed at a load of 91.76 kN.

In this slab, first crack was visible at a load of 35.61 kN at the bottom surface of the slab. Corner cracks were also found.

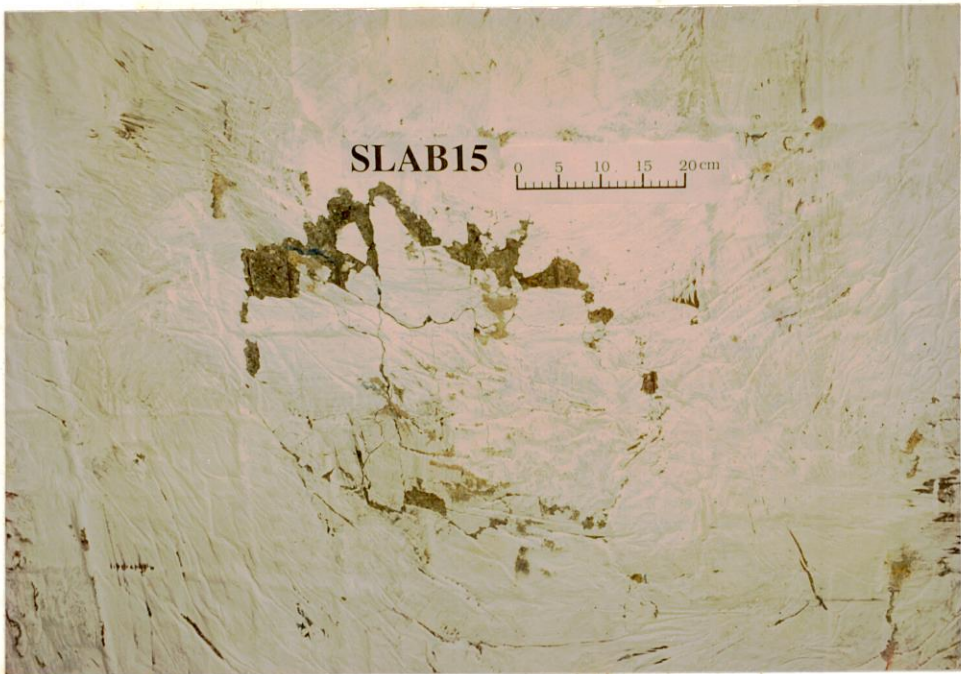
Due to safety reasons, the cracks were no longer marked after the load application of 64.92 kN. The central deflection of the slab measured at this level was 13.21 mm.

After failure of the slab at the load of 91.76 kN, all cracks at the bottom surface of the slab were marked. The cracking pattern of the bottom surface of the slab is shown in the *Figure 4.9b*. From the cracking profile, it is seen a regular deep boundary like crack around the middle portion of slab where spalling of concrete also took place.

The average uniaxial compressive (cylinder) strength of concrete (f_c') for this slab was tested and found to be equal to 33.03 MPa on the day of testing.



(a)



(b)

Figure 4.9 Cracking pattern of bottom surface of (a) SLAB14 and (b) SLAB15

XVI) SLAB16

SLAB16 was larger than other slabs and had a very high level of edge restraint (width of edge beam=340 mm). It had a thickness of 60 mm with moderate percentage of reinforcement ($\rho=1.0$ percent). The predicted failure load for this slab in accordance with ACI 318-95, BS 8110-85, CAN3-A23.3-M84 and CEB-FIP-78 were 71.06 kN, 83.91 kN, 86.27 kN and 103.97 kN, respectively. During the test, the slab actually failed at a load of 171.96 kN.

In this slab, first crack was visible at a load of 35.61 kN at the central portion of the bottom surface of slab. The crack propagation of this slab was very much akin to other restrained slab of 60 mm thickness. No cracks of the top surface of the slab and slab portion adjacent to edge beam were visible.

Due to safety reasons, the marking of crack propagation was not continued once the applied load reached a level around the Code predicted loads. Once again, the central deflection of the slab could not be measured after a load of 152.62 kN to safeguard the LVDT. At this level a central slab deflection of 13.76 mm was recorded. The average uniaxial compressive (cylinder) strength of concrete (f'_c) for this slab was found to be 40.24 MPa on the same day of testing. The cracking pattern of the bottom surface of the slab is shown in the *Figure 4.10*.

The summary of the test results are shown in *Appendix E*.

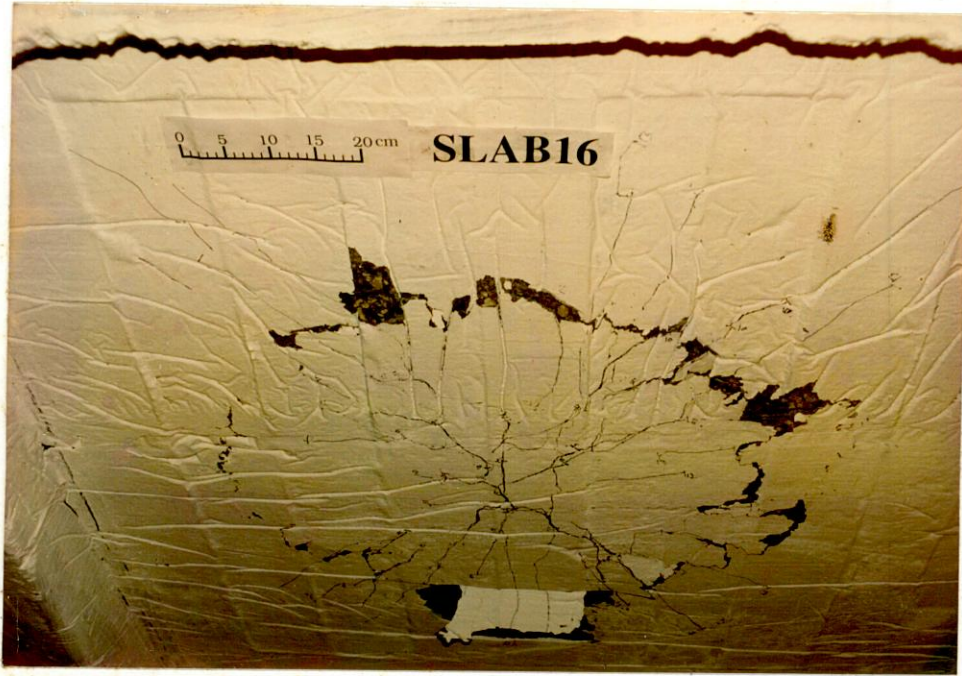


Figure 4.10 Cracking pattern of bottom surface of SLAB16

CHAPTER FIVE

DISCUSSION OF RESULTS

5.1 GENERAL

Test results obtained from this study have been analyzed in this chapter. It has been found that ultimate punching shear capacity and behaviour of slab samples are dependent on reinforcement ratio, restraining action of slab edges, slab thickness, and, of course, span-to-depth ratio of the slab. In this chapter, apart from studying the ultimate punching load capacity, effect of edge restraint, effect of steel reinforcement, effect of span-to-depth ratio and cracking patterns of the model slabs tested in the research, detailed investigation has been carried out in order to find out the deficiency of current Code provisions related to punching shear strength of slabs.

5.2 ULTIMATE LOAD CARRYING CAPACITY

The load-carrying capacity of all the slab models as obtained from test results as well as from the predictions of ACI 318-95, BS 8110-85, CAN3-A23.3-M84 and CEB-FIP are summarized in *Table 5.1*. All terms related to various factor of safety have been put equal to 1.0. It is to be noted that Code-predicted punching shear load have been calculated in accordance with the equations given in Section 2.2. Again, while calculating the predicted strength of slabs, actual compressive (cylinder) strength of concrete on the day of testing have been given as input, whereas compressive cube strength has been estimated to be 25 percent higher than its cylinder strength counterpart.

From the *Table 5.1*, it is clear that the load carrying capacity of all the slab models tested were greater than those predicted by the present-day Codes such as ACI 318, BS 8110, CAN3-A23.3-M84 and CEB-FIP. It is also apparent from this table that the punching shear provision of European Code (CEB-FIP) is more economical than other Codes as described earlier.

Table 5.1 Comparison of Load Carrying Capacity with Code Predictions

Slab Models	Expt. failure load in kN	Predicted Failure Load in kN				Experimental failure load / Code predicted load			
		ACI 318	BS 8110	CAN3 -A23.3	CEB-FIP	Expt./ACI	Expt./BS	Expt./CAN	Expt./CEB
SLAB1	225.16	108.95	104.77	132.06	139.23	2.07	2.15	1.70	1.62
SLAB2	242.09	107.39	132.00	130.17	152.98	2.25	1.83	1.87	1.59
SLAB3	142.95	93.21	144.85	112.98	126.66	1.53	0.99	1.27	1.12
SLAB4	138.12	69.38	66.60	84.10	89.73	1.99	2.07	1.64	1.54
SLAB5	147.59	67.88	83.91	82.28	97.60	2.17	1.76	1.79	1.51
SLAB6	130.51	72.67	96.05	88.09	106.89	1.80	1.36	1.48	1.22
SLAB7	181.64	100.01	132.00	121.22	139.12	1.82	1.38	1.50	1.31
SLAB8	133.27	72.11	66.60	87.40	94.45	1.85	2.00	1.52	1.41
SLAB9	115.51	64.59	83.91	78.29	91.34	1.79	1.38	1.48	1.26
SLAB10	188.89	107.44	132.00	130.22	153.06	1.76	1.43	1.45	1.23
SLAB11	112.88	71.34	66.60	86.48	93.12	1.58	1.69	1.31	1.21
SLAB12	115.73	68.29	83.91	82.77	98.38	1.69	1.38	1.40	1.18
SLAB13	171.96	107.82	132.00	130.69	158.80	1.59	1.30	1.32	1.08
SLAB14	84.73	66.10	66.60	88.12	84.11	1.28	1.27	0.96	1.01
SLAB15	91.76	64.48	83.91	78.16	91.14	1.42	1.09	1.17	1.01
SLAB16	171.96	71.17	83.91	86.27	103.97	2.42	2.05	1.99	1.65
Average						1.81	1.57	1.49	1.31

5.3 EFFECT OF EDGE RESTRAINT

91690
All the slab panels, including those with low-percentage ($\rho=0.5$ percent) to high percentage ($\rho=1.5$ percent) of steel, with and without edge restrained failed in a punching shear mode. An analysis of test results is presented in *Table 5.2*, where non-dimensional punching shear strength ($P_u/f_c'b_0d$) and normalized punching shear strength ($P_u/\sqrt{f_c'} b_0d$) of each specimen have been given. In this case non-dimensional punching shear strength has been calculated by dividing the corresponding ultimate load by the product of the compressive strength of concrete and critical surface at half the effective depth away from the perimeter of loaded area. Again, the experimental punching shear strength have been normalized by dividing the corresponding load by the product of the square root of compressive strength of concrete and area of the nominal critical surface located at half the effective depth away from the perimeter of the load.

Table 5.2 shows that there was a definite increase in punching load of the slab panels as the degree of edge restraint increased. This trend is also evident in *Figure 5.1* and *Figure 5.2*, where it can be seen that the punching shear capacity increased significantly with the increase in the width of edge beams from zero to 245 mm ($C=0.10 \times 10^8 \text{ mm}^4$ to $2.36 \times 10^8 \text{ mm}^4$).

From *Figure 5.1* and *Table 5.2*, it is clear that the enhancements in the ultimate non-dimensional strength for slab models having 1.0 percent of reinforcement was about 41.89 percent as the width of the edge beam increased from zero to 245 mm ($C=0.21 \times 10^8 \text{ mm}^4$ to $2.36 \times 10^8 \text{ mm}^4$) for the thick slabs ($h = 80 \text{ mm}$) and about 45.17 percent for the slightly thinner slabs ($h=60 \text{ mm}$ and $C= 0.10 \times 10^8 \text{ mm}^4$ to $1.32 \times 10^8 \text{ mm}^4$)

Similar increases in strength were found for 60 mm thick slab models having 0.5 percent and 1.0 percent reinforcement, as it is evident from *Figure 5.2*. It is clear from *Figure 5.2* and *Table 5.2* that for 60 mm thick slabs having 0.5 percent reinforcement the punching shear capacity increased by about 47.91 percent as the width of the edge beam increased to 245 mm from zero restraint.

Table 5.2 Non-dimensional and Normalized Punching Shear Strength of Reinforced Concrete Slabs

Slab	Effective depth (d)	$b_0 = 4(120+d)$	Ultimate Load (P_u)	Cylinder Strength (f'_c)	Non-dimensional strength	Normalized punching strength
	mm	mm	kN	MPa		
SLAB1	70	760	225.16	38.51	0.1099	0.6820
SLAB2	70	760	242.09	37.42	0.1216	0.7439
SLAB3	70	760	142.95	28.19	0.0953	0.5061
SLAB4	50	680	138.12	38.24	0.1062	0.6569
SLAB5	50	680	147.59	36.60	0.1186	0.7175
SLAB6	50	680	130.51	41.95	0.0915	0.5927
SLAB7	70	760	181.64	32.45	0.1052	0.5994
SLAB8	50	680	133.27	41.30	0.0949	0.6099
SLAB9	50	680	115.51	33.14	0.1025	0.5902
SLAB10	70	760	188.89	37.45	0.0948	0.5802
SLAB11	50	680	112.88	40.43	0.0821	0.5221
SLAB12	50	680	115.73	37.04	0.0919	0.5593
SLAB13	70	760	171.96	37.72	0.0857	0.5263
SLAB14	50	680	84.73	34.71	0.0718	0.4230
SLAB15	50	680	91.76	33.03	0.0817	0.4696
SLAB16	50	680	171.96	40.24	0.1257	0.7973

The present exercise reveals that the edge restraint has a significant effect on the ultimate punching load of reinforced concrete slabs, resulting in a great increase of punching shear resistance in the slabs and enhancing effectively the load-carrying capacity of the member subjected to punching load. The enhancement in the punching load carrying capacity of slabs due to edge continuity may be attributed to the possible influence of in-plane restraint, as advocated by other researchers like Kuang and Morley (1992), Lovrovich and McLean (1990), McLean, et al. (1990) and Rankin and Long (1987a). Similar to the findings of other researchers, compressive membrane forces were, in fact, developed in the slabs due to edge restraints. This may be due to the lateral slab expansion and possible outward movement of the edge beams. Continuous slabs deflect less than similar simply-supported slabs under the action of load. This helps the slabs having edge continuity to sustain more punching load.

5.4 EFFECT OF STEEL REINFORCEMENT

The ultimate non-dimensional shear strengths of various slab, have been plotted in *Figure 5.3* against the reinforcement ratio for the specimens having width of edge beam equal to 245 mm. As it can be expected, the load-carrying capacity of the test slab panels increased with the addition of steel reinforcement, increasing significantly as the reinforcement ratio increased from 0.5 percent to 1.0 percent. The corresponding increases in the ultimate non-dimensional strength were 10.65 percent for the slabs with 80 mm thickness and 11.68 percent for those with 60 mm thickness. However, in contrast to the findings of Kuang and Morley (1992), when the percentage of steel was over 1.0 percent, the non-dimensional punching shear strength decreased, by about 14 percent for slabs with 60 mm thickness and 13 percent for those with 80 mm thickness, with respect to the similar slabs having 0.5 percent reinforcement. Kuang and Morley (1992) reported virtually no change in non-dimensional punching shear strength in this cases.

It is worth mentioning here that whereas the British and CEB Codes recognize the role of the amount of reinforcement on the punching shear carrying capacity of slabs, American and Canadian Code equations simply ignore its effect.

Thus it is clear from the above discussion that steel reinforcement has an important effect on the punching shear strength. This indicates that whereas steel reinforcement has a positive effect on the punching shear strength for the lightly reinforced restrained slabs, for those that are heavily reinforced such effects may become negative. Excessive amount of reinforcement sometimes make structural concrete brittle as reported by Seraj, et al. (1995). The present decline in punching strength at higher level of reinforcement may also be due to such effects. However, additional tests are needed to investigate, in detail, the influence of the reinforcement ratio on punching load capacity of restrained concrete slabs, especially those with lower level of edge restraint.

5.5 EFFECT OF SLAB THICKNESS

The slab thickness is an important factor affecting the punching load capacity of a reinforced concrete slab with a given degree of restraint. Keeping the clear span as well as other parameters of the slab samples constant, it has been found that higher the slab thickness the higher the punching shear strength of slab.

Figure 5.1 and *Table 5.1* show that for the same clear span (1200 mm) and the same percentage of reinforcement ($\rho=1.0$ percent), average of the non-dimensional strength of 80 mm thick slabs was 3.19 percent above than that of 60 mm thick slabs. Again, from *Figure 5.3*, it is evident that for the same width of edge beam ($b = 245$ mm), the average of the non-dimensional strengths was 3.32 percent higher for 80 mm thick slab samples in comparison to 60 mm thick slabs .

Thus, it appears that the thickness is an important factor affecting the punching load capacity of a reinforced concrete slab with a given degree of restraint, despite the fact that thickness is already in the denominator of the expression for dimensionless shear strength. From this it seems that thickness may, perhaps, has a more positive influence on such strengths than what is currently recognized by the present-day Codes.

5.6 DEFLECTION

The variation of slab deflection with applied load is shown in *Figure 5.4*. The individual as well as group load-deflection curves of all the slab tested are given in Appendix D. It may be recalled that complete load-deflection curves of all the slab tested could not be traced due to limitation of available instruments.

It is, however, clear from *Figure 5.4* that central slab deflections were smaller for the slabs restrained by edge beams. The value of deflection decreased, in general, as the degree of edge restraint increased. Again, the heavily reinforced slabs, on the whole, underwent lesser deflections and showed slightly higher stiffness.

5.7 CRACKING

During the tests, the development of cracking and the width of cracks were carefully observed and monitored at various load increments. Cracking on the underside of the slabs developed as a series of cracks radiating from the centrally loaded area. As the load increased, the widths of the cracks increased as expected. The crack widths of the normally reinforced ($\rho=1.0$ percent) and heavily reinforced ($\rho=1.5$ percent) slabs were found to be smaller than those of lightly reinforced slabs ($\rho=0.5$ percent). Whereas the cracks of the slabs with reinforcement level of 0.5 percent propagated more readily towards the edges, similar cracks for other slabs having more reinforcement were, somewhat, concentrated in the middle portion of the slab.

Similarly, whereas cracks were fine and large in number in case of strongly restrained slabs, for moderately restrained slabs such cracks were found to be wider and fewer in number. In case of strongly restrained slabs, due to the presence of in-plane forces, the width of the cracks was less and consequently the total energy due to punching was distributed among a large number of fine cracks. On the other hand, in slab having lesser amount of lateral restraint, initially produced cracks could widen and thereby, the total energy was cater for less number of wider cracks. The discontinuity on the

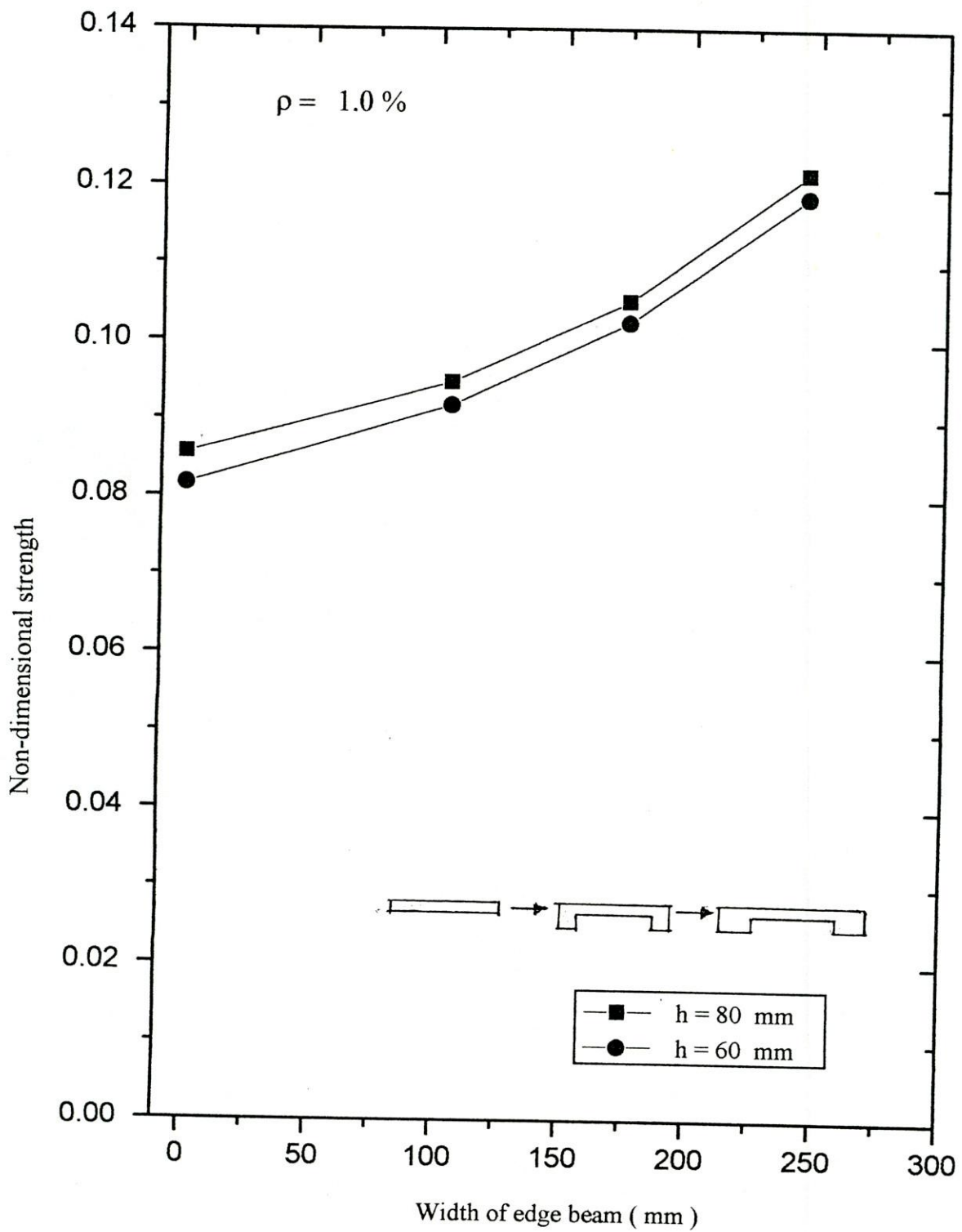


Figure 5.1 : Effect of edge restraint for 1.0 percent reinforcement

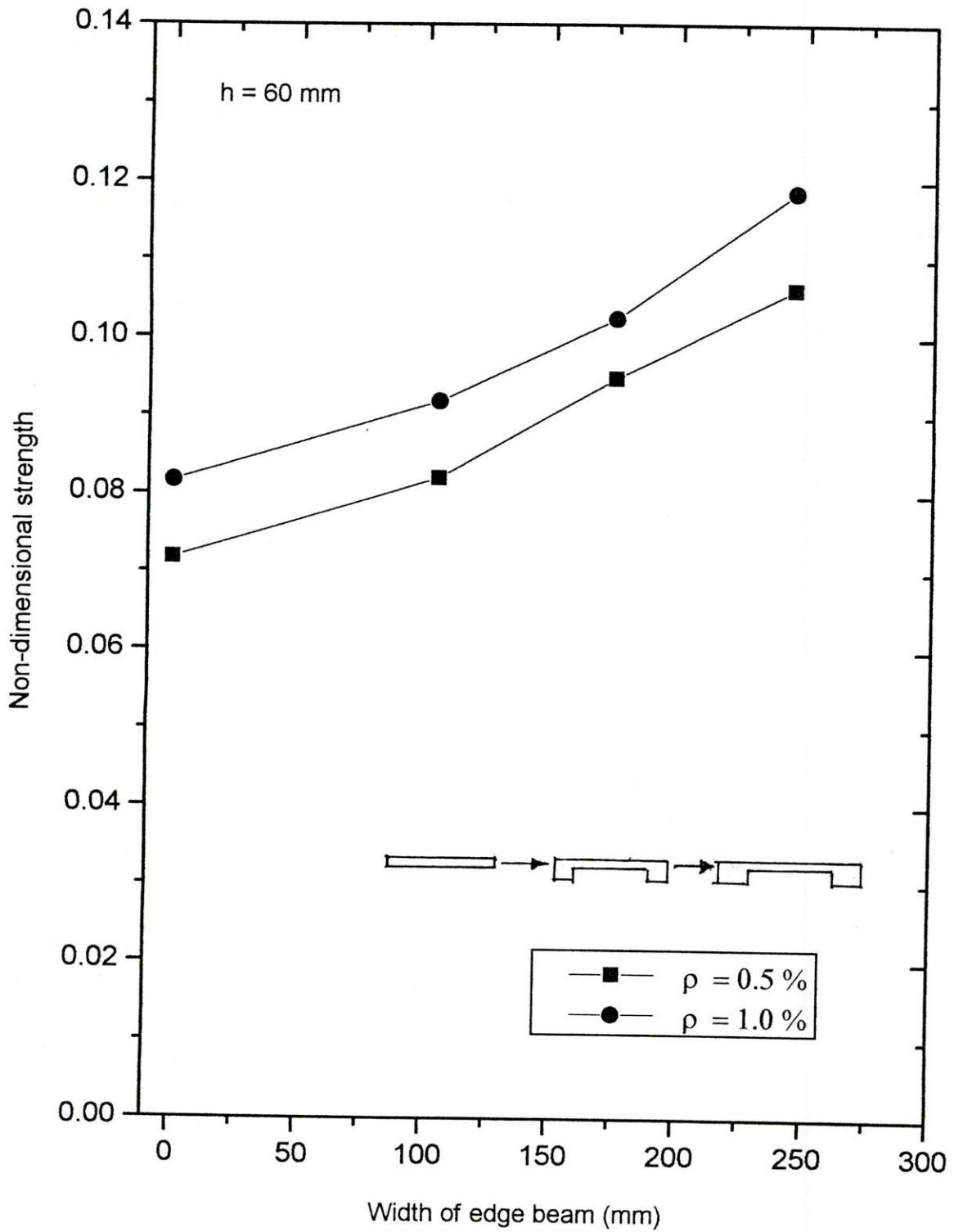


Figure 5.2 : Effect of edge restraint for slab thickness of 60 mm

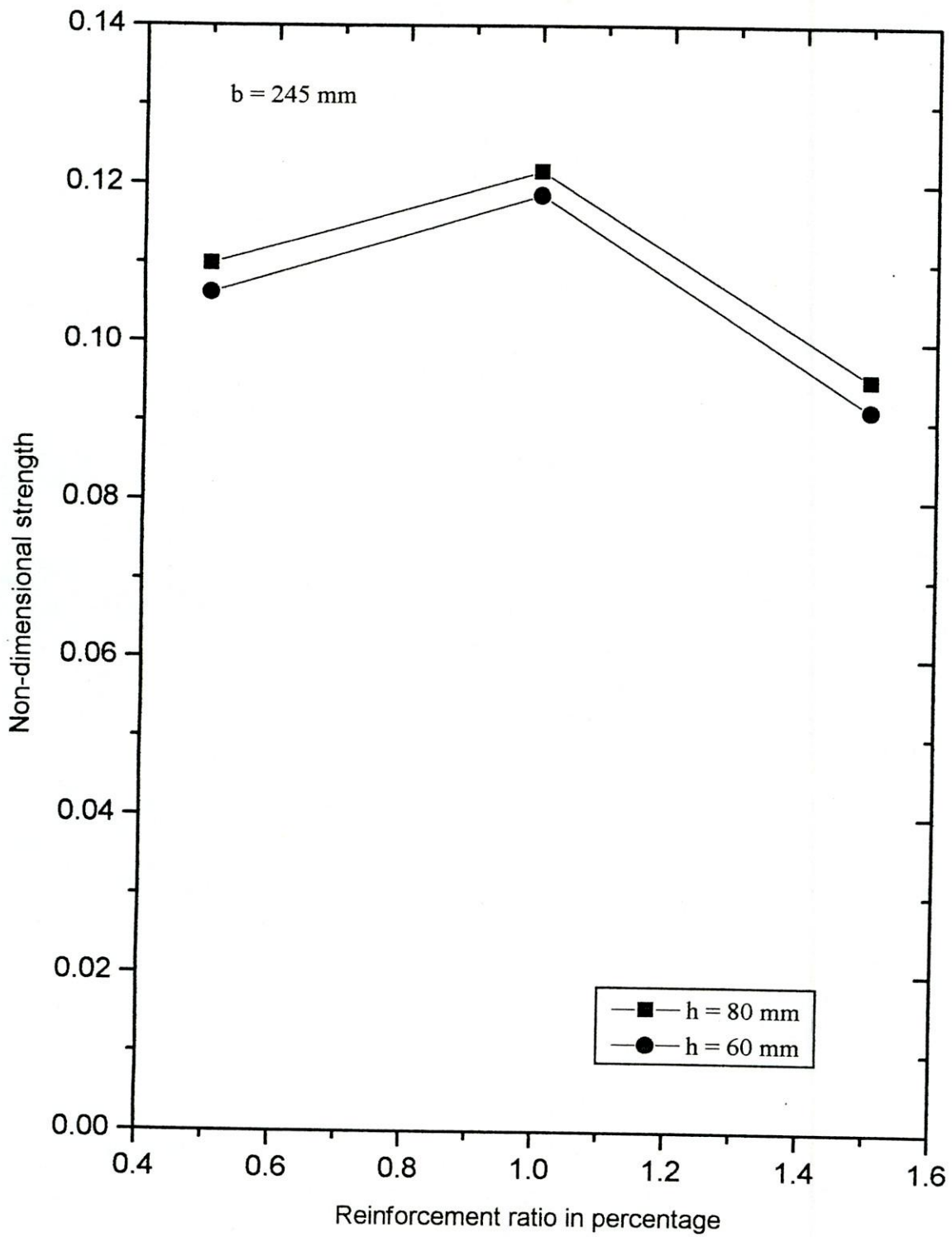


Figure 5.3 : Effect of reinforcement ratio for same width edge beam

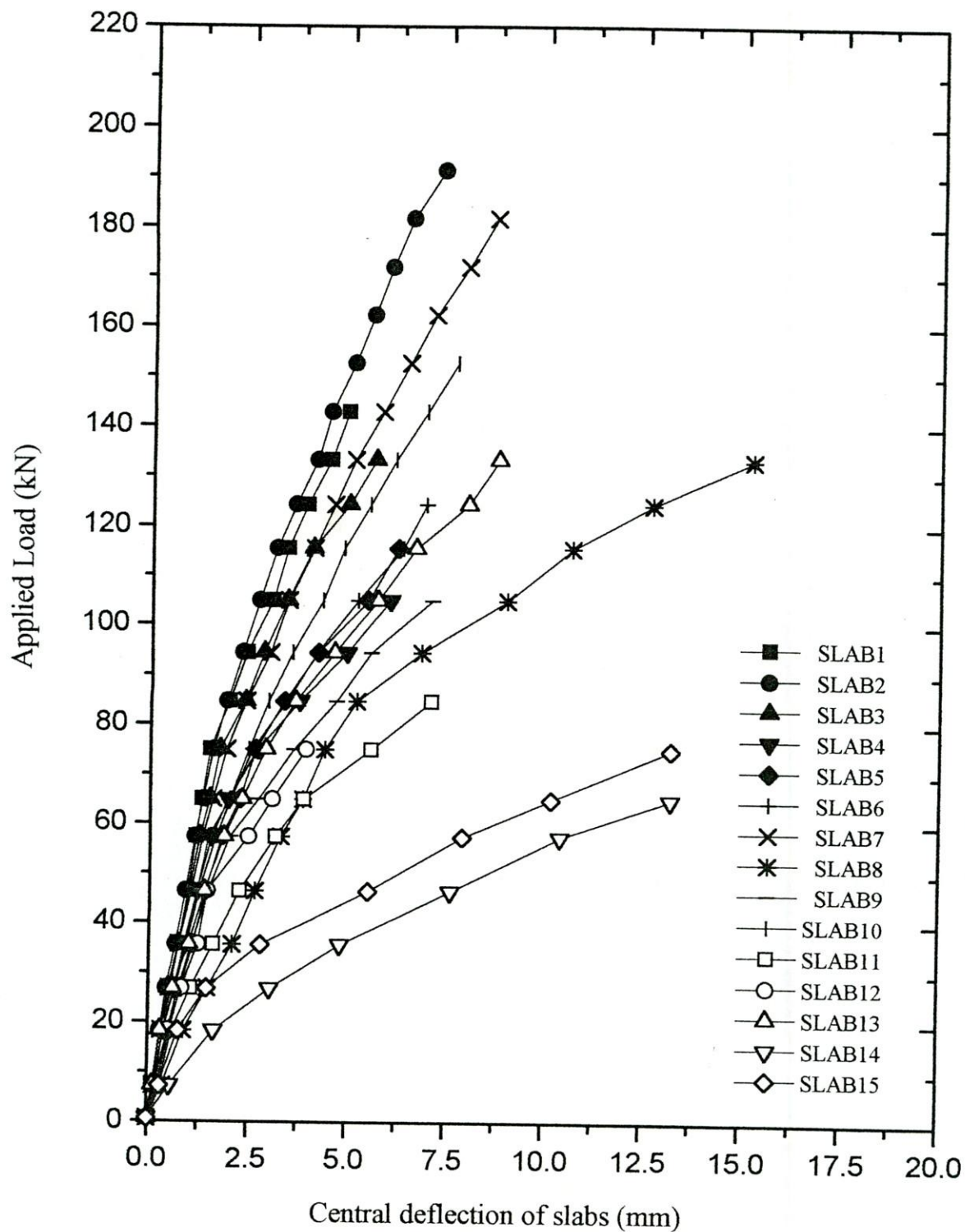


Figure 5.4 : Central deflection of all slabs under different loading

top surface of the slabs after punching typically took the square geometry of the punching plate.

5.8 DETERMINATION OF SIZE SENSITIVITY VIA SLAB16

SLAB16 was a 60 mm thick slab with 1.0 percent reinforcement ($\rho=1.0$ percent). The width of the edge beam of this slab ($b=340$ mm) was higher than all other slab samples of this study. The clear span of this slab was also greater than all other slab samples and was equal to 1450 mm. The area of this slab was, thus, 46 percent higher than all other slabs investigated in this study. From *Table 5.1* it can be seen that the load carrying capacity of this slab was greater than those predicted by ACI 318-95, BS 8110-85, CAN3-A23.3-M84 and CEB-FIP-78 by 2.40, 2.05, 1.99 and 1.65 times, respectively.

Slab thickness and reinforcement ratio of SLAB16 were akin to those of SLAB5, SLAB9, SLAB12 and SLAB15. It is interesting to note from *Table 5.1* that, the degree of enhancement in the punching shear carrying capacity of SLAB16 was, in fact, slightly higher than the model slabs having smaller plan area. This reinforces the notion that the positive influence of edge restraint, is not dependent on slab size and that the general trend shown by model slabs are also reflected in slabs having larger dimensions. However, since only one slab having slightly larger dimension was tested in this study, further tests are, of course, needed to understand the possible influence of size effect on punching load capacity. The findings of the present study, thus, may be considered to be applicable, albeit tentatively, to all sorts of slabs.

5.9 COMPARISON OF TEST RESULTS WITH DIFFERENT CODE PREDICTIONS

A comparison of the experimental failure loads and the punching shear strength predicted by various Codes is shown in *Table 5.1*. A more precise and graphical representation of this comparison has been made and shown in *Figure 5.5*, *Figure 5.6*

and *Figure 5.7*. Partial safety factors, reduction factors, etc. have been removed in this exercise and the strength of concrete of individual slabs has been considered while plotting the graphs.

Figures 5.5 and *5.6*, represent the ultimate load carrying capacity of slabs having different width of edge beams for samples having 1.0 percent reinforcement. It is evident for both 80 mm and 60 mm thick slabs that the experimental load carrying capacity is much higher than all the Code predictions. American Code (ACI 318-95) has been found to be more conservative than the others Codes while the European Code (CEB-FIP) was the least conservative. The British Code (BS 8110-85) and the Canadian Code (CAN-3-23.3-M84) predictions fell in between the American and European Codes.

From *Figure 5.7*, it appears that for slab samples having 0.5 percent reinforcement, load carrying capacity predicted by the European and Canadian Codes were closer to the experimental load carrying capacity for slabs having zero restraint. In this case, for restrained slabs, European Code was, once again, found to be less conservative than all other Codes. American and British Codes, were most conservative in predicting the capacity of slabs having $\rho=0.5$ percent. They also predicted similar punching capacity.

It is also evident from *Figures 5.5*, *5.6* and *5.7* that the experimental load carrying capacity of the slabs increased with the increase in the degree of edge restraint provided by edge beams of larger widths. This restraining action of slabs has not been taken into consideration in all the Code provisions.

In view of the fact that ACI 318-95 is, perhaps, the most commonly used Code in the world and also seems to form the basis of BNBC (1993), the normalized punching shear strength ($P_u/\sqrt{f'_c} b_0d$) for different edge restraints as well as reinforcement ratios are shown in *Figures 5.8*. It is clear from *Table 5.2* and *Figure 5.8* that whereas the punching shear capacity predicted by ACI 318-95 Code is only 0.33 times $\sqrt{f'_c} b_0d$, in reality it may attain much higher values. Whereas, only further testing may lead to possible modifications in Code provisions due to the dangerous nature of shear failure, CAN3-A23.3-M84 already uses a slightly higher values of 0.4 in a similar equation.

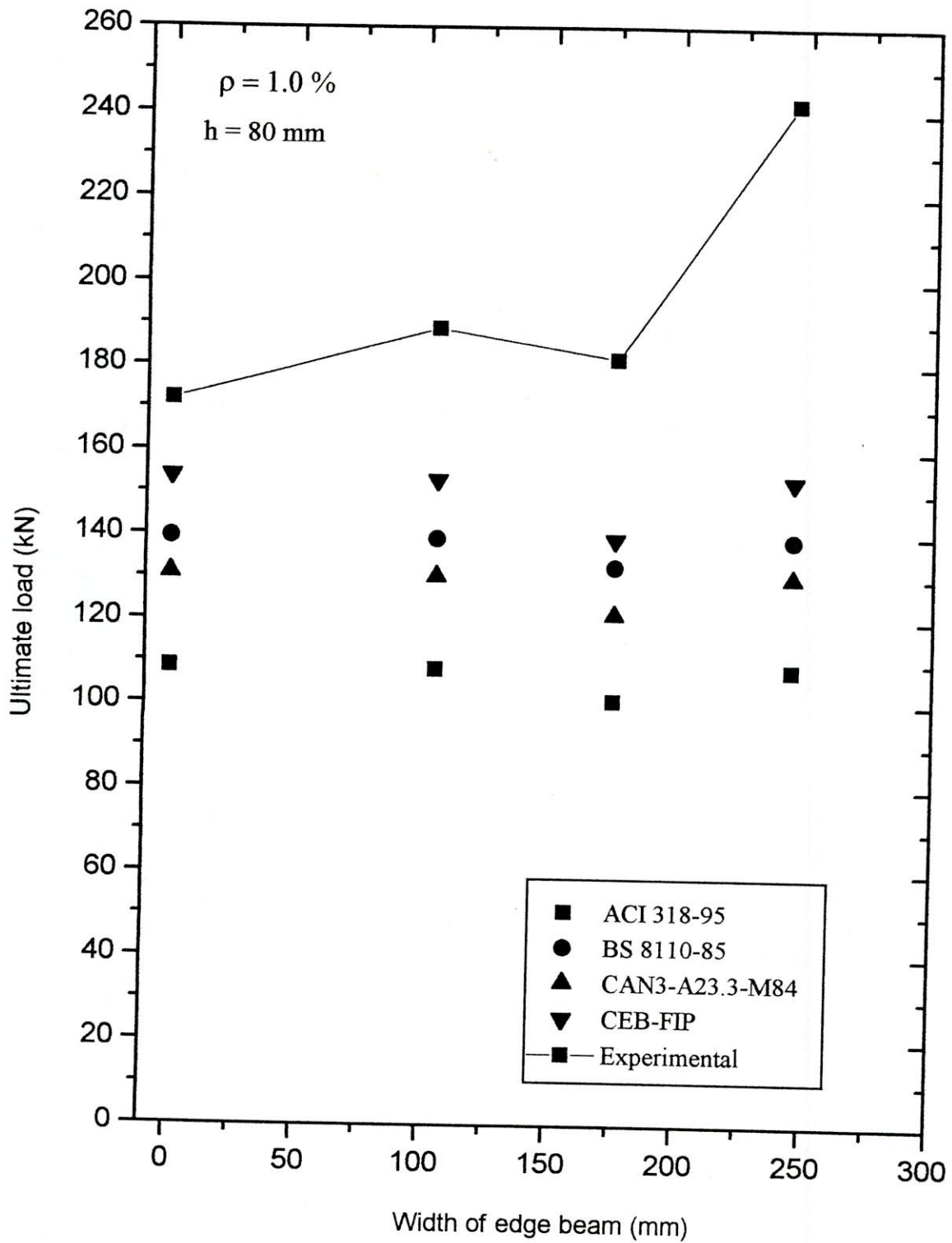


Figure 5.5 : Comparison of ultimate load for different Code predicted load at slab thickness = 80 mm and reinforcement ratio = 1.0 percent

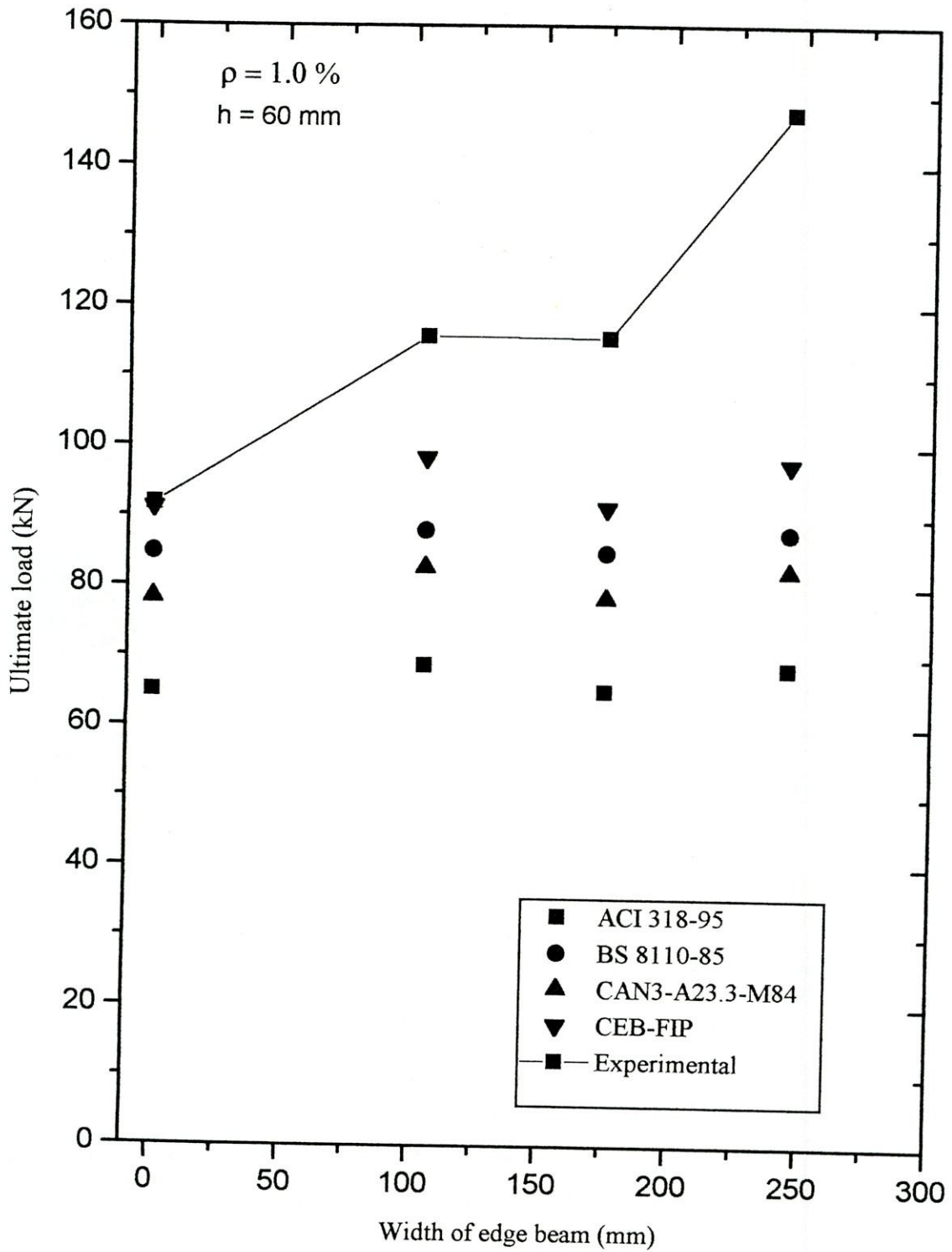


Figure 5.6 : Comparison of ultimate load for different Code predicted load at slab thickness = 60 mm and reinforcement ratio = 1.0 percent

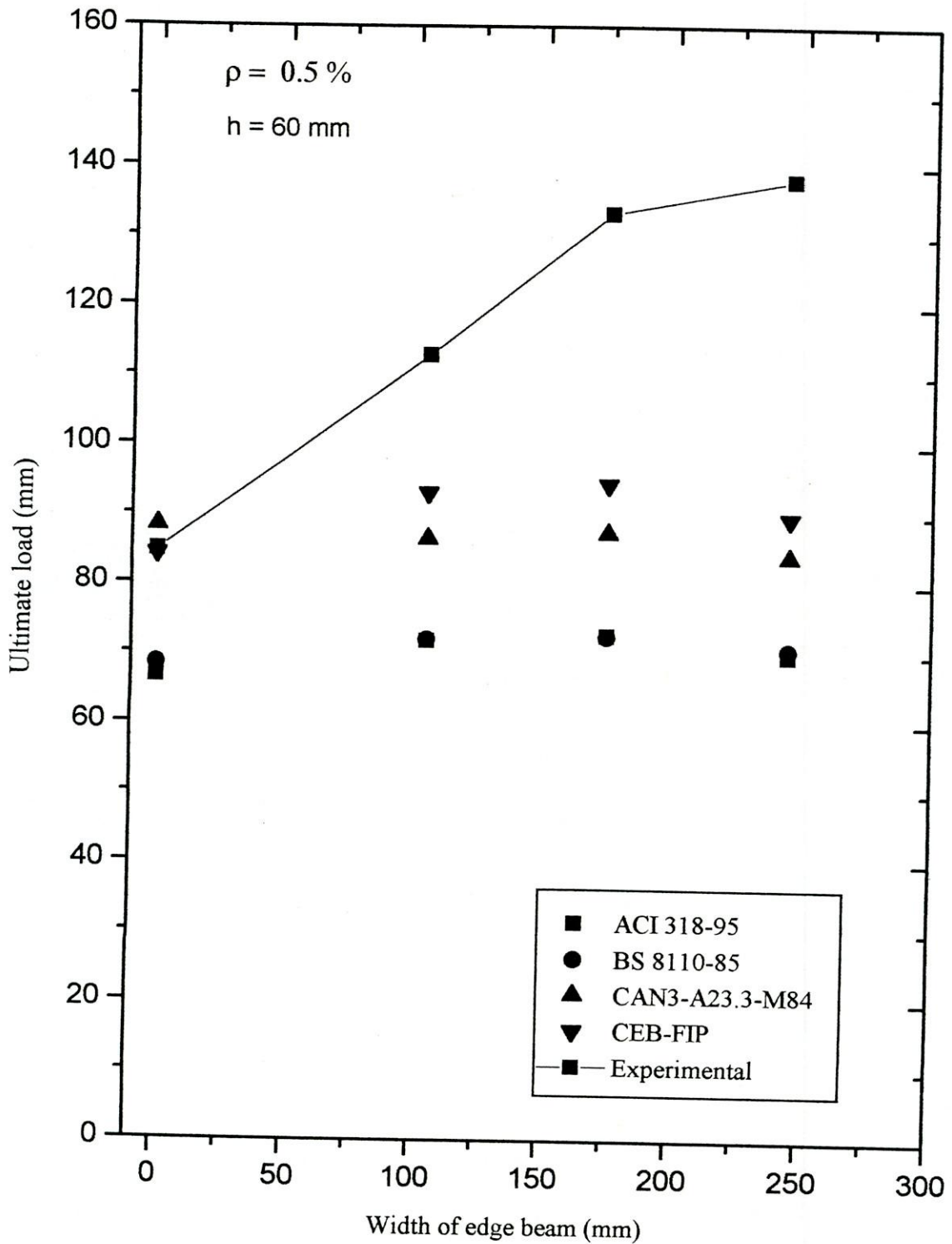


Figure 5.7 : Comparison of ultimate load for different Code predicted load at slab thickness = 60 mm and reinforcement ratio = 0.5 percent

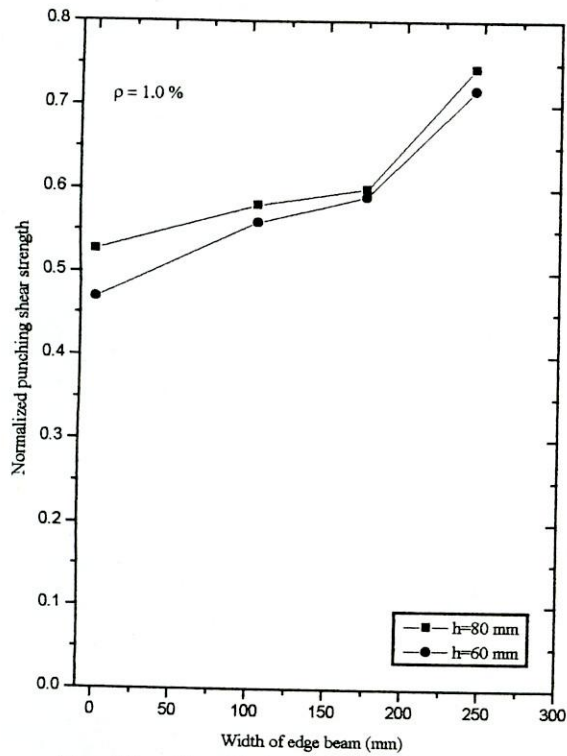


Figure 5.8a : Normalized punching shear strength for 1.0 percent reinforcement

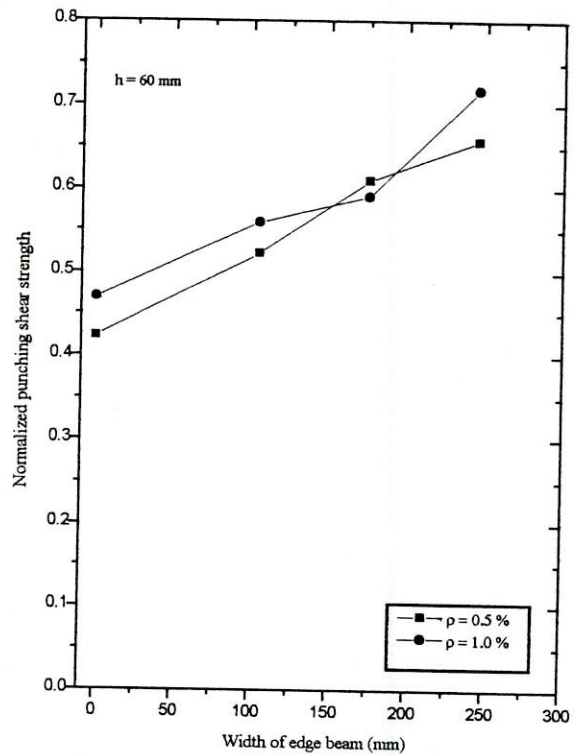


Figure 5.8b : Normalized punching shear strength for slab thickness of 60 mm

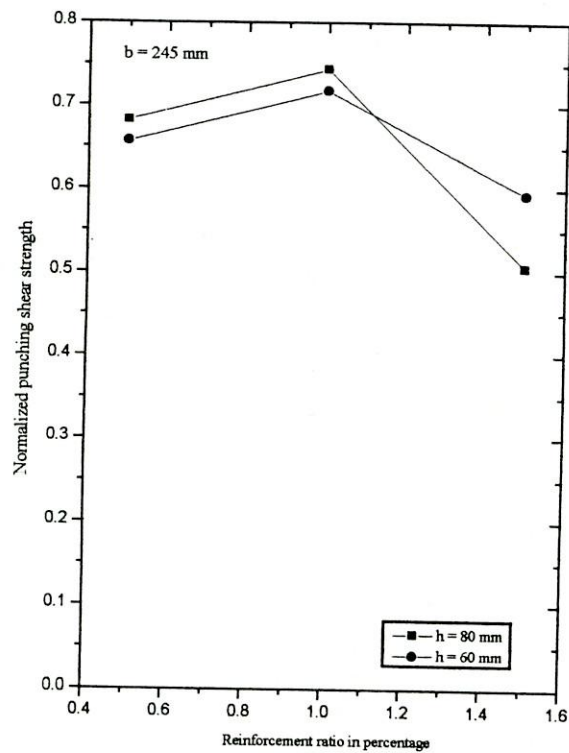


Figure 5.8c : Normalized punching shear strength for same width of edge beam

From the above discussion, it can be concluded that the present Codes are not capable of predicting the punching shear strength of reinforced concrete slabs satisfactorily. For all the slabs tested, the prediction of ACI 318-95 was most conservative. On the other hand, although CEB-FIP Code predictions were very much on the conservation side, its prediction of punching failure load was better than the others. In general, all the Codes failed to cater for the beneficial effect of edge restraint.

CHAPTER SIX

CONCLUSION AND RECOMMENDATIONS

6.1 CONCLUSIONS

Punching tests on sixteen reinforced concrete slabs have been reported in this thesis. Thirteen of these slabs are restrained at the edges to simulate continuous slab construction. The tests results provided basic experimental information on the behaviour of restrained slabs subjected to concentrated loading. All the slab failed in a punching mode when subjected to punching load at the slab centre. The outcome of the present series of tests may become useful for the development of a rational method of analysis. Whereas, the following conclusions may be derived from the limited experimental work reported in this study, further experimental research on a wide range of slabs are, of course, needed to consolidate the findings.

- a) Punching shear strengths observed from punching tests conducted on the restrained reinforced concrete slabs have been found to be higher than the predictions of present-day design provisions. Present Code methods underestimate the punching load capacity of slabs as the Code expressions are based on tests conducted on simply-supported slabs with their edges unrestrained. The magnitude of the strength enhancement increases with the degree of edge restraint.
- b) The degree of enhancement in the punching shear capacity due to continuity at the slab edges (imposed by edge beams) do not diminish with increasing size of slabs.
- c) Whereas the level of steel reinforcement may have a slightly negative effect on the ultimate punching shear capacity of the heavily reinforced slabs, it exerts a positive influence for those lightly reinforced. Again, whereas British and European Codes recognize the influence of percentages of steel, American and

Canadian Codes completely ignore the possible influence of the amount of reinforcement in formulating its equations for punching shear capacity of slabs. The Code provisions of all these Codes may, thus, be reviewed to accommodate the influence of amount of steel in its equations more realistically.

- d) It has been found that for slabs having same size and reinforcement, the punching shear capacity increases with a corresponding increase in the slab thickness. It has been observed that thickness is a very important factor in determining the punching shear capacity of slabs having a given degree of restraint. It appears that slab thickness has, perhaps, a more positive contribution than presently recognized in the Codes.

6.2 RECOMMENDATIONS FOR FUTURE RESEARCH

The following recommendations for future study can be made from the present research :

- a) The findings of the present study may be further consolidated by conducting more tests on several models, as well as, prototype slabs.
- b) In view of the fact that laboratory experimentation is very expensive and time consuming, the punching behaviours of continuous and simply-supported slabs may be studied by using a constant parameter nonlinear finite element model for structural concrete.

REFERENCES

- ACI committee 318 (1983), "Building Code Requirements for Reinforced Concrete (ACI 318-83)," American Concrete Institute, Detroit, 1983.
- ACI committee 318 (1989), "Building Code Requirements for Reinforced Concrete (ACI 318-89)," American Concrete Institute, Detroit, 1989.
- ACI committee 318 (1995), "Building Code Requirements for Reinforced Concrete (ACI 318-95)," American Concrete Institute, Detroit, 1995.
- Bangladesh National Building Code (1993), Prepared for Housing and Building Research Institute, Dhaka, Bangladesh. 1993.
- Bazant, Z. P. and Coa, Z. (1987), "Size Effect in Punching Shear Failure of Slabs," *ACI Structural Journal*, Jan.-Feb. 1987, pp 44-51.
- BS 8110 (1985), "Structural use of Concrete: Part 1: Code of Practice for Design and Construction," British Standard Institution, London, 1985.
- CAN3-A23.3-M84 (1984), "Design of Concrete for Buildings," Canadian Standards Association, Rexdale, 1984.
- CEB-FIP (1978), "Model Code for Concrete Structures," Comite Euro-International du Beton, Cement and Concrete Association, London, 1978.
- Ferguson, P. M., Breen, J. E. and Jirsa, J. O., "Reinforced Concrete Fundamentals", (Fifth edition), Published by John Wiley & Sons.
- Gardner, N. J. (1990), "Relationship of the Punching Shear Capacity of Reinforced Concrete Slabs with Concrete Strength," *ACI Structural Journal*, V.87, No.1, Jan.-Feb. 1990, pp 66-71.

- Hammil, N and Ghali, A. (1994), "Punching Shear Resistance of Corner Slab-Column Connections," *ACI Structural Journal*, V.91, No.6, Nov.-Dec., 1994, pp 697-707.
- Kuang, J. S. and Morley, C. T. (1992), "Punching Shear Behaviour of Restrained Reinforced Concrete Slabs," *ACI Structural Journal*, V.89, No.1, Jan.-Feb. 1992, pp 13-19.
- Lovrovich, J. S. and McLean, D. I. (1990), "Punching Shear Behaviour of Slabs with varying Span-Depth Ratios," *ACI Structural Journal*, V.87, No.5, Sept.-Oct. 1990, pp 507-511.
- McLean, D. I. , Phan, L. T. and White, R. N. (1990), "Punching Shear Behaviour of Light Concrete," *ACI Structural Journal*, V.87, No.4, July-Aug. 1990, pp 386-392.
- Nilson, A. H. and Winter, G., "Design of Concrete Structures", (11th edition), Published by McGraw-Hill Book Company.
- Rankin, G. I. B. and Long, A. E. (1987a), "Predicting the Punching Strength of Conventional Slab Column Specimens," *Proceedings the Institute of Civil Engineers (London)*, V.82, Part 1, April. 1987 pp 327-346.
- Rankin, G. I. B. and Long, A. E. (1987b), "Predicting the Punching Strength of Interior Slab Column Connection," *Proceedings the Institute of Civil Engineers (London)*, V.82, Part 1, Dec. 1987, pp 1185-1186.
- Regan, P. E., Jorabi, H. R. (1988), "Shear Resistance of One Way Slabs Under Concentrated Load," *ACI Structural Journal*, V.85, No.2, March-April, 1988, pp 150-157.

Seraj, S. M., Kotsovos, M. D. and Pavlovic, M. N. (1995), "Behaviour of High-Strength Mix Reinforced Concrete Beams", *Journal of Archives of Civil Engineers, Proceedings Polish Academy of Sciences*, V. 41, No. 1, pp. 31-67.

Shukry, M. E. S. and Goode, C. D. (1990), "Punching Shear Strength of Composite Construction," *ACI Structural Journal*, V. 87, No. 1, Jan.-Feb. 1990, pp 12-22.

Shetty, M. S., "Concrete Technology", Published by S. Chand & Company Ltd., Ram Nagar, New Delhi-110055.

Yamada, T., Nanni, A. and Endo, K. (1992), "Punching Shear Resistance of Flat Slabs : Influence of Reinforcement Type and Ratio," *ACI Structural Journal*, V.88, No. 4, Sept.-Oct. 1992, pp 555-563.

APPENDIX A

Details section and reinforcement of all slabs

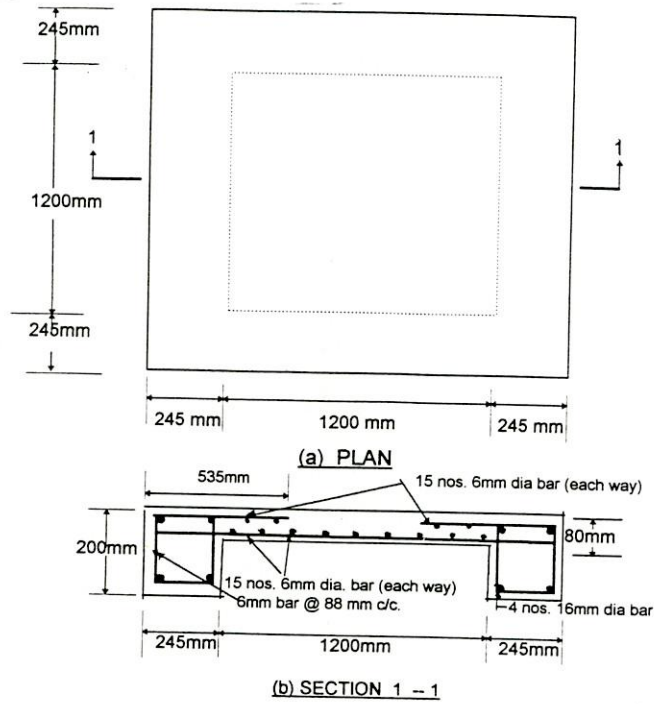


Figure A-1 (a) Plan (b) Section and reinforcement details of SLAB1

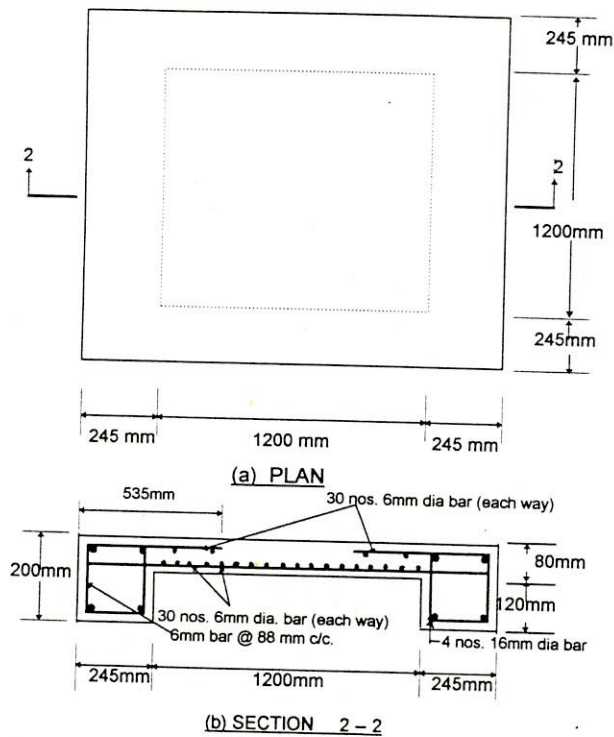


Figure A-2 (a) Plan (b) Section and reinforcement details of SLAB2

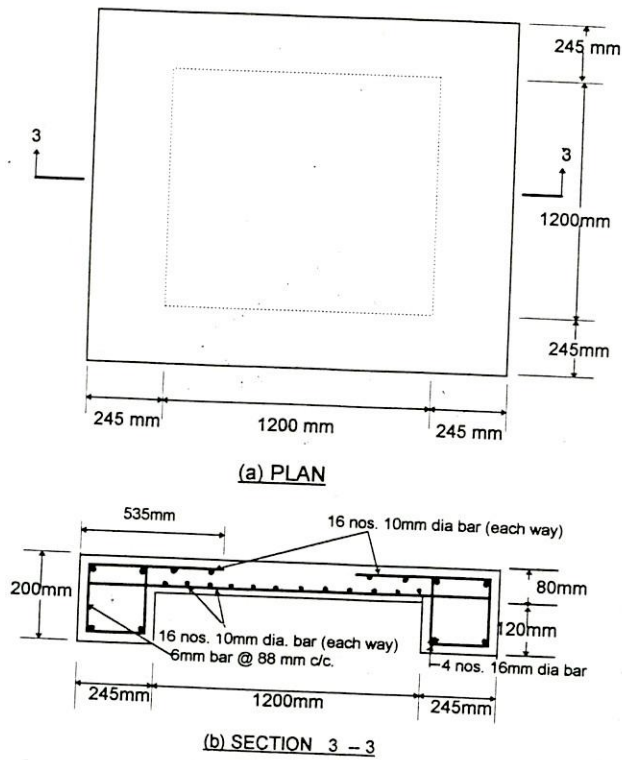


Figure A-3 (a) Plan (b) Section and reinforcement details of SLAB3

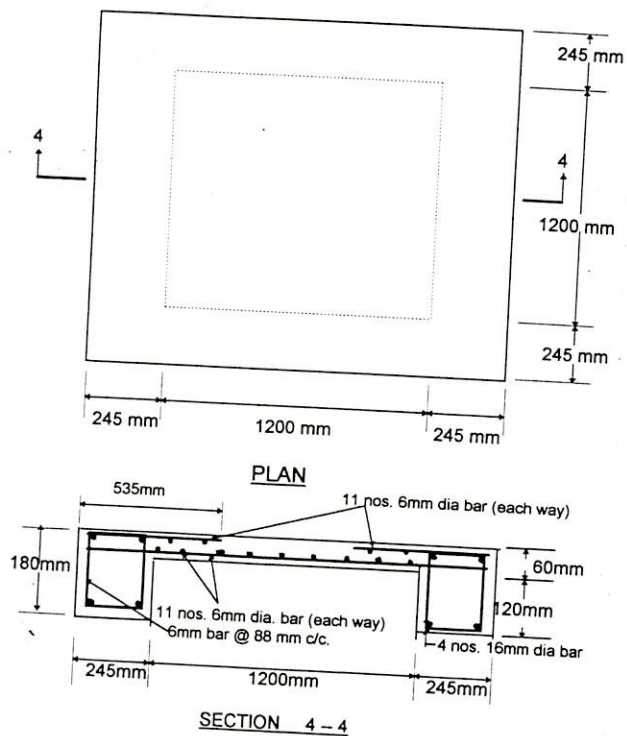


Figure A-4 (a) Plan (b) Section and reinforcement details of SLAB4

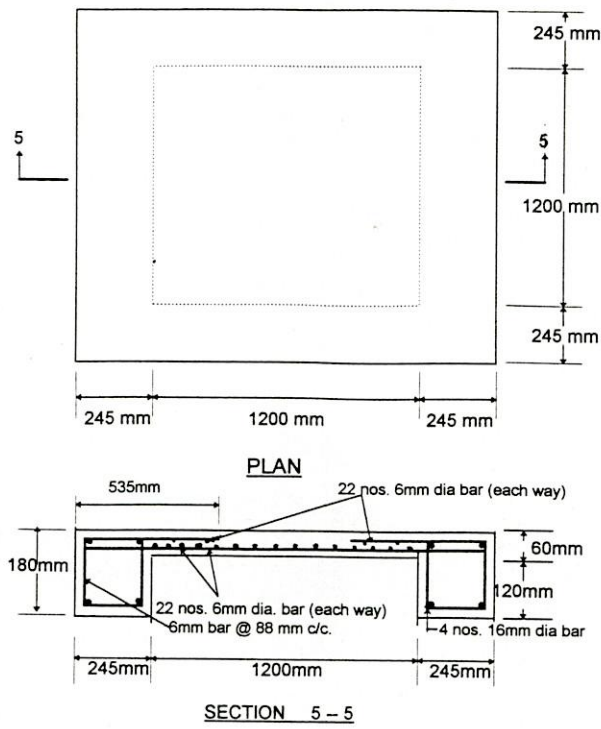


Figure A-5 (a) Plan (b) Section and reinforcement details of SLAB5

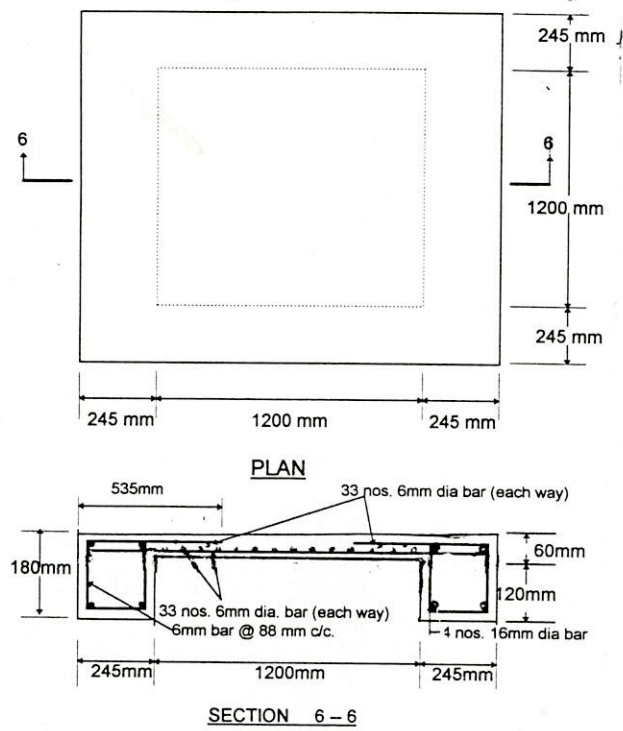


Figure A-6 (a) Plan (b) Section and reinforcement details of SLAB6

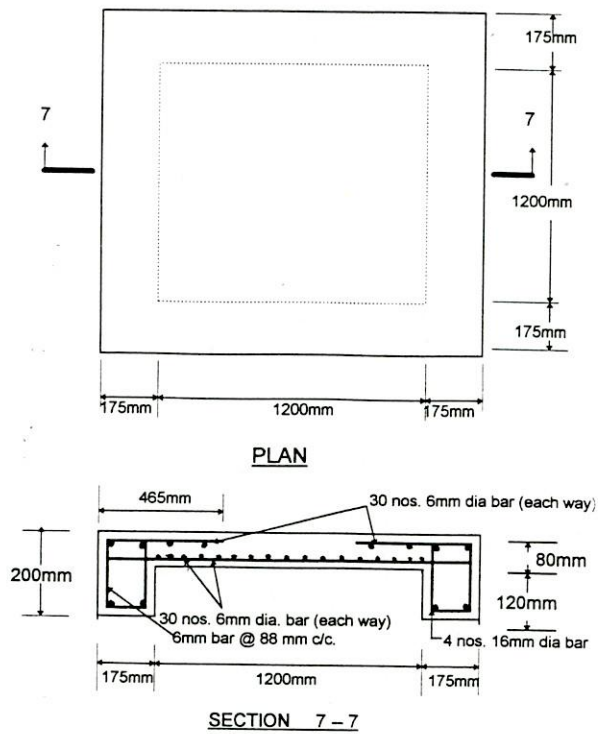


Figure A-7 (a) Plan (b) Section and reinforcement details of SLAB7

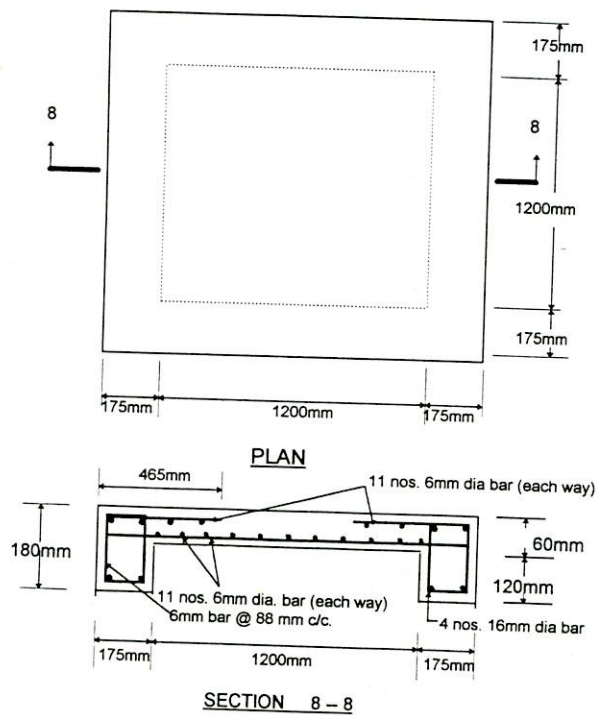


Figure A-8 (a) Plan (b) Section and reinforcement details of SLAB8

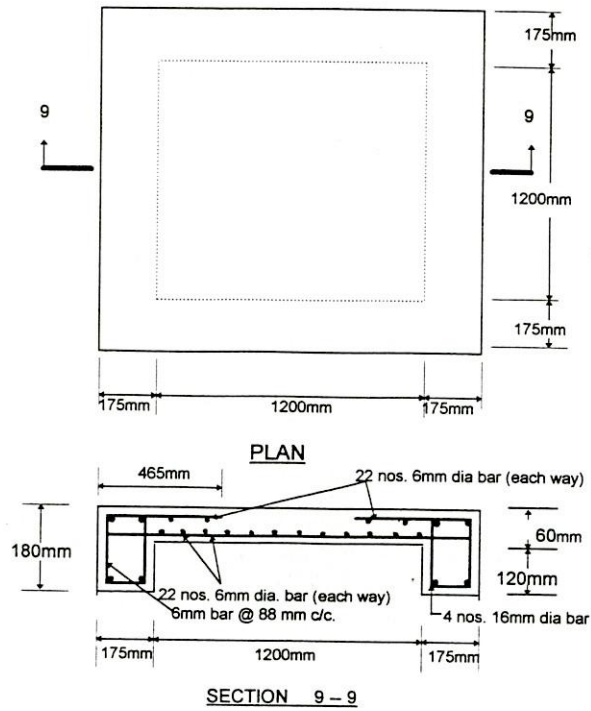


Figure A-9 (a) Plan (b) Section and reinforcement details of SLAB9

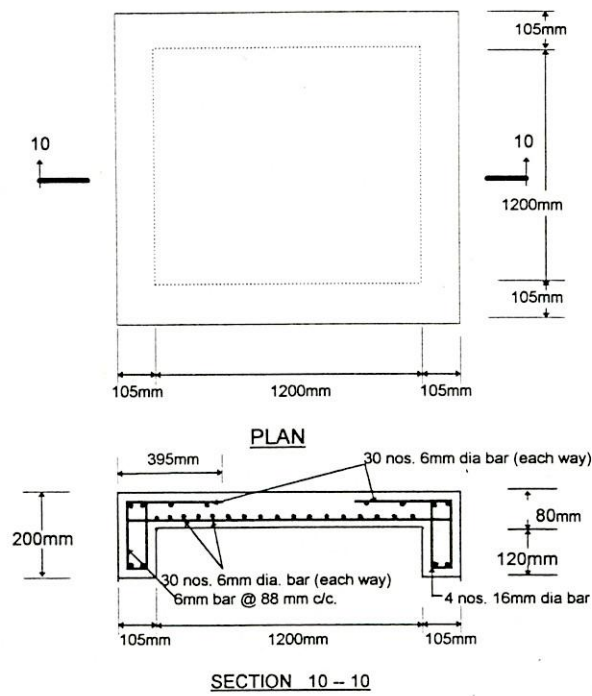


Figure A-10 (a) Plan (b) Section and reinforcement details of SLAB10

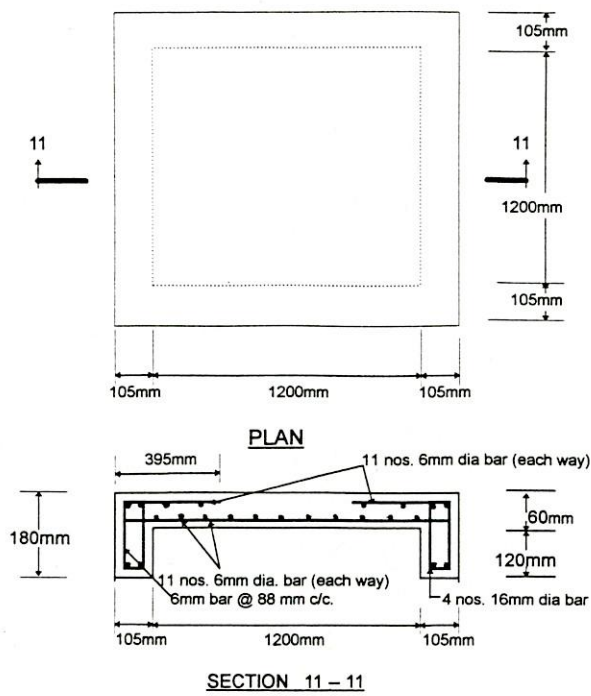


Figure A-11 (a) Plan (b) Section and reinforcement details of SLAB 11

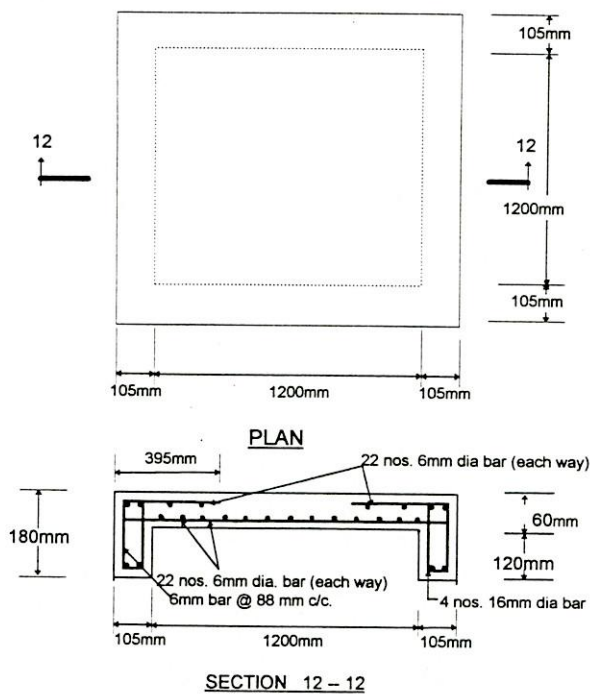


Figure A-12 (a) Plan (b) Section and reinforcement details of SLAB 12

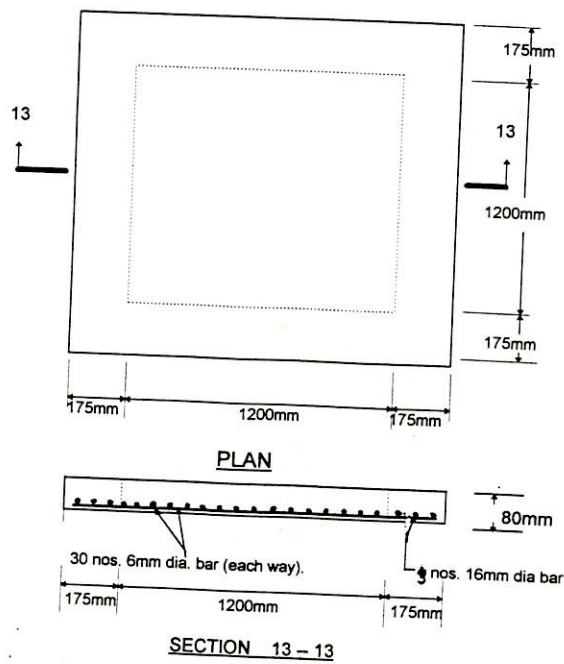


Figure A-13 (a) Plan (b) Section and reinforcement details of SLAB13

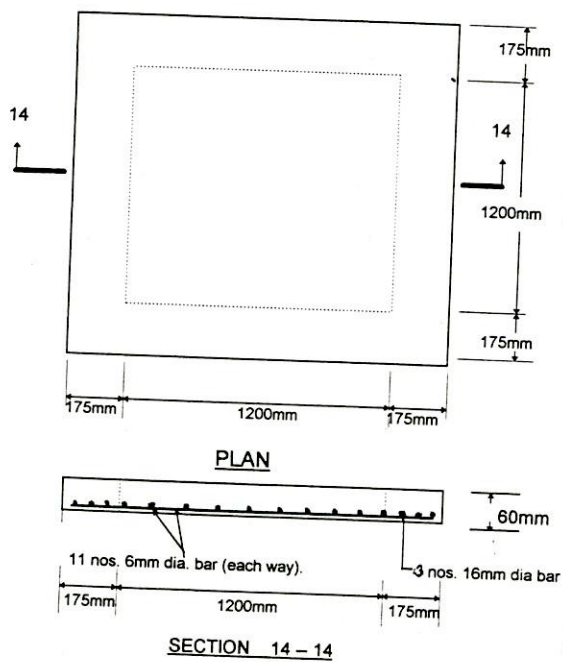


Figure A-14 (a) Plan (b) Section and reinforcement details of SLAB14

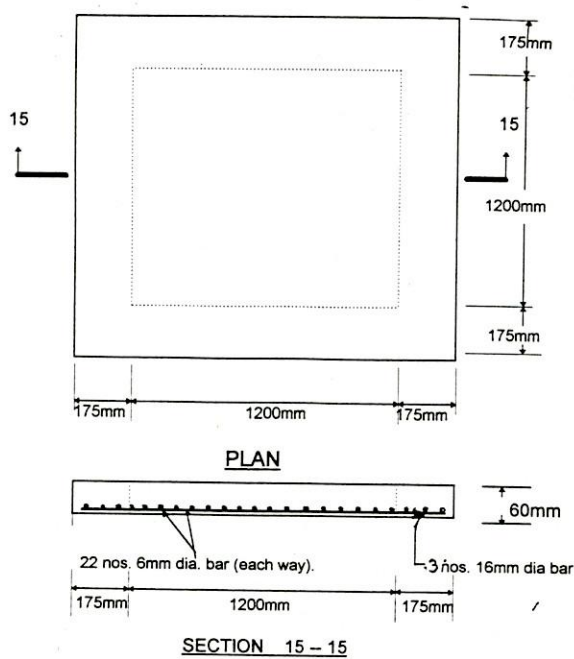


Figure A-15 (a) Plan (b) Section and reinforcement details of SLAB15

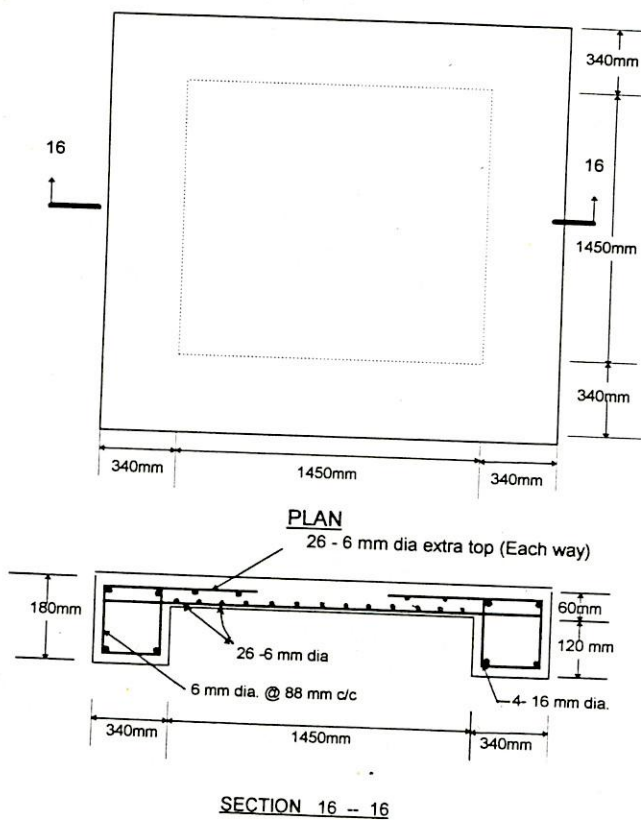


Figure A-16 (a) Plan (b) Section and reinforcement details of SLAB16

APPENDIX B

Calculation of design strength and torsional rigidity of slabs

DESIGN B-1 Design of slab samples of slab thickness = 80 mm (SLAB1, SLAB2, SLAB3, SLAB7, SLAB10 and SLAB13)

Design data :

$$d = 70 \text{ mm}$$

$$c = \text{length of loaded area} = 120 \text{ mm (Section 3.3)}$$

$$b_0 = 4(d+c) = 4(70+120) = 760 \text{ mm}$$

$$f'_c = 36 \text{ MPa}$$

(I) According to ACI 318-89 Code provision

From equation (2.3b)

Punching shear strength,

$$\begin{aligned} V_c &= 0.33 \times \sqrt{36} \times 760 \times 70 / 1000 \text{ kN} \\ &= 105.34 \text{ kN} \end{aligned}$$

(II) According to BS 8110-85 Code provision

$$f'_{cu} = f'_c / 0.80 = 36 / 0.80 \text{ MPa} = 45.00 \text{ MPa} > 40.00 \text{ MPa}$$

Accepted $f'_{cu} = 40.00 \text{ MPa}$

$$400/d = 400/70 = 5.7143 > 1.00 \text{ O.K}$$

Accepted $400/d = 5.7143$

(a) for $\rho = 0.5 \text{ percent}$

From equation (2.4),

Punching shear strength,

$$\begin{aligned} V_p &= 3.16 \sqrt[3]{100 \times 0.5 / 100} \sqrt[3]{40 / 25} \sqrt[4]{400 / 70} (120 + 3 \times 70) 70 / 1000 \text{ kN} \\ &= 104.77 \text{ kN} \end{aligned}$$

(b) for $\rho = 1.0 \text{ percent}$

$$\begin{aligned} V_p &= 3.16 \sqrt[3]{100 \times 1.0 / 100} \sqrt[3]{40 / 25} \sqrt[4]{400 / 70} (120 + 3 \times 70) 70 / 1000 \text{ kN} \\ &= 132.00 \text{ kN} \end{aligned}$$

(c) for $\rho = 1.5 \text{ percent}$

$$V_p = 3.16 \sqrt[3]{100 \times 1.5 / 100} \sqrt[3]{40 / 25} \sqrt[4]{400 / 70} (120 + 3 \times 70) 70 / 1000 \text{ kN}$$

$$= 151.10 \text{ kN}$$

(III) According to CAN3-A23.3-M84 Code provision

From equation (2.5)

Punching shear strength,

$$V_p = 0.4 \times \sqrt{36} \times 760 \times 70 / 1000 \text{ kN}$$

$$= 127.68 \text{ kN}$$

(IV) According to CEB-FIP Code provision

From equation (2.6)

$$\tau_{rd} = 0.075 (f_c)^{2/3} = 0.075 (36)^{2/3} = 0.8177$$

$$k = 1.6 - d/1000 = 1.6 - 70/1000 = 1.53 > 1.0$$

Accepted $k = 1.53$

(a) for $\rho = 0.5$ percent

$$v_c = 1.6 \tau_{rd} k (1 + \rho/2)$$

$$= 1.6 \times 0.8177 \times 1.53 (1 + 0.5/2)$$

$$= 2.5022$$

Punching shear strength,

$$V_p = v_c b_0 d = 2.5022 \times 760 \times 70 / 1000 \text{ kN}$$

$$= 133.12 \text{ kN}$$

(b) for $\rho = 1.0$ percent and $\rho = 1.5$ percent

Accepted $\rho = 0.8$ percent

$$v_c = 1.6 \times 0.8177 \times 1.53 (1 + 0.8/2)$$

$$= 2.8025$$

Punching shear strength,

$$V_p = v_c b_0 d = 2.8024 \times 760 \times 70 / 1000 \text{ kN}$$

$$= 149.09 \text{ kN}$$

DESIGN B-2 Design of slab samples of slab thickness = 60 mm (SLAB4, SLAB5, SLAB6, SLAB8, SLAB9, SLAB11, SLAB12, SLAB14, SLAB15 and SLAB16)

Design data :

$$d = 50 \text{ mm}$$

$$c = \text{Edge length of loaded area} = 120 \text{ mm (Section 3.3)}$$

$$b_0 = 4(d+c) = 4(50+120) = 680 \text{ mm}$$

$$f'_c = 36 \text{ MPa}$$

(I) According to ACI 318-89 Code provision

From equation (2.3b)

Punching shear strength,

$$\begin{aligned} V_c &= 0.33 \times \sqrt{36} \times 680 \times 50 / 1000 \text{ kN} \\ &= 67.32 \text{ kN} \end{aligned}$$

(II) According to BS 8110-85 Code provision

$$f_{cu} = f'_c / 0.80 = 36 / 0.80 \text{ MPa} = 45.00 \text{ MPa} > 40.00 \text{ MPa}$$

Accepted $f_{cu} = 40.00 \text{ MPa}$

$$400/d = 400/50 = 8.00 > 1.00 \quad \text{O.K}$$

Accepted $400/d = 8.00$

(a) *for $\rho = 0.5$ percent*

From equation (2.4),

Punching shear strength,

$$\begin{aligned} V_p &= 3.16 \sqrt[3]{100 \times 0.5 / 100} \sqrt[3]{40 / 25} \sqrt[4]{400 / 50} (120 + 3 \times 50) 50 / 1000 \text{ kN} \\ &= 66.60 \text{ kN} \end{aligned}$$

(b) *for $\rho = 1.0$ percent*

$$\begin{aligned} V_p &= 3.16 \sqrt[3]{100 \times 1.0 / 100} \sqrt[3]{40 / 25} \sqrt[4]{400 / 50} (120 + 3 \times 50) 50 / 1000 \text{ kN} \\ &= 83.91 \text{ kN} \end{aligned}$$

(c) for $\rho = 1.5$ percent

$$V_p = 3.16 \sqrt[3]{100 \times 1.5 / 100} \sqrt[3]{40 / 25} \sqrt[4]{400 / 50} (120 + 3 \times 50) 50 / 1000 \text{ kN} \\ = 96.05 \text{ kN}$$

(III) According to CAN3-A23.3-M84 Code provision

From equation (2.5)

Punching shear strength,

$$V_p = 0.4 \times \sqrt{36} \times 680 \times 50 / 1000 \text{ kN} \\ = 81.6 \text{ kN}$$

(IV) According to CEB-FIP Code provision

From equation (2.6)

$$\tau_{rd} = 0.075 (f_c)^{2/3} = 0.075 (36)^{2/3} = 0.8177$$

$$k = 1.6 - d/1000 = 1.6 - 50/1000 = 1.55 > 1.0$$

Accepted $k = 1.55$

(a) for $\rho = 0.5$ percent

$$v_c = 1.6 \tau_{rd} k (1 + \rho/2) \\ = 1.6 \times 0.8177 \times 1.55 (1 + 0.5/2) \\ = 2.535$$

Punching shear strength,

$$V_p = v_c b_0 d = 2.535 \times 680 \times 50 / 1000 \text{ kN} \\ = 86.19 \text{ kN}$$

(b) for $\rho = 1.0$ percent and $\rho = 1.5$ percent

Accepted $\rho = 0.8$ percent

$$v_c = 1.6 \times 0.8177 \times 1.55 (1 + 0.8/2) \\ = 2.839$$

Punching shear strength,

$$V_p = v_c b_0 d = 2.839 \times 680 \times 50 / 1000 \text{ kN} \\ = 96.53 \text{ kN}$$

B-3 Calculation of torsional rigidity of slabs

For a reinforced concrete torsional restraining member, torsional rigidity is given by the following equation :

$$\text{Torsional rigidity, } C = \sum \left(1 - 0.63 \frac{x}{y}\right) \frac{x^3 y}{3}$$

Here, for L section x and y should be measured as follow,

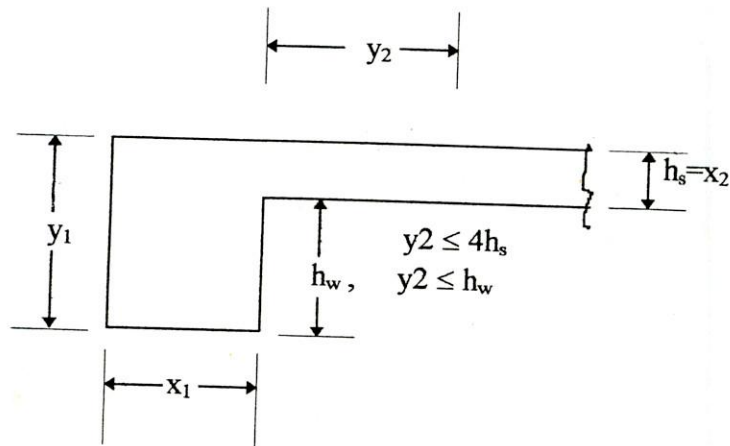


Figure B-1 Dimension of L - section for torsional rigidity.

Calculations for SLAB1-SLAB3

Here,

$$x_1 = 245 \text{ mm}, y_1 = 200 \text{ mm}$$

$$x_2 = 80 \text{ mm}, y_2 = 120 \text{ mm}$$

Thus, Torsional rigidity,

$$\begin{aligned} C &= \left(1 - 0.63 \frac{245}{200}\right) \frac{245^3 \cdot 200}{3} + \left(1 - 0.63 \frac{80}{120}\right) \frac{80^3 \cdot 120}{3} \text{ mm}^4 \\ &= 2.36 \times 10^8 \text{ mm}^4 \end{aligned}$$

Calculations for SLAB4-SLAB6

Here,

$$x_1 = 245 \text{ mm}, y_1 = 180 \text{ mm}$$

$$x_2 = 60 \text{ mm}, y_2 = 120 \text{ mm}$$

Thus, Torsional rigidity,

$$C = (1 - 0.63 \frac{245}{180}) \frac{245^3 \cdot 180}{3} + (1 - 0.63 \frac{60}{120}) \frac{60^3 \cdot 120}{3} \text{ mm}^4$$
$$= 1.32 \times 10^8 \text{ mm}^4$$

Calculations for SLAB7

Here,

$$x_1 = 175 \text{ mm}, y_1 = 200 \text{ mm}$$

$$x_2 = 80 \text{ mm}, y_2 = 120 \text{ mm}$$

Thus, Torsional rigidity,

$$C = (1 - 0.63 \frac{175}{200}) \frac{175^3 \cdot 200}{3} + (1 - 0.63 \frac{80}{120}) \frac{80^3 \cdot 120}{3} \text{ mm}^4$$
$$= 1.72 \times 10^8 \text{ mm}^4$$

Calculations for SLAB8-SLAB9

Here,

$$x_1 = 175 \text{ mm}, y_1 = 180 \text{ mm}$$

$$x_2 = 60 \text{ mm}, y_2 = 120 \text{ mm}$$

Thus, Torsional rigidity,

$$C = (1 - 0.63 \frac{175}{180}) \frac{175^3 \cdot 180}{3} + (1 - 0.63 \frac{60}{120}) \frac{60^3 \cdot 120}{3} \text{ mm}^4$$
$$= 1.31 \times 10^8 \text{ mm}^4$$

Similarly, for SLAB10, $C = 0.64 \times 10^8 \text{ mm}^4$,

for SLAB11 and SLAB12, $C = 0.50 \times 10^8 \text{ mm}^4$,

for SLAB13, $C = 0.21 \times 10^8 \text{ mm}^4$,

for SLAB14 and SLAB15, $C = 0.10 \times 10^8 \text{ mm}^4$.

APPENDIX C

Weight of the sample and slab movement

Table C-1 Weight of the Sample

Slab	Weight	
	In kilo-gram (kg)	In kilo-Newton (kN)
SLAB1	959	9.39
SLAB2	959	9.39
SLAB3	959	9.39
SLAB4	822	8.04
SLAB5	822	8.04
SLAB6	822	8.04
SLAB7	741	7.25
SLAB8	625	6.12
SLAB9	625	6.12
SLAB10	541	5.29
SLAB11	446	4.36
SLAB12	446	4.36
SLAB13	463	4.53
SLAB14	347	3.40
SLAB15	347	3.40
SLAB16	1359	13.30
Average	705.19	6.9

Table C-2 The Actual Load and Monitored Load.

Rig Reading	Actual Load		Rig Reading	Actual Load	
	In Pounds	In kilo-Newton		In Pounds	In kilo-Newton
0	141	0.627	13.5	28963	128.833
0.5	878	3.906	14.0	29961	133.273
1.0	1614	7.179	14.5	31048	138.108
1.5	2864	12.740	15.0	32136	142.947
2.0	4114	18.300	15.5	33223	147.783
2.5	5069	22.548	16.0	34310	152.618
3.0	6023	26.792	16.5	35397	157.453
3.5	7051	31.364	17.0	36485	162.293
4.0	8005	35.608	17.5	37572	167.128
4.5	9251	41.150	18.0	38659	171.963
5.0	10423	46.364	18.5	39746	176.798
5.5	11669	51.906	19.0	40834	181.638
6.0	12913	57.440	19.5	41921	186.473
6.5	13790	61.341	20.0	43008	191.308
7.0	14595	64.921	20.5	44095	196.143
7.5	15764	70.121	21.0	45183	200.983
8.0	16860	74.997	21.5	46270	205.818
8.5	17954	79.863	22.0	47357	210.653
9.0	19049	84.734	22.5	48444	215.489
9.5	20143	89.600	23.0	49532	220.328
10.0	21234	94.462	23.5	50619	225.163
10.5	22419	99.724	24.0	51706	229.999
11.0	23602	104.986	24.5	52793	234.834
11.5	24784	110.244	25.0	53881	239.673
12.0	25967	115.506	25.5	54968	244.509
12.5	26966	119.950	26.0	56055	249.344
13.0	27967	124.403	26.5	57142	254.179



Figure C-1 Lifting of the slab at the casting yard.



Figure C-2 Slab placed on trolley.



Figure C-3 Trolley along with slab being pushed and pulled towards the laboratory.



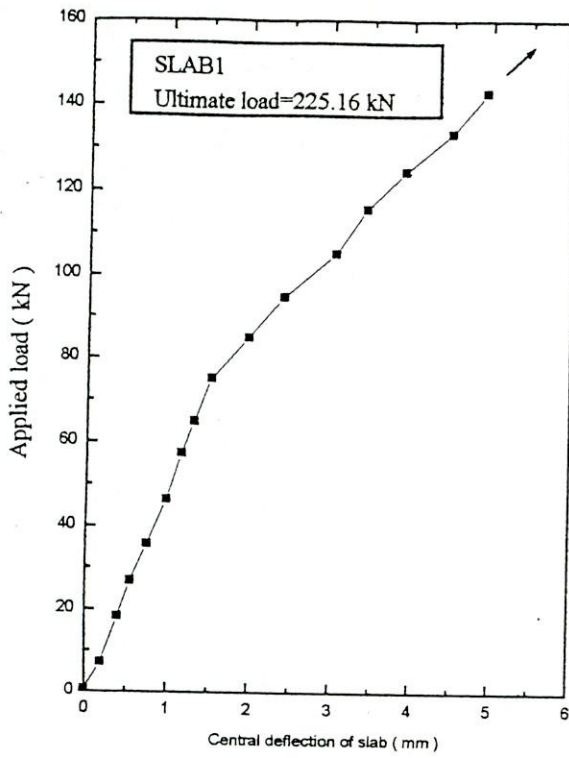
Figure C-4 Lifting of slab with two cranes for placement in the test rig.



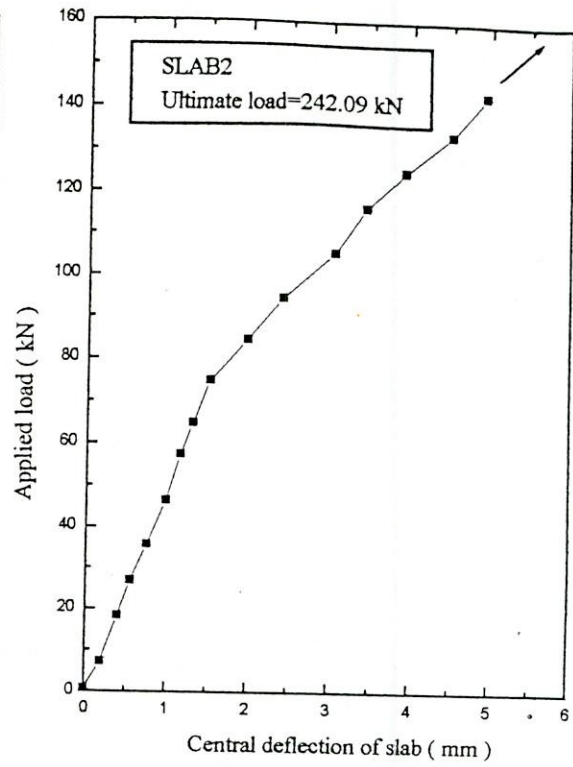
Figure C-5 Slab without edge beam (SLAB13-SLAB15) placed on test rig.

APPENDIX D

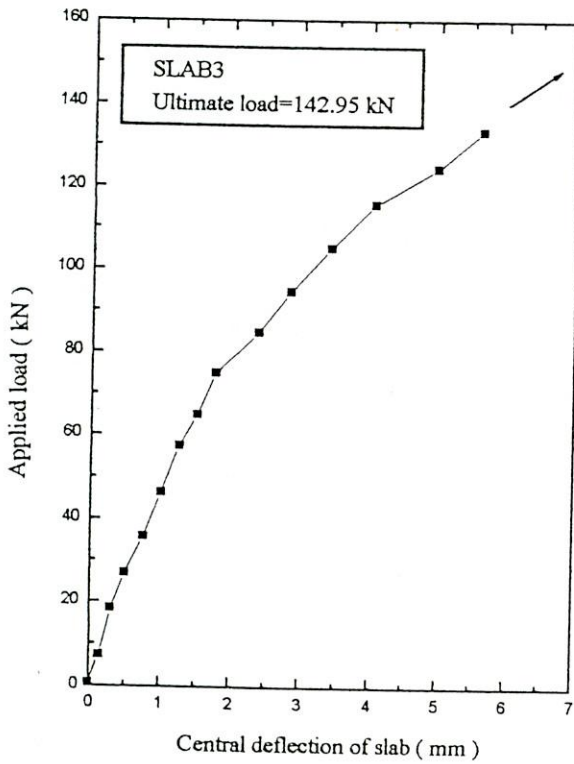
Deflections of slab and edge beam



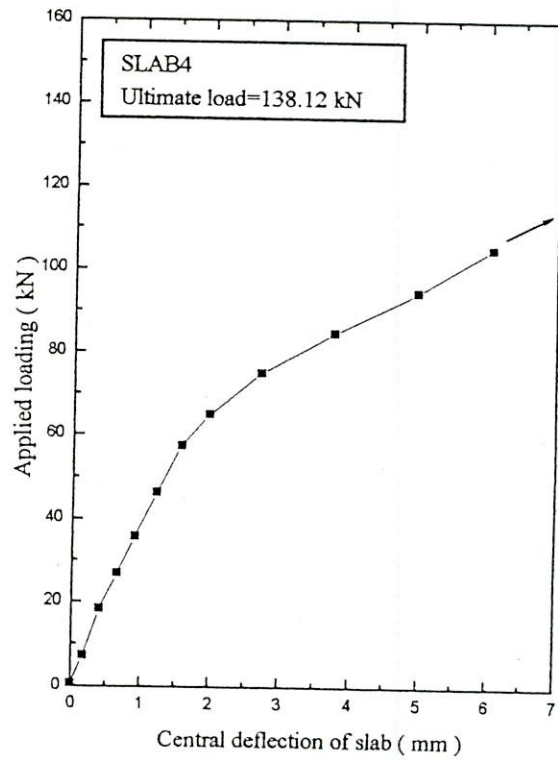
(a)



(b)

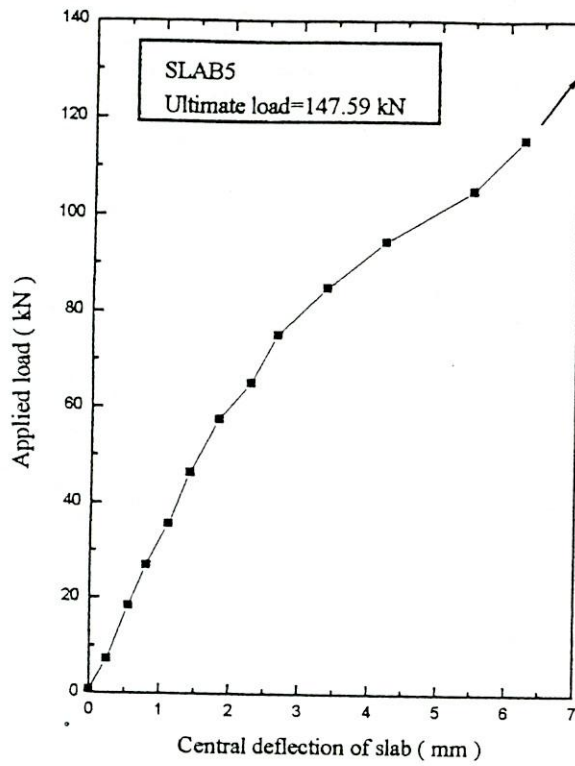


(c)

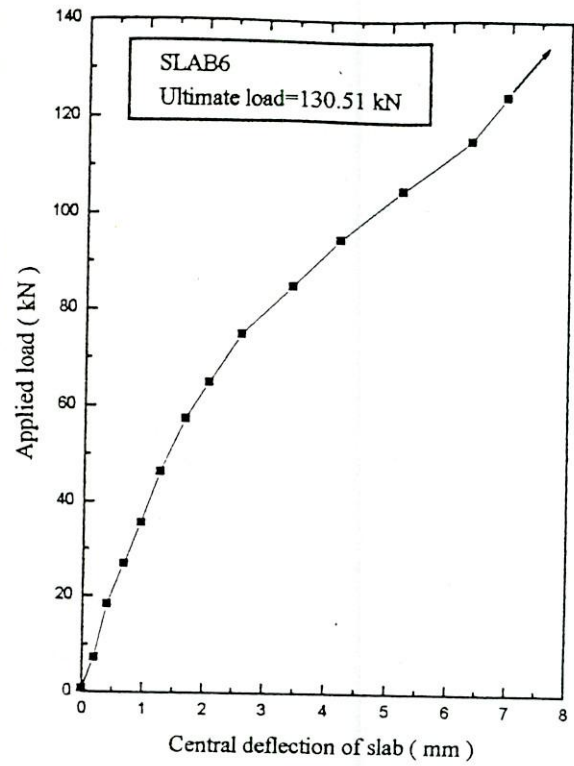


(d)

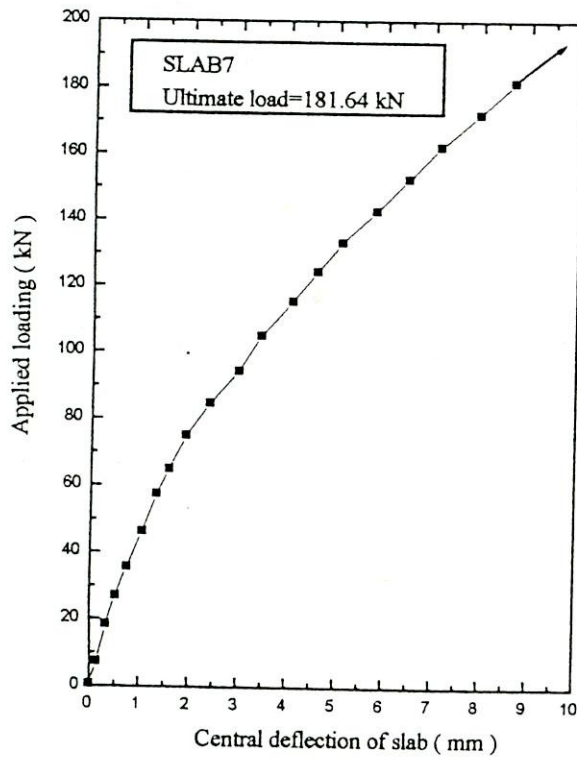
Figure D-1 : Central deflection of slab for different loading of (a) SLAB1, (b) SLAB2, (c) SLAB3 and (d) SLAB4



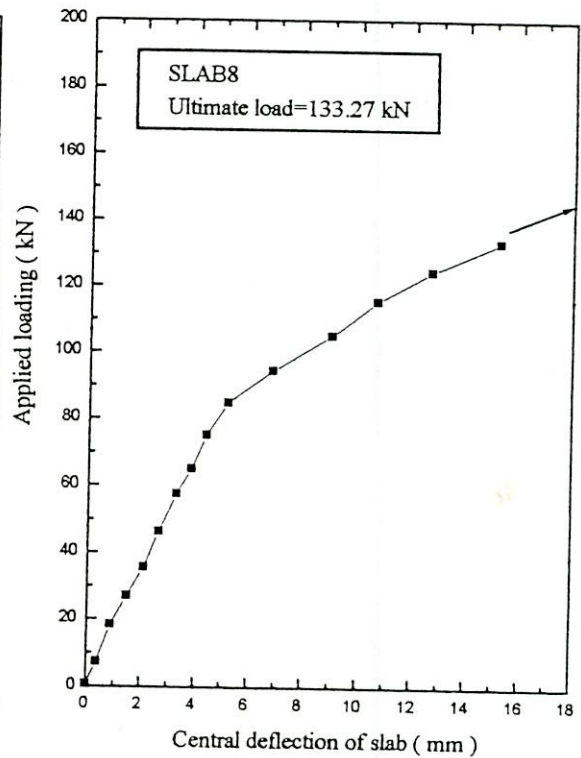
(a)



(b)

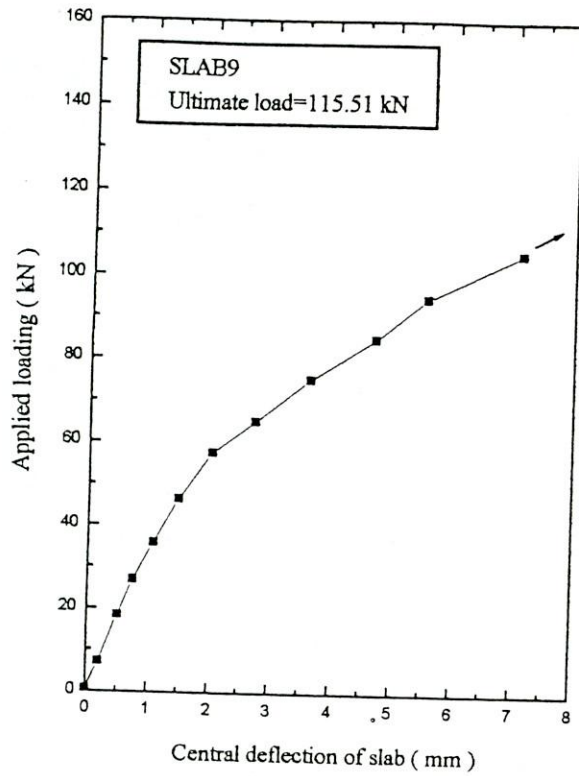


(c)

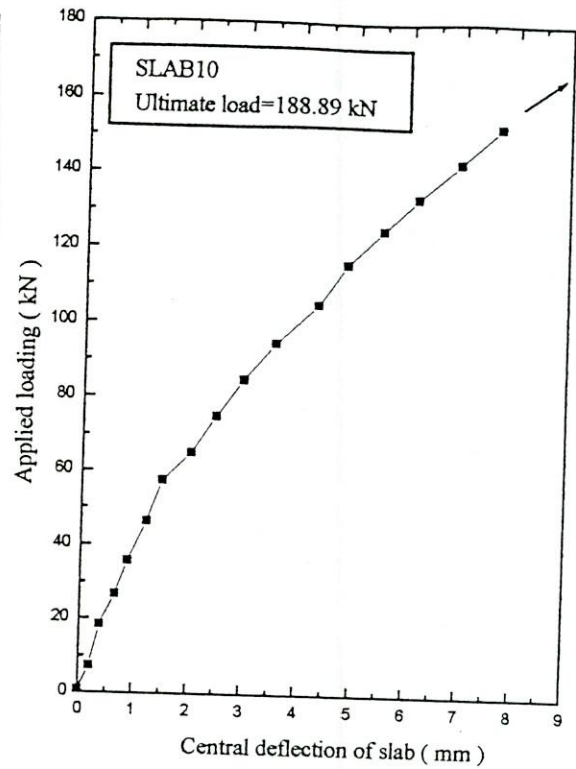


(d)

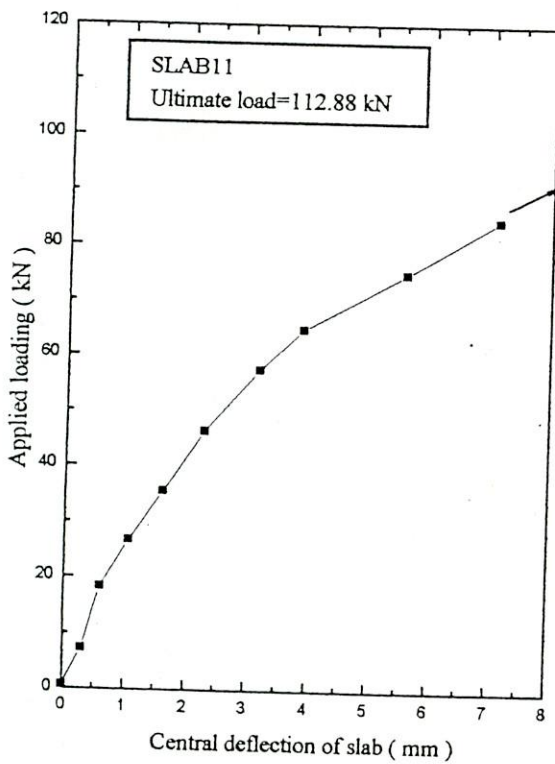
Figure D-2 : Central deflection of slab for different loading of (a) SLAB5, (b) SLAB6, (c) SLAB7 and (d) SLAB8



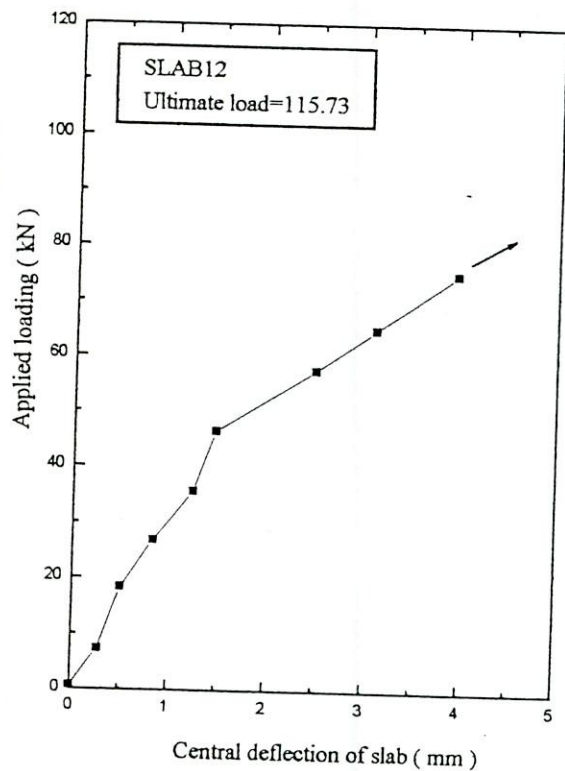
(a)



(b)

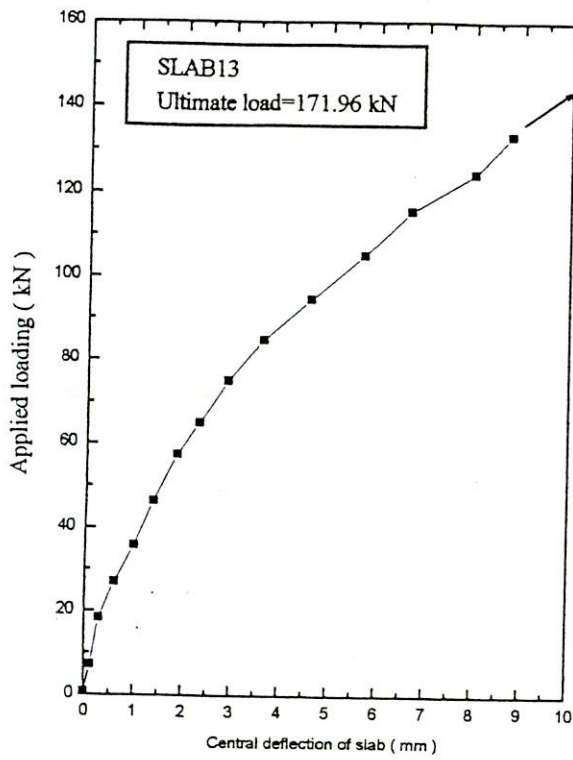


(c)

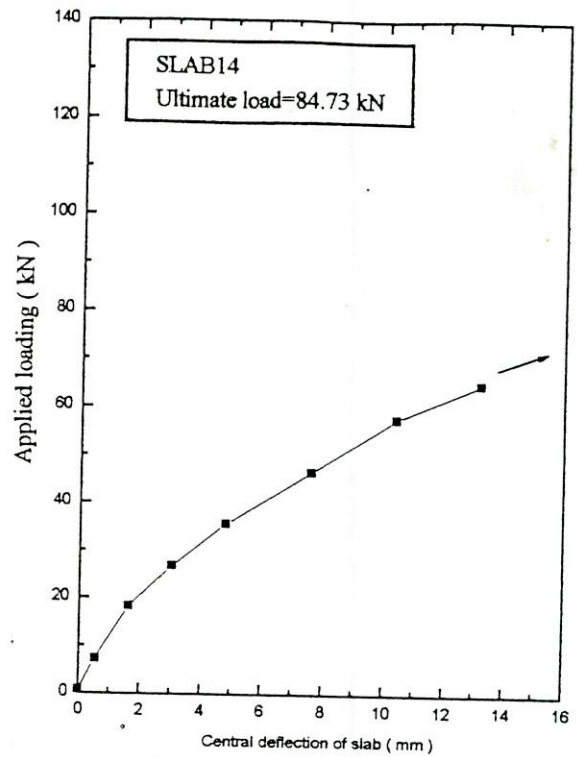


(d)

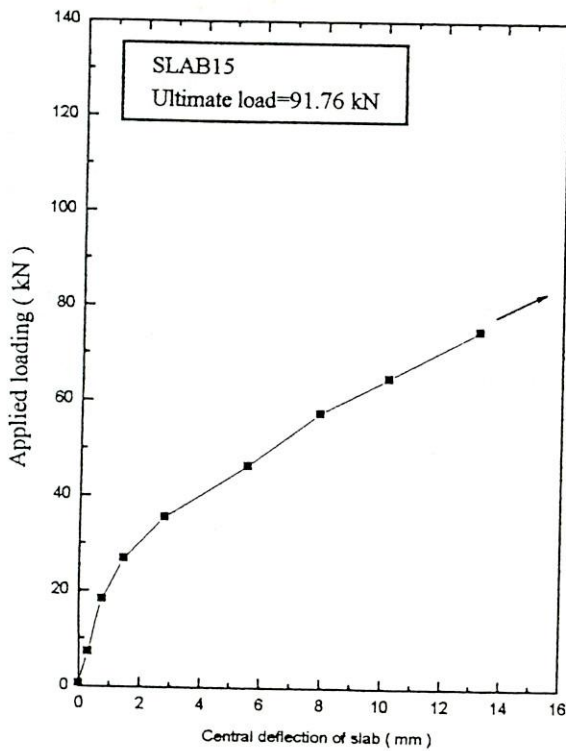
Figure D-3 : Central deflection of slab for different loading of (a) SLAB9, (b) SLAB10, (c) SLAB11 and (d) SLAB12



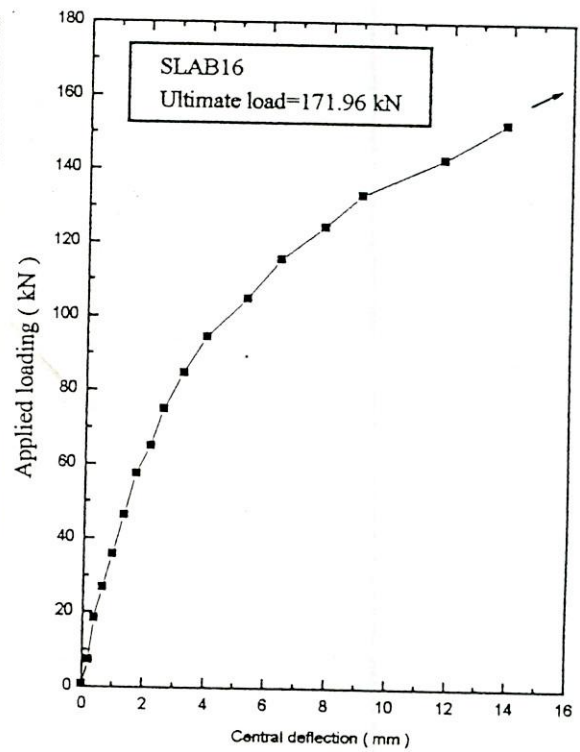
(a)



(b)

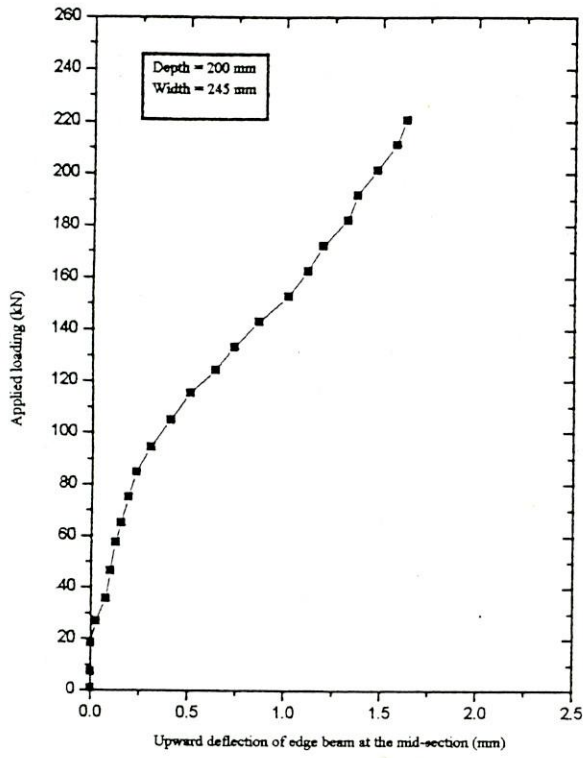


(c)

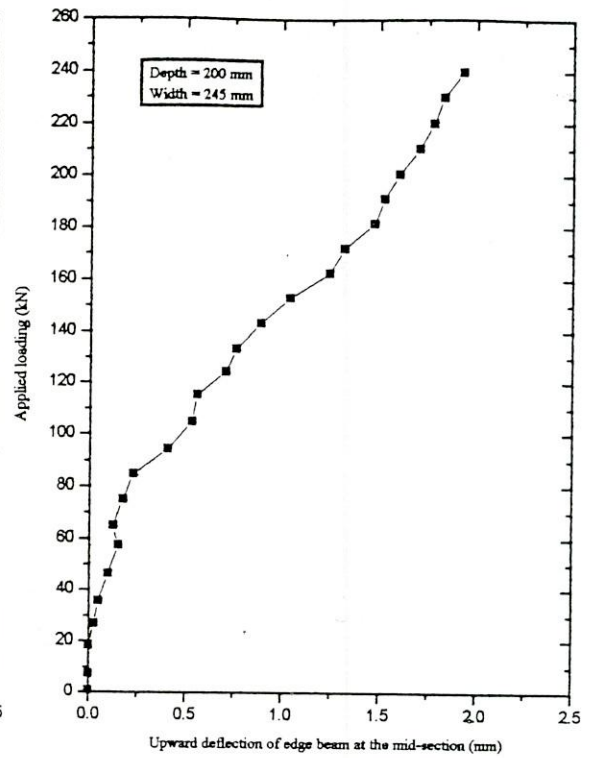


(d)

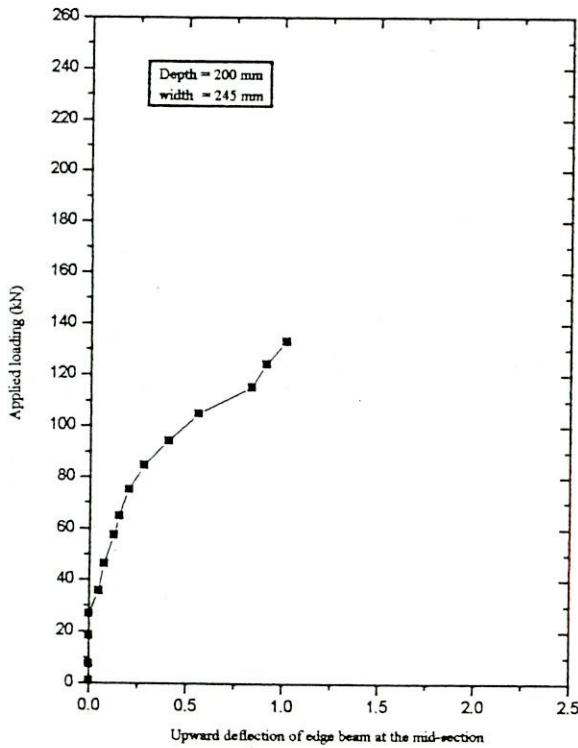
Figure D-4 : Central deflection of slab for different loading of (a) SLAB13, (b) SLAB14, (c) SLAB15 and (d) SLAB16



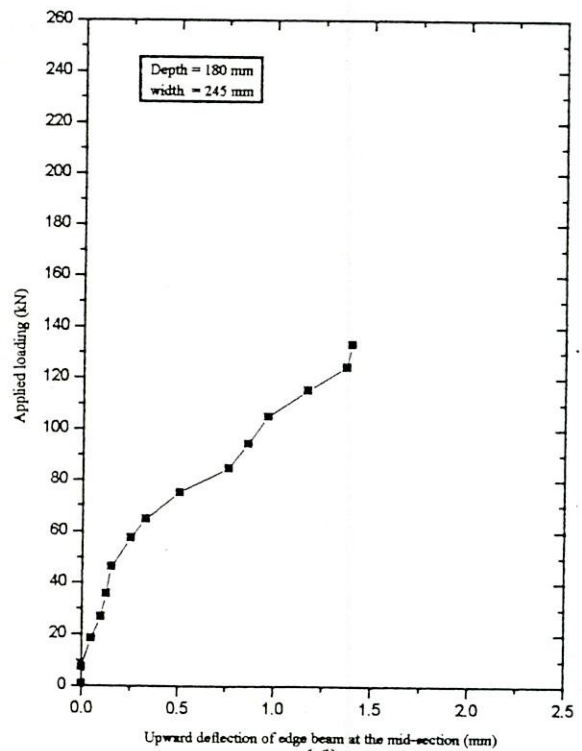
(a)



(b)

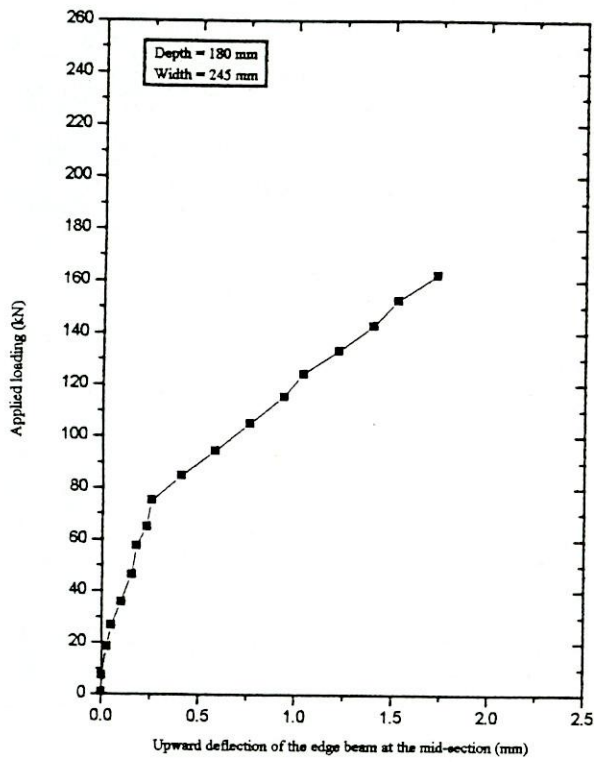


(c)

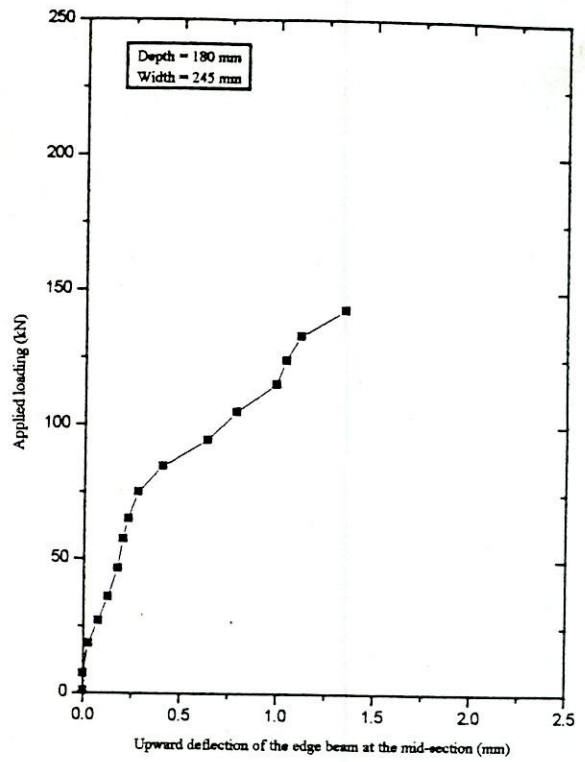


(d)

Figure D-5 : Upward deflection of edge beam at the mid-section under different loading of (a) SLAB1 (b) SLAB2 (c) SLAB3 and (d) SLAB4

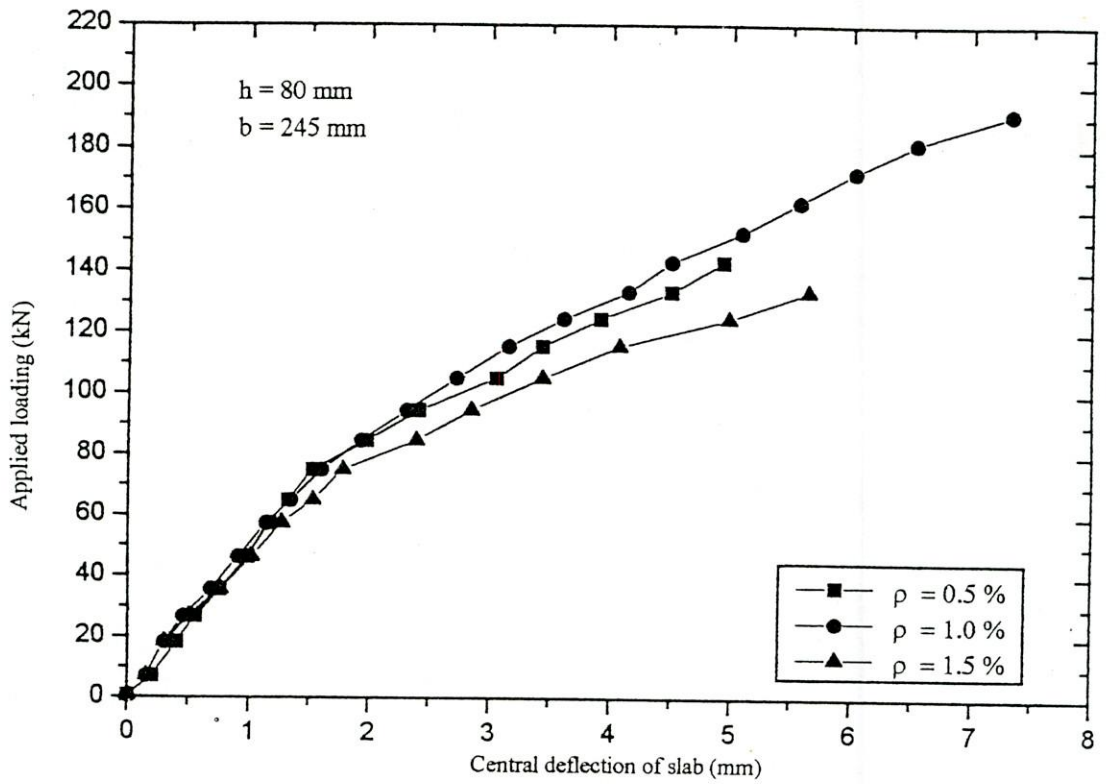


(a)

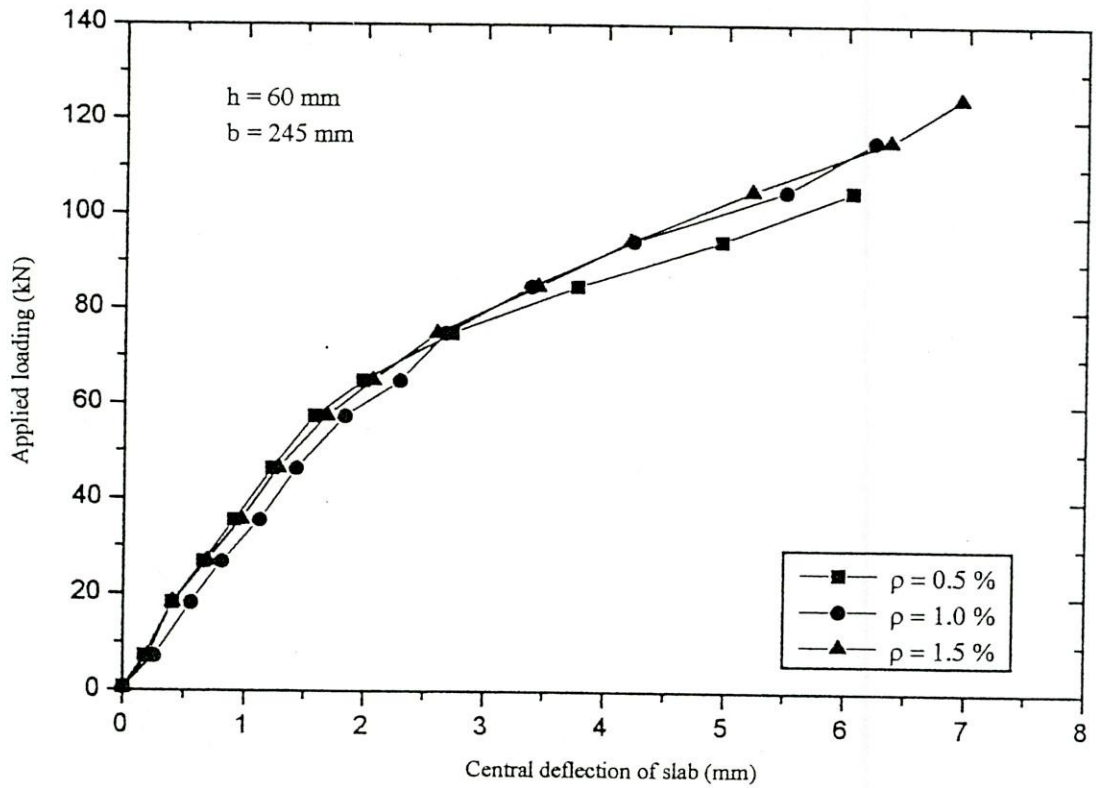


(b)

Figure D-6 : Upward deflection of the edge beam at the mid-section under different loading of (a) SLAB5 and (b) SLAB6

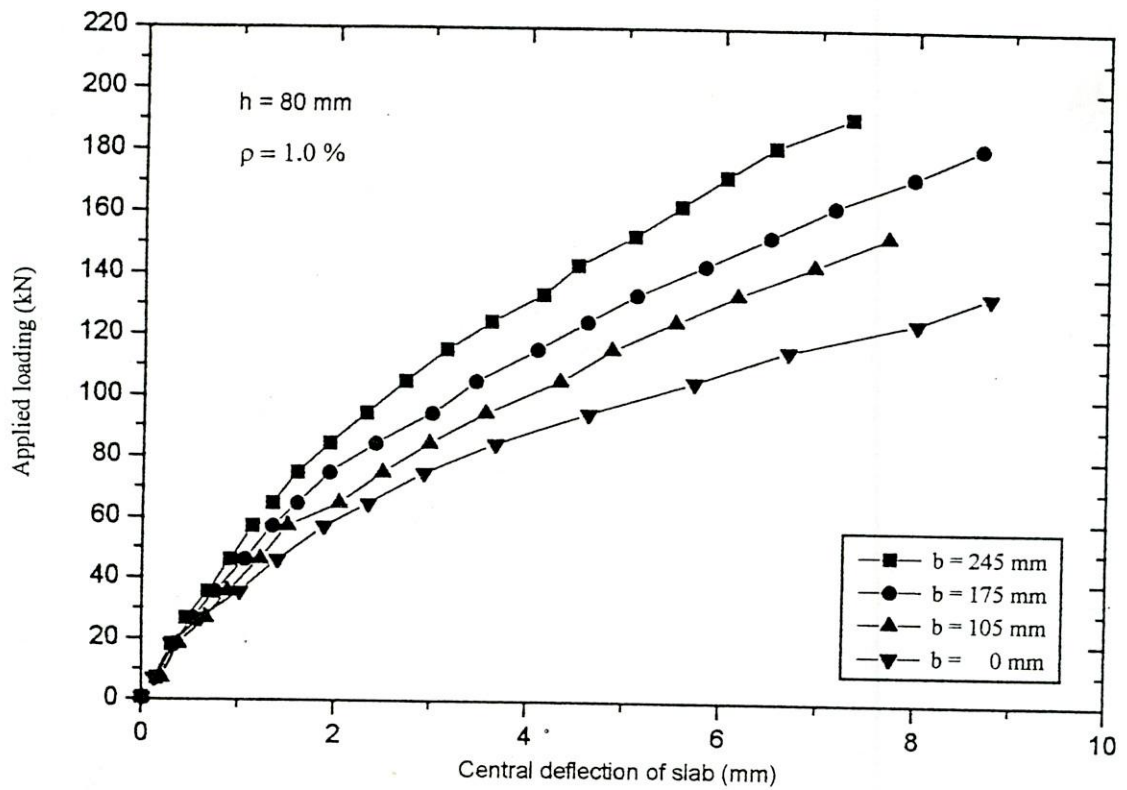


(a)

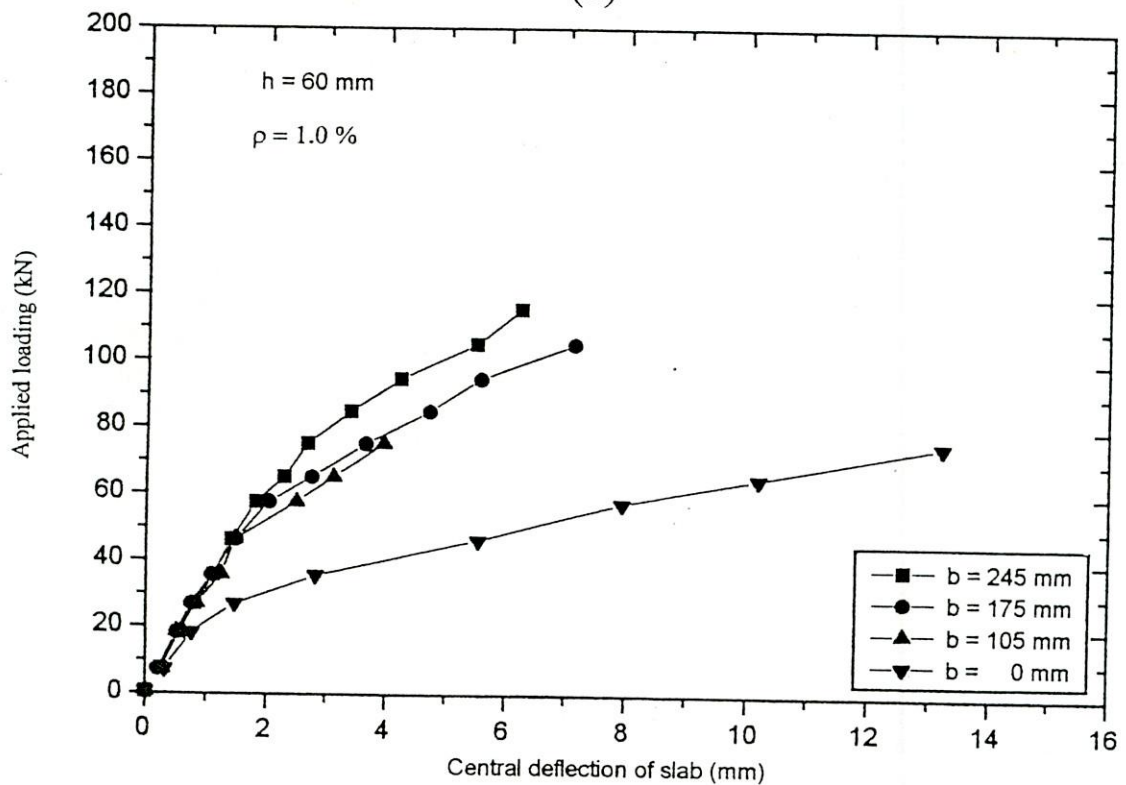


(b)

Figure D-7: Central deflection of slab under different loading of same width of edge beam (245 mm) for (a) $h=80$ mm and (b) $h=60$ mm.



(a)



(b)

Figure D-8: Central deflection of slab under applied loading for various width of edge beam at same reinforcement ratio (ρ) = 1.0 percent for (a) $h=80$ mm and (b) $h=60$ mm.

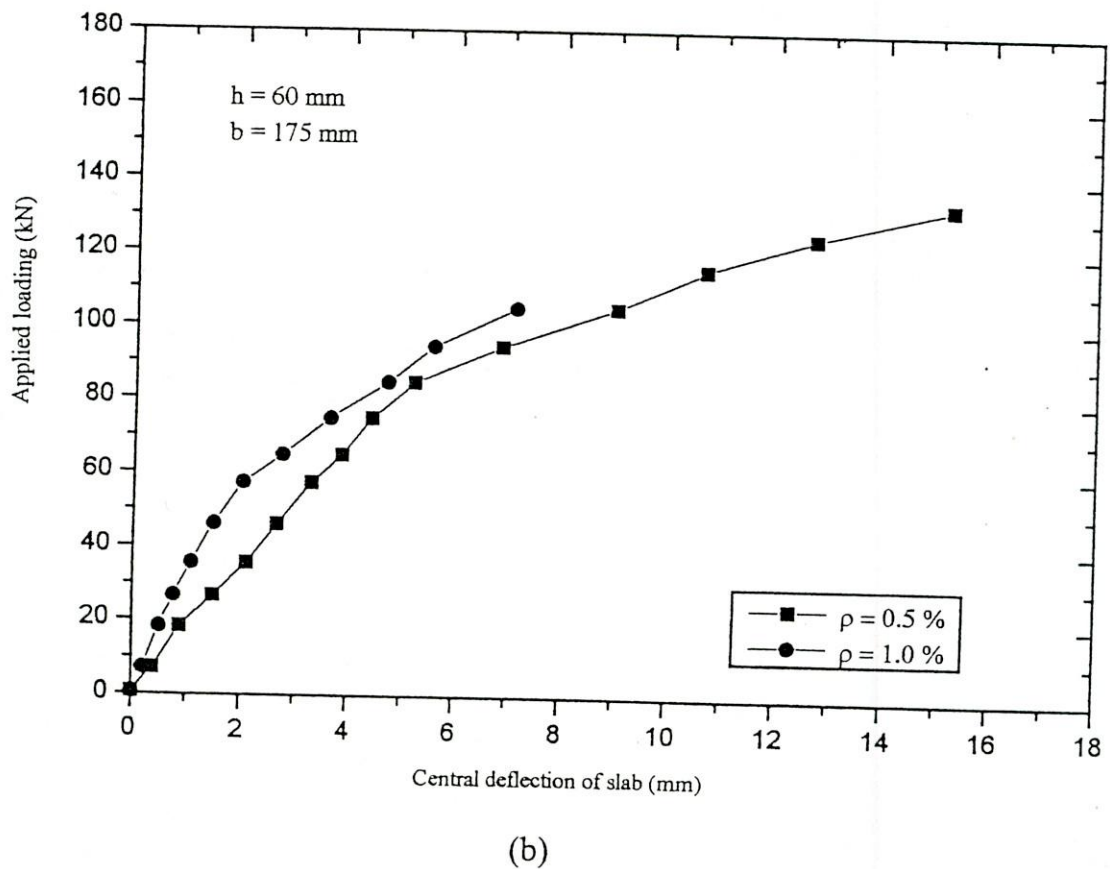
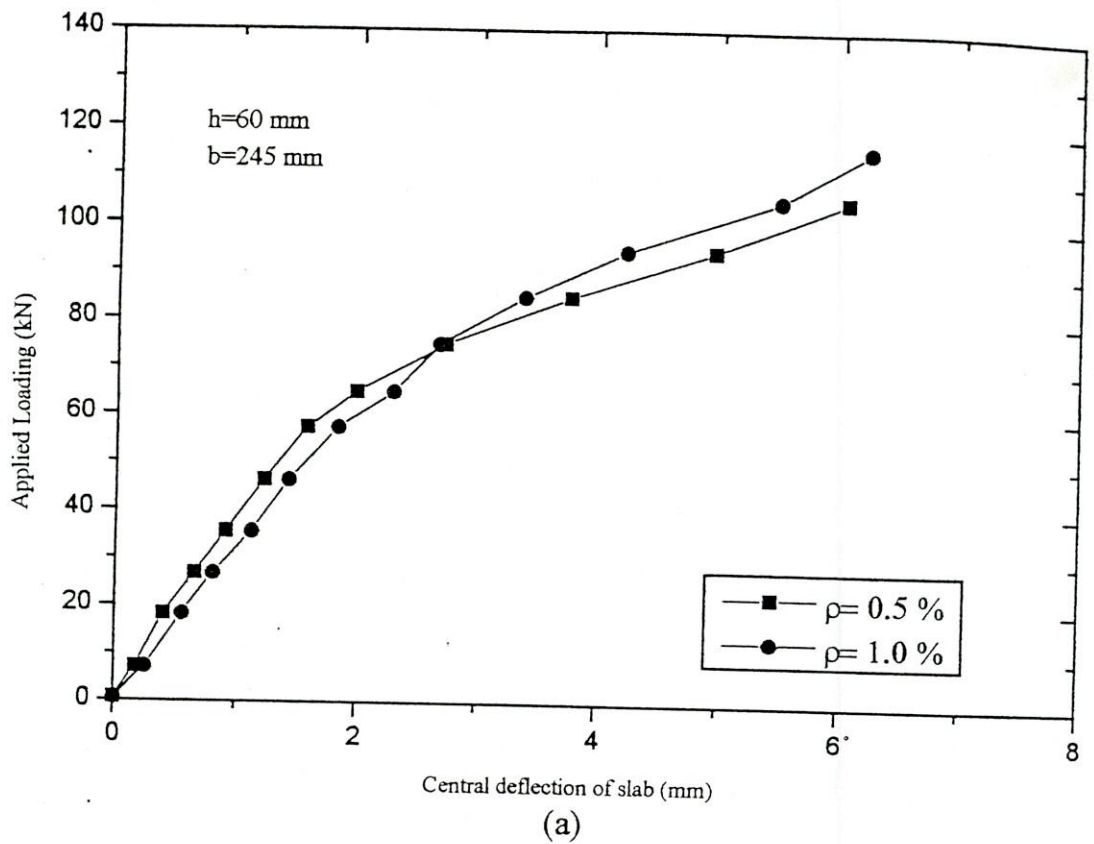
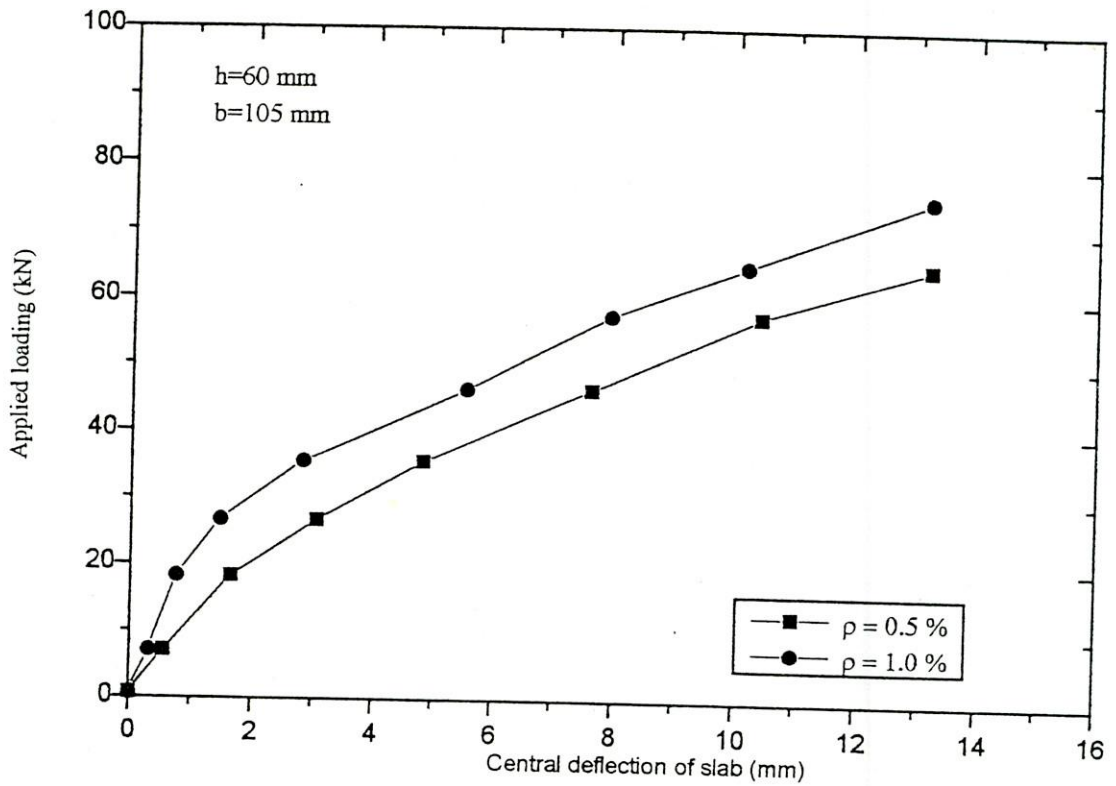
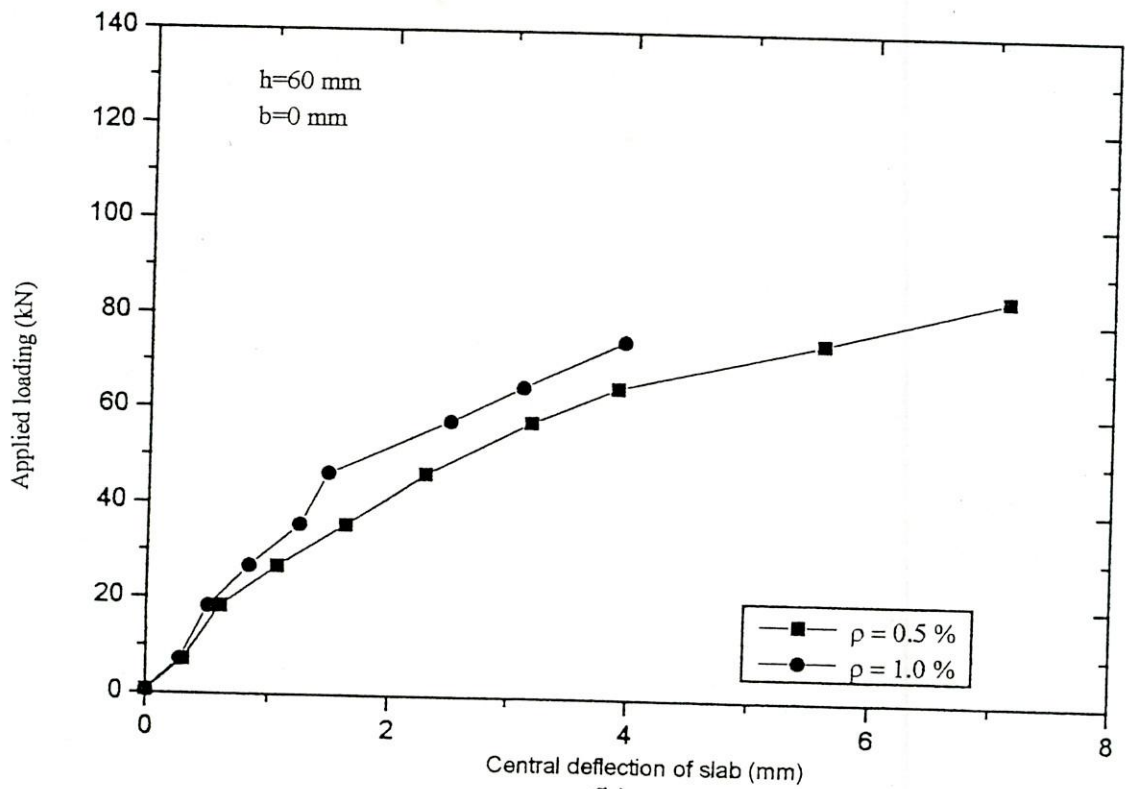


Figure D-9a: Central deflection of slab under different loading of same slab thickness (60 mm) for (a) $b = 245$ mm and (b) $b = 175$ mm.



(a)



(b)

Figure D-9b : Central deflection of slab under different loading of same slab thickness (60 mm) for (a) $b=105$ mm and (b) $b=0$ mm.

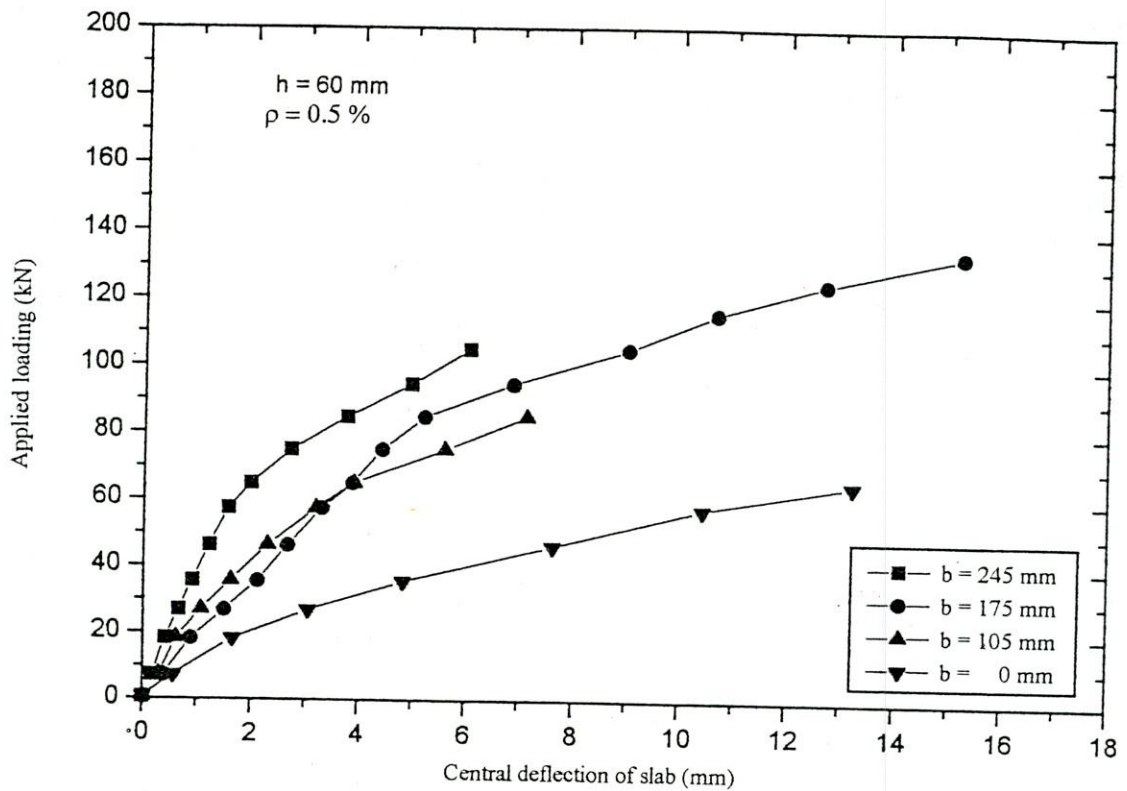


Figure D-10 : Central deflection of slab under applied loading for various width of edge beam (b) at slab thickness (h) = 60 mm and reinforcement ratio (ρ) = 0.5 %

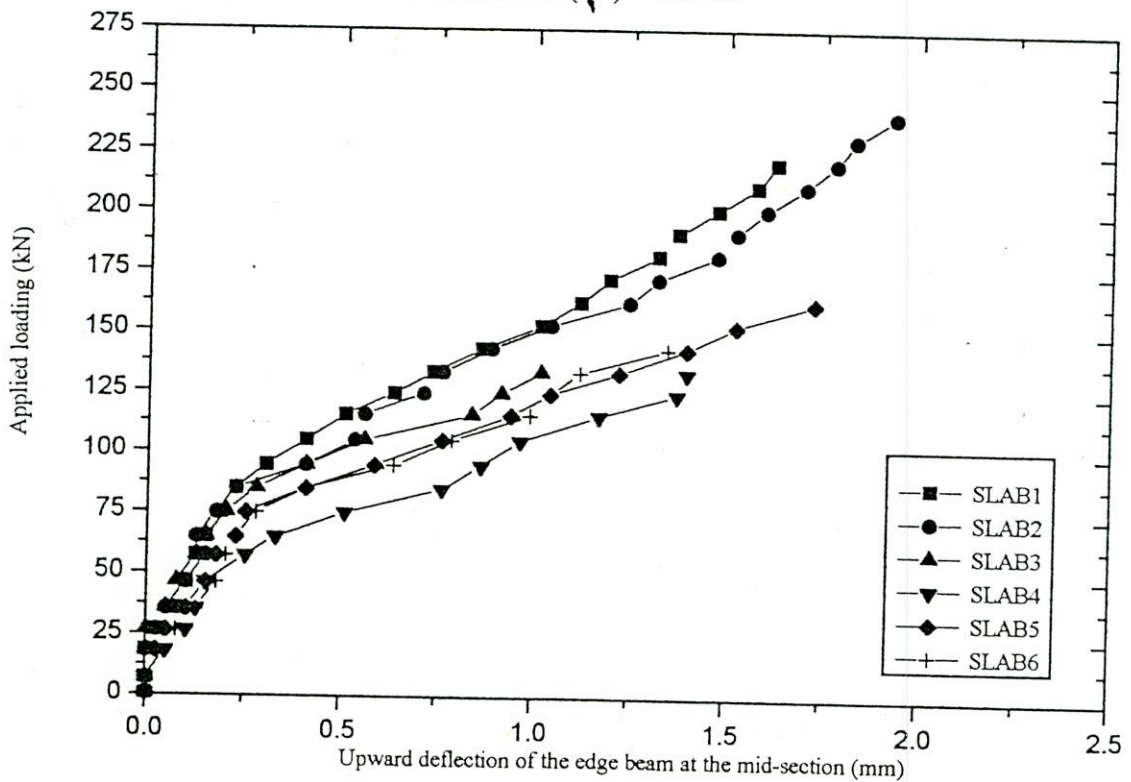


Figure D-11 : Upward deflection of edge beam at the mid-section of SLAB1 to SLAB6

APPENDIX E

Test Results in table

Table E-1 Ultimate Strength of Slabs and Cylinder Strength of Concrete.

SLAB SAMPLE	Width of Edge Beam	Slab Thickness	Crushing Strength of Concrete (f'_c)	Ultimate Load
	(mm)	(mm)	(MPa)	(kN)
SLAB 1	245	80	38.51	225.16
SLAB 2	245	80	37.42	242.09
SLAB 3	245	80	28.19	142.95
SLAB 4	245	60	38.24	138.12
SLAB 5	245	60	36.60	147.59
SLAB 6	245	60	41.95	130.51
SLAB 7	175	80	32.45	181.64
SLAB 8	175	60	41.30	133.27
SLAB 9	175	60	33.14	115.51
SLAB 10	105	80	37.45	188.89
SLAB 11	105	60	40.43	112.88
SLAB 12	105	60	37.04	115.73
SLAB 13	0	80	37.72	171.96
SLAB 14	0	60	34.71	84.73
SLAB 15	0	60	33.03	91.76
SLAB 16	340	60	40.24	171.96

Table E-2a

Central Deflection of Slab for Different Loading of SLAB1 to SLAB6.

Applied load (kN)	Deflection at the Center Point of Slabs in mm.					
	SLAB 1	SLAB 2	SLAB 3	SLAB 4	SLAB 5	SLAB 6
0.627	0	0	0	0	0	0
7.179	0.2032	0.1524	0.1524	0.1778	0.254	0.2032
18.300	0.4064	0.3048	0.3048	0.4064	0.5588	0.4064
26.792	0.5588	0.4572	0.508	0.6604	0.8128	0.6858
35.608	0.762	0.6858	0.762	0.9144	1.1176	0.9652
46.364	0.9906	0.9144	1.016	1.2192	1.4224	1.27
57.440	1.1684	1.143	1.27	1.5748	1.8288	1.6764
64.921	1.3208	1.3462	1.524	1.9812	2.286	2.0574
74.997	1.524	1.6002	1.778	2.7178	2.667	2.5908
84.734	1.9812	1.9304	2.3876	3.7592	3.3782	3.429
94.462	2.413	2.3114	2.8448	4.953	4.2164	4.191
104.986	3.048	2.7178	3.429	6.0452	5.4864	5.207
115.506	3.429	3.1496	4.064	--	6.223	6.35
124.403	3.9116	3.6068	4.9784	--	--	6.9342
133.273	4.4958	4.1402	5.6388	--	--	--
142.947	4.9276	4.4958	--	--	--	--
152.618	--	5.08	--	--	--	--
162.293	--	5.5626	--	--	--	--
171.963	--	6.0198	--	--	--	--
181.638	--	6.5278	--	--	--	--
191.308	--	7.3152	--	--	--	--

Table E-2b

Central Deflection of Slab for Different Loading of SLAB7 to SLAB12.

Applied load (kN)	Deflection at the Center Point of Slabs in mm.					
	SLAB 7	SLAB 8	SLAB 9	SLAB 10	SLAB 11	SLAB 12
0.627	0	0	0	0	0	0
7.179	0.1524	0.381	0.2032	0.2032	0.3048	0.2794
18.300	0.3302	0.889	0.508	0.381	0.6096	0.508
26.792	0.5334	1.4986	0.762	0.6604	1.0668	0.8382
35.608	0.762	2.1082	1.0922	0.889	1.6256	1.2446
46.364	1.0668	2.667	1.4986	1.2192	2.286	1.4732
57.440	1.3462	3.302	2.032	1.4986	3.175	2.4892
64.921	1.6002	3.8608	2.7432	2.032	3.8862	3.0988
74.997	1.9304	4.4196	3.6322	2.4892	5.588	3.937
84.734	2.413	5.207	4.699	2.9718	7.112	--
94.462	2.9972	6.858	5.5626	3.556	--	--
104.986	3.4544	9.017	7.112	4.318	--	--
115.506	4.0894	10.668	--	4.8514	--	--
124.403	4.5974	12.7	--	5.5118	--	--
133.273	5.1054	15.24	--	6.1468	--	--
142.947	5.8166	--	--	6.9342	--	--
152.618	6.477	--	--	7.6962	--	--
162.293	7.1374	--	--	--	--	--
171.963	7.9502	--	--	--	--	--
181.638	8.6614	--	--	--	--	--

Table E-2c

**Central Deflection of Slab for Different Loading of SLAB13
to SLAB16.**

Applied load (kN)	Deflection at the Center Point of Slabs in mm.			
	SLAB 13	SLAB 14	SLAB 15	SLAB 16
0.627	0	0	0	0
7.179	0.127	0.5588	0.3048	0.2032
18.300	0.3048	1.651	0.762	0.381
26.792	0.6096	3.048	1.4732	0.635
35.608	1.016	4.826	2.8194	0.9652
46.364	1.397	7.62	5.5372	1.3208
57.440	1.8796	10.414	7.9248	1.7018
64.921	2.3368	13.208	11.176	2.1844
74.997	2.921	--	13.208	2.5908
84.734	3.6576	--	--	3.2258
94.462	4.6228	--	--	3.9624
104.986	5.715	--	--	5.2832
115.506	6.6802	--	--	6.3754
124.403	8.001	--	--	7.7978
133.273	8.763	--	--	9.017
142.947	--	--	--	11.7348
152.618	--	--	--	13.7922

